

UNIVERSITY OF CALIFORNIA, SAN DIEGO

I/O-Efficient Data-Intensive Computing

A dissertation submitted in partial satisfaction of the
requirements for the degree of Doctor of Philosophy

in

Computer Science

by

Alexander Carlin Rasmussen

Committee in charge:

Professor Amin Vahdat, Chair
Professor Alin Deutsch
Professor Tara Javidi
Professor Bill Lin
Professor Geoffrey M. Voelker

2013

Copyright

Alexander Carlin Rasmussen, 2013

All rights reserved.

The Dissertation of Alexander Carlin Rasmussen is approved and is acceptable in quality and form for publication on microfilm and electronically:

Chair

University of California, San Diego

2013

EPIGRAPH

Speed provides the one genuinely modern pleasure.

Aldous Huxley

Obviously, the highest type of efficiency is that which can utilize existing material to the best advantage.

Jawaharlal Nehru

Efficiency is doing things right; effectiveness is doing the right things.

Peter Drucker

Phil: Birdman, this is Dvd, our new efficiency expert.

Harvey: Interesting name. Norweg...?

Dvd: Was "David". I eliminated the vowels to save time.

Phil: Brillnt!

Harvey: Hmm... Hrvy... wait, is Y a vowel?

Harvey Birdman: Attorney at Law – s1e18 – Gone Efficien...t

TABLE OF CONTENTS

Signature Page	iii
Epigraph	iv
Table of Contents	v
List of Figures	ix
List of Tables	xii
Acknowledgements	xiii
Vita	xvi
Abstract of the Dissertation	xvii
Chapter 1 Introduction	1
1.1 The Rise of Partition-Parallel Architectures	2
1.2 Scale-Out, but not Scale-Up	3
1.3 Sources of Inefficiency in Existing Systems	4
1.4 Hypothesis	5
1.5 Organization	6
Chapter 2 Background	7
2.1 Problem Formulation: Sorting	7
2.2 Problem Formulation: MapReduce	8
Chapter 3 Architectural and Design Principles	10
3.1 Building a “Balanced” System	10
3.2 Design Considerations	10
3.3 Hardware Architecture	11
3.4 Software Architecture	14
Chapter 4 TritonSort: I/O-Efficient Large-Scale Sorting	16
4.1 Introduction	16
4.2 Design Challenges	18
4.2.1 Software Architecture	18
4.3 Design and Implementation	20
4.3.1 Architecture Overview	20
4.3.2 Sort Architecture	21
4.3.3 TritonSort Architecture: Phase One	22
4.3.4 TritonSort Architecture: Phase Two	29

4.3.5	Stage and Buffer Sizing	31
4.4	Optimizations	31
4.4.1	Network	31
4.4.2	Minimizing Disk Seeks	35
4.4.3	The Importance of File Layout	35
4.4.4	CPU Scheduling	36
4.4.5	Pipeline Demand Feedback	37
4.4.6	System Call Behavior	38
4.5	MinuteSort: An In-Memory Sort Implementation	38
4.6	Measuring TritonSort’s Energy Efficiency	39
4.6.1	Measuring the Switch	40
4.6.2	Measuring the Nodes	40
4.6.3	Calculating Energy	43
4.6.4	Measurement Results	47
4.7	Evaluation	48
4.7.1	Evaluation Environment	48
4.7.2	Comparison to Alternatives	49
4.7.3	Examining Changes in Balance	49
4.7.4	TritonSort Scalability	51
4.8	Conclusions	52
4.9	Acknowledgments	52
Chapter 5	Themis: I/O-Efficient MapReduce	53
5.1	Introduction	53
5.2	The Challenge of Skew	55
5.3	System Architecture	57
5.3.1	Core Architecture	57
5.3.2	MapReduce Overview	57
5.3.3	Phase One: Map and Shuffle	58
5.3.4	Phase Two: Sort and Reduce	59
5.4	Memory Management and Flow Control	61
5.4.1	Memory Allocation Interface	61
5.4.2	Policy 1: Pool-Based Management	62
5.4.3	Policy 2: Quota-Based Management	64
5.4.4	Policy 3: Constraint-Based Management	65
5.5	Skew Mitigation	67
5.5.1	Mechanism	68
5.5.2	Sampling Policies	69
5.6	Evaluation	69
5.6.1	Workloads and Evaluation Overview	70
5.6.2	Job Implementation Details	74
5.6.3	Performance	75

5.6.4	Memory Management	78
5.6.5	Skew Mitigation	80
5.6.6	Write Sizes	82
5.7	Conclusions	83
5.8	Acknowledgments	84
Chapter 6	I/O-Efficient Fault Tolerance	85
6.1	Introduction	85
6.2	Motivation	87
6.2.1	Fault Tolerance for “Dense” Clusters	88
6.2.2	Modeling Node Failure Rates	90
6.2.3	Modeling Expected Job Completion Time	91
6.3	Alternative Fault Tolerance Methods	93
6.3.1	Replication	93
6.3.2	Upstream backup	94
6.3.3	Parallel Recovery	94
6.3.4	Process-Pairs	94
6.3.5	Provenance and Selective Replay	95
6.3.6	Scan-Sharing	95
6.4	Design	96
6.4.1	Goals	96
6.4.2	Recovery in MapReduce	96
6.4.3	Write Recovery Approach	97
6.4.4	Read Recovery Approach	98
6.5	Implementation	98
6.5.1	Themis: I/O-Efficient MapReduce	99
6.5.2	Recovery Mechanism	101
6.5.3	Multi-Tenancy in Themis	107
6.5.4	Job Dispatch	108
6.5.5	Input Files and Distributed Storage	109
6.5.6	Responding to Failures	110
6.6	Per-Record Replay Proportionality	111
6.7	Evaluation	116
6.7.1	Methodology	116
6.7.2	Proportionality of Recovery	117
6.7.3	Scan Sharing Overhead	120
6.8	Conclusions	120
6.9	Acknowledgments	120
Chapter 7	Related Work	122
7.1	Large-Scale Sorting Systems	122
7.2	Achieving Per-Resource Balance	123
7.3	Architectural Influences	123

7.4	Fault Tolerance Techniques	124
7.5	Multi-Query Optimization and Scan Sharing	125
7.6	Improving MapReduce's Performance	125
7.7	Skew Mitigation in MapReduce	126
Chapter 8	Conclusions and Future Directions	127
8.1	Summary	127
8.2	Limitations and Future Work	129
	Bibliography	131

LIST OF FIGURES

Figure 4.1.	Performance of the Heaper-Merger sort implementation in microbenchmark on a 200GB per disk parallel external merge-sort as a function of the number of files merged per disk.	19
Figure 4.2.	Block diagram of TritonSort’s phase one architecture. The number of workers for a stage is indicated in the lower-right corner of that stage’s block, and the number of disks of each type is indicated in the lower-right corner of that disk’s block.	22
Figure 4.3.	The NodeDistributor stage, responsible for partitioning records by destination node.	23
Figure 4.4.	The Sender stage, responsible for sending data to other nodes. . . .	23
Figure 4.5.	The Receiver stage, responsible for receiving data from other nodes’ Sender stages.	25
Figure 4.6.	The LogicalDiskDistributor stage, which is responsible for distributing records across logical disks and buffering sufficient data to allow for large writes.	26
Figure 4.7.	Block diagram of TritonSort’s phase two architecture. The number of workers for a stage is indicated in the lower-right corner of that stage’s block, and the number of disks of each type is indicated in the lower-right corner of that disk’s block.	29
Figure 4.8.	Comparing the scalability of single-threaded and multi-threaded Receiver implementations.	32
Figure 4.9.	Microbenchmark indicating the ideal disk throughput as a function of write size.	34
Figure 4.10.	Power consumed by a representative node during a JouleSort run, comparing the results of the two power meters used.	44
Figure 4.11.	Throughput when sorting 1 TB per node as the number of nodes increases.	51
Figure 5.1.	Stages of Phase One (Map/Shuffle) in Themis.	57
Figure 5.2.	Stages of Phase Two (Sort/Reduce) in Themis.	59

Figure 5.3.	A diagrammatic overview of pool-based memory management. Note that memory in each pool is divided into fixed-size regions, and that any memory not allocated to pools cannot be utilized by stages.	62
Figure 5.4.	A diagrammatic overview of quota-based memory management. In this figure, $Quota_A$ provides a memory quota between Stage 1 and Stage 4. Stages 2 and 3 use unmanaged memory created with standard <code>malloc</code> and <code>free</code> syscalls.	63
Figure 5.5.	A diagrammatic overview of constraint-based memory management. All stages' memory requests are satisfied by a central memory manager that schedules these requests according to the stage graph's structure.	65
Figure 5.6.	Performance of evaluated MapReduce jobs. Maximum sequential disk throughput of approximately 90 MB/s is shown as a dotted line. Our TritonSort record from 2011 is shown on the left for comparison.	76
Figure 5.7.	Effects of allocation policy on mean allocation times across workers.	78
Figure 5.8.	Memory quota usage of the Reader Converter stage. The network was made artificially slow in the time period designated by the dashed lines.	80
Figure 5.9.	Partition sizes for various Themis jobs. Error bars denoting the 95% confidence intervals are hard to see due to even partitioning.	81
Figure 5.10.	Median write sizes for various Themis jobs.	82
Figure 6.1.	A lower-bound of the expected benefit of job-level fault tolerance for varying cluster sizes, given that an error-free execution of a job with task-level fault tolerance takes five minutes (a), an hour (b), or ten hours (c) to complete.	88
Figure 6.2.	A diagrammatic overview of Themis' phases.	99
Figure 6.3.	Illustrative example of disk failure and recovery in a two-node cluster with two intermediate disks per node and eight intermediate partitions. The rectangles representing each partition are labeled with the disk or disks on which data for that partition is stored. ...	102

Figure 6.4.	Illustrative example of node failure and recovery in a two-node cluster with two intermediate disks per node and eight intermediate partitions. A ‘?’ indicates that it is unknown whether the data has been lost or not.	103
Figure 6.5.	An overview of multi-tenancy in Themis. Input records are mapped by both job A and job B’s map functions, and intermediate records are routed based on each job’s partition function independently. . .	107
Figure 6.6.	Comparing the performance of unmodified HDFS, HDFS with whole file replication for the primary replica, and reading and writing from raw disks.	109
Figure 6.7.	Time to sequentially scan a 13.5 GB file vs. selectively reading a percentage of records.	112
Figure 6.8.	The negative impact of both scanning through and selectively reading from the same file simultaneously.	113
Figure 6.9.	The negative impact of running a scan on one file while selectively reading records from a second file.	114
Figure 6.10.	Runtime of recovery from a disk failure during an 800GB sort with an increasing number of failed disks.	117
Figure 6.11.	Runtime of recovery from node failures during an 800GB sort. . . .	118
Figure 6.12.	Comparing the baseline performance of an 800GB sort with the performance of scan-sharing that sort with disk failure recovery jobs. . .	119

LIST OF TABLES

Table 1.1.	Large scale sorting results over time, and their associated per-node and per-disk efficiency. Results extracted from [6, 62, 69, 70].	6
Table 3.1.	Resource options considered for constructing a cluster for a balanced sorting system. These values are estimates as of January, 2010. . . .	12
Table 4.1.	Median stage runtimes for a 52-node, 100TB sort, excluding the amount of time spent waiting for buffers.	31
Table 4.2.	Average power consumed by a node throughout a sort benchmark run for the first four trials of our JouleSort experiments.	45
Table 4.3.	Total energy measured for each 100TB trial by both WattsUp and ILO meters.	46
Table 4.4.	Statistics for the energy measurements presented in Table 4.3.	47
Table 4.5.	Effect of increasing speed of intermediate disks on a two node, 500GB sort.	50
Table 4.6.	Effect of increasing the amount of memory per node on a two node, 2TB sort.	50
Table 5.1.	Themis’s three phase architecture.	58
Table 5.2.	A comparison of Themis’s memory allocator implementations. . . .	61
Table 5.3.	A summary of the Themis memory allocator API.	61
Table 5.4.	A description and table of abbreviations for the MapReduce jobs evaluated in this section. Data sizes take into account 8 bytes of metadata per record for key and value sizes.	70
Table 5.5.	Performance comparison of Hadoop and Themis.	77
Table 5.6.	Performance of allocation policies.	79
Table 6.1.	Component-level failure rates observed in a Google data center as reported in [30].	89
Table 6.2.	Table summarizing Themis’ response to various kinds of failures at different points in the job.	104

ACKNOWLEDGEMENTS

First and foremost, thanks to my parents. Throughout the past six years, being close to home was a great source of comfort. I love you both, and could not have asked for better parents.

I would like to acknowledge Professor Amin Vahdat for his support as the chair of my committee, and for his advice and patience throughout this whole process.

I would also like to acknowledge George Porter, whose Herculean efforts in co-authorship, cluster management, grant writing and advising have helped both myself and so many others.

This dissertation would not have been possible without the hard work and support of my co-authors, whose contributions I would like to acknowledge individually. Mike Conley was heavily involved in both the TritonSort and Themis efforts, and wrote Themis' constraint-based memory management system and the current record-setting MinuteSort implementation. His determination and enthusiasm were valuable beyond expression. Harsha Madhyastha was involved from the earliest days of the TritonSort effort, and was present for the first successful sort. Radhika Niranjana Mysore put a lot of work into the initial Heaper-Merger version of the TritonSort architecture, and contributed significantly to MinuteSort. Alexander Pucher wrote the first iteration of our radix sort code, and helped me write what would become the final version of TritonSort in a single, crazed 48-hour push. Rishi Kapoor handled the mammoth port of CloudBurst to Themis with exceptional graciousness and tenacity. Terry Lam wrote Themis' PageRank implementation and input generators, and served as our first real user, helping to make Themis more robust.

Most computer science departments dream of having a system administrator as deeply knowledgeable, accommodating, and hospitable as Brian Kantor. Thank you for fighting the never-ending battle against entropy and keeping everything running through

innumerable deadlines.

Chris Nyberg, Mehul Shah and Naga Govindaraju provided conscientious and patient shepherding of TritonSort through the sort benchmark validation process. Thanks for keeping us honest and giving us a target to hit. I never got to meet Jim Gray, but the sort benchmark that he pioneered has had a profound impact on this phase of my life.

Joe Hellerstein gave me the exposure to computer science research that convinced me to go to graduate school, the recommendation letter that helped get me in, and the startup opportunity that got me out. Along the way, he provided feedback on papers and a great deal of valuable advice.

The work in this dissertation was funded by the National Science Foundation and generous donations from Cisco and NetApp. Special thanks to Landon Curt Noll for being our advocate inside Cisco for so many years.

I have been fortunate to make many new friends while at UCSD, and to keep in touch with friends from Berkeley, Monrovia High and before. Thanking each of you properly would double the length of this dissertation. You are all wonderful people, and I couldn't have finished this without you. I am so incredibly fortunate to have all of you in my life.

Chapter 4 contains material as it appears in the Proceedings of the USENIX Symposium on Networked Systems Design and Implementation (NSDI) 2011. Rasmussen, Alexander; Porter, George; Conley, Michael; Madhyastha, Harsha; Niranjan Mysore, Radhika; Pucher, Alexander; Vahdat, Amin. The dissertation author was the primary investigator and author of this paper.

Chapter 5 contains material as it appears in the Proceedings of the ACM Symposium on Cloud Computing (SoCC) 2012. "Themis: An I/O-Efficient MapReduce". Rasmussen, Alexander; Conley, Michael; Kapoor, Rishi; Lam, Vinh The; Porter, George; Vahdat, Amin. The dissertation author was the primary investigator and author of this

paper.

Chapter 6 contains material submitted for publication as “I/O-Efficient Fault Tolerance for MapReduce”. Rasmussen, Alexander; Porter, George; Vahdat, Amin. The dissertation author was the primary investigator and author of this paper.

VITA

2007 B.S., University of California, Berkeley
2010 M.S., University of California, San Diego
2013 Ph.D., University of California, San Diego

PUBLICATIONS

“Themis: An I/O-Efficient MapReduce” ACM Symposium on Cloud Computing, October 2012.
“TritonSort: A Balanced Large-Scale Sorting System” USENIX Symposium on Networked Systems Design and Implementation, April 2011.
“Short Paper: Improving the Responsiveness of Internet Services with Automatic Cache Placement” European Conference in Computer Systems, April 2009.

ABSTRACT OF THE DISSERTATION

I/O-Efficient Data-Intensive Computing

by

Alexander Carlin Rasmussen

Doctor of Philosophy in Computer Science

University of California, San Diego, 2013

Professor Amin Vahdat, Chair

There is a growing need for scalable, data-intensive processing platforms to analyze and filter large volumes of data. The effectiveness of these systems is measured by the quantity and quality of data that they can process in a reasonable amount of time; thus, these systems have very high I/O and storage requirements.

Existing systems are very effective at scaling to large cluster sizes. Unfortunately, there exists a significant gap between the performance these systems provide and the underlying capacity of the hardware infrastructure on which they are deployed.

In this dissertation, we endeavor to bridge this performance gap by focusing on

efficient I/O as a first-class architectural concern. In particular, we present two systems, TritonSort and Themis. TritonSort is a high-performance large-scale sorting system capable of sorting 100TB of data on a modestly-sized cluster at about 82% of that cluster's peak hardware performance. Themis is a successor system to TritonSort that supports the popular MapReduce programming paradigm and can run a wide spectrum of MapReduce jobs at nearly the speed at which TritonSort can sort. We conclude with the implementation of a fault tolerance scheme for Themis that provides proportional fault tolerance without imposing additional rounds of I/O during common-case operation.

Chapter 1

Introduction

The quantity of data the world generates and stores is growing at a staggering rate. Walmart handles more than a million customer transactions per hour, and the size of its customer database is estimated at 2.5 petabytes [27]. Search engines like Google construct complex indices over the entire public Internet, which is estimated to consist of at least 14 billion pages [51]. Facebook’s users upload more than 300 million photos per day [41]. Scientific instruments like the Australian Square Kilometer Array, the Large Hadron Collider and the Pan-STARRS array of telescopes can generate petabytes of data per day [38].

Capturing this data, while a technically challenging feat in and of itself, is not enough. To be useful, the data must be analyzed, aggregated, filtered, and transformed. The aforementioned data sets are but a few examples of a new class of “big data” – data sets that are so large and complex that they become difficult to process using traditional techniques and technologies.

Some data-intensive problems allow every record to be processed in parallel without knowing anything about any other records. These problems are known as “embarrassingly parallel”, and can be scaled out easily. An example of an embarrassingly parallel problem is searching a corpus of text for occurrences of a word; each document in the corpus can be scanned independently and the results of the scan over each document

can be trivially merged together afterward.

However, a much larger class of problems are not embarrassingly parallel. These problems require some form of aggregation or combination across records (analogous to the group-by and join operations in relational database systems) in addition to per-record processing. One canonical example of this class of problems is counting the number of times each word occurs in a corpus of text. The occurrences of each word can be counted in each document independently, but these counts must be subsequently added together. Performing this aggregation efficiently is one of the primary challenges facing designers of systems for processing “big data”.

1.1 The Rise of Partition-Parallel Architectures

In recent years, a range of large-scale, data-intensive systems have been developed to tackle jobs like the word count example above. One of the most popular frameworks for this form of analysis is MapReduce [22]. A MapReduce computation is specified by two functions. The first function, `map`, takes a record as input and produces zero or more records; it performs the per-record processing portion of the job. The second function, `reduce`, takes all records with the same key as input and produces zero or more records; it performs the aggregation portion of the job. Both `map` and `reduce` functions are assumed to be deterministic and side-effect free, although this is sometimes not the case in practice.

MapReduce’s strength lies in the simplicity of its programming model. Users of MapReduce need only write `map` and `reduce` functions without concerning themselves with dividing the data among nodes, performing inter-node communication or recovering from failures. The `map` function’s signature and its idempotent nature make it embarrassingly parallel, while the `reduce` function’s parallelism can be adjusted from completely serial to extremely parallel based on the number of distinct keys in the records produced

by the map function.

MapReduce was developed by Google in the early 2000s for tasks like inverted index generation and PageRank [64] computation over Google's cache of the web. Engineers at Yahoo! wrote an open-source version of MapReduce called Hadoop [90] in 2005 that has since become extremely popular and is widely deployed in both academic and industrial settings.

1.2 Scale-Out, but not Scale-Up

While systems like MapReduce scale quite well, they do not utilize their clusters' resources to nearly the extent that they should. As one example, in 2009 a cluster of 3452 nodes running Hadoop sorted 100 TB of data in 173 minutes [62]. At a high level, this performance is quite impressive – an average of 578 GB of data sorted per minute. However, this high-level performance masks a great deal of inefficiency. In the aforementioned record-setting sort, each node in the cluster's average rate was approximately 2.8 MBps, a small fraction of the speed at which that can read from and write to its disks. This performance gap is even more apparent when one considers that a significant fraction of the data (approximately 27 TB) could conceivably have been buffered in the cluster's main memory.

These efficiency problems are not limited to Hadoop. Anderson and Tucek [6] examined a collection of large-scale data-intensive processing systems and found a widespread lack of efficiency among them.

The tempting solution to the problem of inefficiency is to simply increase the size of the cluster, splitting the data being processed among progressively more nodes. This decreases both the amount of data that each node must process and (to the extent allowed by Amdahl's Law [4]) increases the throughput of the system. However, this approach has several negative consequences.

Larger clusters have a proportionately large capital expense and operational cost. Google, one of the pioneers in large-scale data-intensive systems, has contracted over 260MW to power its data centers [23]. When it filed its IPO in 2011, Facebook reported that it spent \$606 million on constructing and equipping its data centers in 2011 and expected to spend another \$500 million in 2012 [81]. As problem sizes increase, these expenses must by necessity also increase unless system efficiency is improved.

Large data centers also have an environmental cost. McKinsey and Company estimates that the carbon dioxide emissions from data centers will surpass emissions from the airline industry by 2020 [31]. Further, larger clusters are harder to manage and experience faults more frequently than smaller clusters do because of the increased number of nodes in those clusters. We will explore the implications of increased failure further in Chapter 6.

1.3 Sources of Inefficiency in Existing Systems

While a thorough study of the sources of per-node inefficiency in existing systems has not been performed, we can broadly classify three different sources of inefficiency in systems that are I/O-bound:

Inefficient I/O Current-generation large scale data processing systems read from and write to large collections of magnetic hard drives. These magnetic drives are characterized by their fast sequential access and slow random access. Fundamentally, systems that desire a high throughput from these devices should write to them sequentially as much as possible. However, existing systems often treat disks as a “black box” without consideration for the overheads of non-sequential access.

Too much I/O per record Existing systems may read and write each record to disk several times during the course of a job, either because of memory pressure or for increased fault tolerance. These additional reads and writes incur significant additional overhead, as writing to disk is at least an order of magnitude slower than accessing other levels in the node’s memory hierarchy.

Imbalanced hardware configurations Often, the hardware platforms on which these systems are deployed are configured such that the system will run out of network bandwidth or memory before they can maximize their disks’ throughput. In Chapter 4, we argue that a degree of software/hardware co-design can lead to radically more efficient software and hardware architectures.

1.4 Hypothesis

The hypothesis of this dissertation is that systems built with efficient disk I/O as a first-order architectural concern can realize an order of magnitude improvement in performance versus existing large-scale data-intensive systems without compromising their scalability or generality.

We argue that the chief challenges of building such a system lie both in minimizing the number of I/O operations per record and in ensuring that disk I/O is done sequentially as much as possible. We also argue that significant increases in per-node efficiency can be realized by considering fault tolerance models that prioritize efficient I/O both in failure-free operation and during recovery.

We explore the design of radically more efficient data processing systems through two main prototype systems: TritonSort, a large-scale sorting system, and Themis, an implementation of the MapReduce programming model. Table 1.1 compares the performance of TritonSort and Themis with previous sort benchmark record holders.

Table 1.1. Large scale sorting results over time, and their associated per-node and per-disk efficiency. Results extracted from [6, 62, 69, 70].

Year	Name	Nodes	Disks	MB/s	MB/s/node	MB/s/disk
2012	Themis (35TB)	20	320	4656	232.8	14.6
2011	Themis	52	832	12080	232.4	14.5
2011	TritonSort	52	832	15633	300.6	18.8
2009	Hadoop	3452	13808	9633	2.79	0.69
2009	DEMSort	195	780	9400	48.2	12.1

TritonSort and Themis have each improved on the per-node performance of systems in their respective problem domains by almost an order of magnitude, approaching the maximum throughput possible on the clusters on which they are deployed. At time of writing, TritonSort and Themis hold four world records in large-scale sorting.

1.5 Organization

Chapter 2 provides background on the problem domains of large-scale sorting and MapReduce. Chapter 3 provides an overview of the architecture and design principles that underpin both the systems presented in this dissertation. Chapter 4 presents the design and implementation of TritonSort, our large-scale sorting system. Chapter 5 presents the design and implementation of Themis, our MapReduce implementation, focusing in particular on its differences from TritonSort’s design. Chapter 6 takes an in-depth look at fault tolerance in Themis, looking first at the trade-off between fault tolerance and I/O-efficiency, and then presenting the design and implementation of an I/O-efficient fault tolerance scheme for Themis. Chapter 7 explores related work. The dissertation concludes with Chapter 8, which describes some open problems and future directions.

Chapter 2

Background

This section makes the problem domains tackled by TritonSort and Themis more concrete, and describes the architectural features that both systems share in common.

2.1 Problem Formulation: Sorting

TritonSort seeks to meet the specifications laid out in the GraySort benchmark [80]. For this benchmark, the data to be sorted consists of 100 byte records, each of which has a 10-byte key and a 90-byte value. We target deployments with input datasets that are tens to hundreds of terabytes in size; the GraySort benchmark’s current data size is 100 terabytes.

Input data is stored as a collection of files across the cluster’s disks. TritonSort’s goal is to transform this input data set into an ordered set of output files, also stored across the cluster’s disks, such that an in-order concatenation of these output files is a sorted permutation of the input data set.

Sorting large datasets places great stress on a cluster’s resources. First, storing tens to hundreds of terabytes of data demands a large amount of storage capacity. Given the capacity of modern hard drives, the data must be stored across several drives and almost certainly across many machines. Second, performing reads and writes to all these disks simultaneously places load on both the disks themselves and the I/O controllers

connecting them to the CPU. Third, since the records to be sorted are assumed to be distributed randomly across input files, almost all of the dataset to be sorted will have to be sent over the network at some point. Finally, comparing records requires a non-trivial amount of compute power. This combination of demands makes it challenging to design an efficient large-scale sorting system that utilizes the cluster's resources well.

2.2 Problem Formulation: MapReduce

As mentioned in Chapter 1, a MapReduce computation is specified by two functions, `map` and `reduce`, with `map` responsible for per-record processing and `reduce` responsible for aggregation. MapReduce treats a data set as a collection of *records*, each of which consists of a *key* and a *value*. Both the key and the value can be arbitrary. A record with key k and value v will be denoted $\langle k, v \rangle$. Throughout this dissertation we will refer to records that are produced by the `map` function as *intermediate records* or *mapped records* and records produced by the `reduce` function as *output records* or *reduced records*.

A canonical example MapReduce job is the problem of counting the occurrences of each word in a text corpus. For this problem, the user might write a `map` function that takes a line of text as input and produces the record $\langle \text{word}, 1 \rangle$ for each word in the line. The `reduce` function would then receive all records for a given word, add their values together, and produce a single record $\langle \text{word}, n \rangle$.

The `map` and `reduce` functions can produce an arbitrary number of arbitrarily-sized records. This is in sharp contrast to the GraySort benchmark, where records can be assumed to be the same size. Additionally, keys can be arbitrarily distributed throughout the space of possible keys. This makes the problem of evenly dividing key ranges among nodes difficult, as we will see in Chapter 5.

Since each `reduce` function is responsible for processing all records with the

same key, the system running a MapReduce job must ensure that all records with the same key are available on the same node. This property requires that the system perform a distributed sort of all intermediate records by key before applying the reduce function to each key's records. In this way, the problem of efficiently running MapReduce jobs is a superset of the problem of efficiently sorting at scale; in fact, a sort job in MapReduce is simply a job with "no-op" map and reduce functions that emit any records they receive unmodified. As we will see later in this dissertation, we applied many of the lessons learned in designing an efficient large-scale sorting system to the problem of building an efficient MapReduce platform.

Chapter 3

Architectural and Design Principles

3.1 Building a “Balanced” System

Both TritonSort and Themis aim to ensure good resource utilization by being “balanced” systems. We define a balanced system as one that drives all cluster resources at as close to 100% utilization as possible. For any given application and workload, there will be an ideal balanced hardware configuration in keeping with the application’s demands on a cluster’s resources. In practice, however, the set of hardware configurations is limited by the availability of components; for example, one cannot currently buy a processor with precisely 13 cores. As a result, a hardware configuration must be chosen that best meets the application’s demands. Once the appropriate hardware configuration is determined, the application must be architected to exploit the hardware’s capabilities. In the following sections, we outline our considerations in designing a balanced system, including our choices of hardware and software architectures.

3.2 Design Considerations

Our system’s design is motivated by three main considerations. First, we rely only on commodity hardware components. This is both to keep the costs of our system relatively low and to have our system be representative of today’s data centers so that

the lessons we learn can be applied more generally. Hence, we do not make use of networking substrates like Infiniband that provide high network bandwidth at high cost. Also, despite the recent emergence of solid state drives (SSDs) that provide higher I/O rates, we chose to use hard disks because they continue to provide the most affordable option for high capacity storage and streaming I/O.

Second, we focus our software architecture on minimizing disk I/O and random disk access. In the particular hardware configuration we chose, the key bottleneck among the various system resources is disk bandwidth. The main challenge in sustaining peak bandwidth is to minimize the amount of time the disks spend seeking, because the disk cannot do any effective data transfer while seeking from one location to another.

Additionally, we seek to minimize the number of times each record is transferred from disk. Sorting data on clusters that have less memory than the total amount of data to be sorted requires every input record to be read and written at least twice [1]. Since a distributed sort by key is the kernel of any MapReduce job, this lower-bound also applies to MapReduce. Since every additional read and write to disk fundamentally increases the time to sort, we seek to achieve exactly this lower bound to maximize system performance.

Third, we choose to focus on hardware architectures whose total memory cannot contain the entire dataset, because such a design would significantly drive up costs and be infeasible for input datasets at the scales that we consider in this dissertation. Significant improvements in efficiency are possible when the dataset fits in memory; we explore sorting in-memory briefly in Chapter 4.

3.3 Hardware Architecture

To determine the right hardware configuration for our application, we make the following observations about our workloads. Since the “working set” for our data is

Table 3.1. Resource options considered for constructing a cluster for a balanced sorting system. These values are estimates as of January, 2010.

Storage			
Type	Capacity	R/W throughput	Price
7.2k-RPM	500 GB	90-100 MBps	\$200
15k-RPM	150 GB	150 MBps	\$290
SSD	64 GB	250 MBps	\$450

Network	
Type	Cost/port
1 Gbps Ethernet	\$33
10 Gbps Ethernet	\$480
40 Gbps Ethernet	\$3700

Server	
Type	Cost
8 disks, 8 CPU cores	\$5,050
8 disks, 16 CPU cores	\$5,450
16 disks, 16 CPU cores	\$7,550

so large, it does not make sense to separate the cluster into computation-heavy and storage-heavy regions, because this would necessitate large network transfer between the two. Instead, we provision each server in the cluster with an equal amount of processing power and disks.

Second, almost all of the data needs to be exchanged between machines as part of the shuffle step of the computation. To balance the system, we need to ensure that this all-to-all shuffling of data can happen in parallel without network bandwidth becoming the overall bottleneck. Since we focus on using commodity components, we use an Ethernet network fabric. Commodity Ethernet is available in a set of discrete bandwidth levels—1 Gbps, 10 Gbps, and 40 Gbps—with cost increasing proportional to throughput (see Table 3.1). Assuming 7.2k RPM 500GB disk drives, a 1 Gbps network can accommodate at most one disk per server without the network throttling disk I/O. Therefore, we settle

on a 10 Gbps network; 40 Gbps Ethernet has yet to mature at the end host and hence is still cost-prohibitive. To balance a 10 Gbps network with disk I/O, we use a server that can host 16 disks. Based on the options available commercially for such a server, we use a server that hosts 16 disks and 8 CPU cores. The choice of 8 cores was driven by the available processor packaging: two physical quad-core CPUs. The larger the number of separate threads, the more stages that can be isolated from each other. In our experience, the actual speed of each of these cores was a secondary consideration, since the workloads we consider are mostly heavily I/O-bound.

Third, our problem domains require both significant capacity and I/O requirements from storage, since tens to hundreds of TB of data is to be stored and all the data is to be read and written twice. To determine the best storage option given these requirements, we survey a range of hard disk options shown in Table 3.1. We find that 7.2k-RPM SATA disks provide the most cost-effective option in terms of balancing cost per GB and cost per read/write MBps (assuming we can achieve streaming I/O). To allow 16 disks to operate at full streaming I/O throughput, we require storage controllers that are able to sustain at least 1600 MBps of streaming bandwidth. Our hardware design necessitated two 8x PCI drive controllers, each supporting 8 disks, because of the PCI bus' bandwidth limitations.

The final design choice in provisioning our cluster is the amount of memory each server should have. The primary purpose of memory in our system is to enable large amounts of data buffering so that we can read from and write to the disk in large chunks. The larger these chunks become, the more data can be read or written before seeking is required. We initially provisioned each of our machines with 12 GB of memory; however, during development we realized that 24 GB was required to provide sufficiently large writes, and so the machines were upgraded. One of the key takeaways from our work is the important role that buffering plays in enabling high utilization of the network, disk,

and CPU, and the efficient, dynamic management of that buffering is a key contribution of this work.

The cluster we used for the research described in this dissertation consists of 70 HP DL380G6 servers, each with two Intel E5520 CPUs (2.27 GHz), 24 GB of memory, and 16 500GB 7,200 RPM 2.5" SATA drives. Each hard drive is configured with a single XFS partition. Each server has two HP P410 drive controllers with 512MB on-board cache, as well as a Myricom 10 Gbps network interface. The network interconnect we used to evaluate TritonSort is a 52-port Cisco Nexus 5020 datacenter switch. During the development of Themis, we upgraded the switch to a Cisco Nexus 5596UP.

3.4 Software Architecture

TritonSort and Themis are staged, pipeline-oriented dataflow processing systems. Both systems are implemented as directed graphs of *stages*. Each stage implements part of the data processing pipeline and either sources, sinks, or transmutes data flowing through it.

Each stage is implemented by a collection of *workers*, each of which is a separate thread. Workers receive input *work units*, which are typically in-memory buffers, by dequeuing them from a collection of per-stage queues. In the process of running, a worker can produce work for a downstream stage, and optionally direct that work to a specific worker. If a worker does not specify a destination worker, work units are assigned according to a per-stage work queuing policy that defaults to round-robin. All workers in a given stage graph run in parallel.

When a work unit arrives, the worker executes a stage-specific `run()` method that implements the specific function of the stage. Workers process work in one of three ways. First, a worker can accept an individual work unit, execute the `run()` method over it, and then wait for new work. Second, it can accept a batch of work (up to a configurable size)

that has been enqueued to one of its stage's queues. Lastly, it can keep its `run()` method active, polling for the presence of new work units explicitly. TritonSort and Themis contain examples of each of these three kinds of methods.

To maximize cluster resource utilization, we need to design an appropriate software architecture. There are a range of possible software architectures in keeping with our constraint of reading and writing every input tuple at most twice. The class of architectures upon which we focus share a similar basic structure. These architectures consist of two phases separated by a distributed barrier, so that all nodes must complete phase one before phase two begins. In the first phase, input data is read in parallel from the cluster's disks and processed to produce intermediate data that is then routed to the node upon which it will ultimately reside. Each node is responsible for storing a disjoint portion of the key space. When data arrives at its destination node, that node writes the data to its local disks. In the second phase, each node sorts the data on its local disks in parallel. If running a MapReduce job, any `reduce` function processing occurs at this point. At the end of the second phase, each node has a portion of the final output data set stored on its local disks. In the case of sort, the sorted output partitions stored on all nodes can be concatenated together to form the final sorted sequence.

Chapter 4

TritonSort: I/O-Efficient Large-Scale Sorting

This chapter presents TritonSort, a highly efficient, scalable sorting system. It is designed to process large datasets, and has been evaluated against as much as 100 TB of input data spread across 832 disks in 52 nodes at a rate of 0.916 TB/min. When evaluated against the annual Indy GraySort sorting benchmark, TritonSort is 60% better in absolute performance and has over six times the per-node efficiency of the previous record holder. In this paper, we describe the hardware and software architecture necessary to operate TritonSort at this level of efficiency. Through careful management of system resources to ensure cross-resource balance, we are able to sort data at approximately 80% of the disks' aggregate sequential write speed.

4.1 Introduction

In this work we present TritonSort, a highly efficient sorting system designed to sort large volumes of data across dozens of nodes. We have applied it to data sets as large as 100 terabytes spread across 832 disks in 52 nodes. The key to TritonSort's efficiency is its *balanced* software architecture, which is able to effectively make use of a large amount of co-located storage per node, ensuring that the disks are kept as utilized

as possible. Our results show the benefit of our design: evaluating TritonSort against the ‘Indy’ GraySort benchmark[80] resulted in a system that was able to sort 100TB of input records in about 60% of the absolute time of the previous record-holder, but with four times fewer resources, resulting in an increase in per-node efficiency by over a factor of six.

It is important to note that our focus in building TritonSort is to highlight the efficiency gains that can be obtained in building systems that process significant amounts of data through balancing computation, storage, memory, and network. Systems such as Hadoop and Dryad further support data-level replication, transparent node failure, and a generalized computational model, all of which are not currently present in TritonSort. However, in presenting TritonSort’s hardware and software architecture, we describe several lessons learned in its construction that we believe are generalizable to other data processing systems. For example, our design relies on a very high disk-to-node ratio as well as an explicit, application-level management of in-memory buffers to minimize disk seeks and thus increase read and write throughput. We choose buffer sizes to balance time spent processing multiple stages of our sort pipeline, and trade off the utilization of one resource for another.

Our experiences show that for a common datacenter workload, systems can be built with commodity hardware and open-source software that improve on per-node efficiency by an order of magnitude while still achieving scalability. Building such systems will either enable significantly cheaper systems to be able to do the same work or provide the ability to address significantly larger problem sets with the same infrastructure.

4.2 Design Challenges

In this paper, we focus on designing systems that sort large datasets as an instance of the larger problem of building balanced systems. Here, we discuss the challenges involved, and outline the key insights underlying our approach.

4.2.1 Software Architecture

Our initial implementation of TritonSort was designed as a distributed, two-phase, parallel external merge-sort. This architecture, which we will call the Heaper-Merger architecture, is structured as follows. In the first phase, Readers read from the input files into buffers, which are sorted by Sorters. Each sorted buffer is then passed to a Distributor, which splits the buffer into a sorted chunk per node and sends each chunk to its corresponding node. Once received, these sorted chunks are heap-sorted by software elements called Heapers in batches and each resulting sorted batch is written to an intermediate file on disk. In the second phase, software elements called Merger merge-sort the intermediate files on a given disk into a single sorted output file.

The problem with the Heaper-Merger architecture is that it does not scale well. In order to prevent the Heaper in phase one from becoming a bottleneck, the sorted runs that the Heaper generates are usually fairly small, on the order of a few hundred megabytes. As a consequence, the number of intermediate files that the Merger must merge in phase two grows quickly as the size of the input data increases. This reduces the amount of data from each intermediate file that can be buffered at a time by the Merger and requires that the merger fetch additional data from files much more frequently, causing many additional seeks.

To demonstrate this problem, we implemented a simple Heaper-Merger sort module in microbenchmark. We chose to sort 200GB per disk in parallel across all the

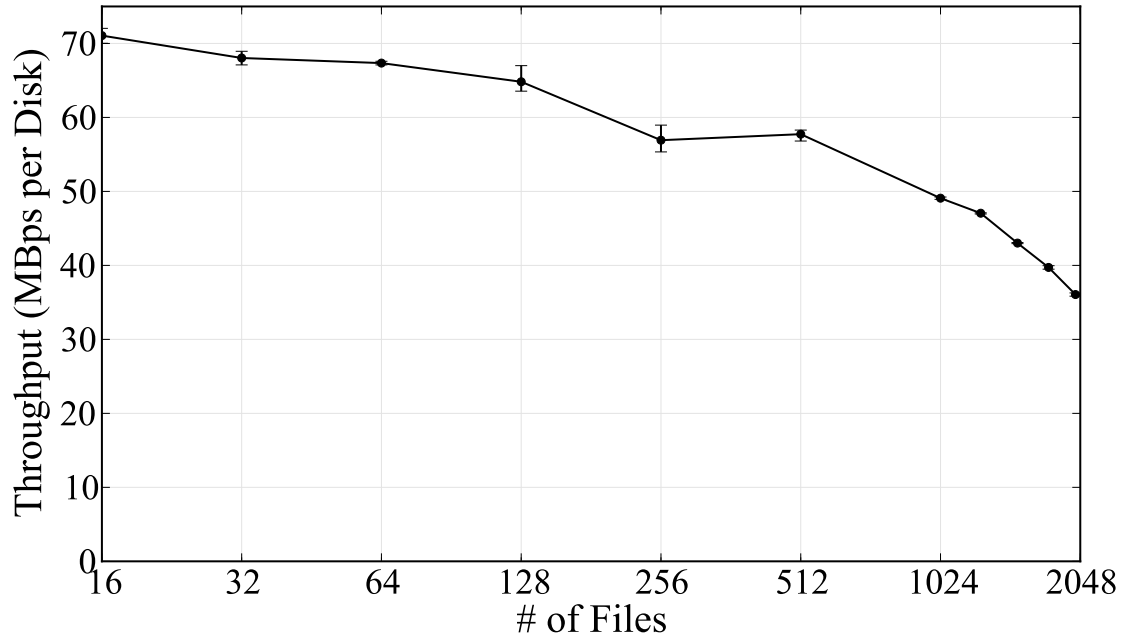


Figure 4.1. Performance of the Heaper-Merger sort implementation in microbenchmark on a 200GB per disk parallel external merge-sort as a function of the number of files merged per disk.

disks to simulate the system’s performance during a 100TB sort. Each disk’s 200GB data set is partitioned among an increasingly large number of files. Each node’s memory is divided such that each input file and each output file can be double-buffered. As shown in Figure 4.1, increasing the number of files being merged causes throughput to decrease dramatically as the number of files increases above 1000.

TritonSort uses an alternative architecture with similar software elements as above and again involving two phases, as mentioned in Chapter 2. We partition the input data into a set of logical *partitions*; with D physical disks and L logical partitions, each logical partition corresponds to a contiguous $\frac{1}{L}$ th fraction of the key space and each physical disk hosts $\frac{L}{D}$ logical partitions. In the first phase, Readers pass buffers directly to Distributors. A Distributor maps the key of every record in its input buffer to its corresponding logical partition and sends that record over the network to the machine that hosts this logical partition. Records for a given logical partition are buffered in memory and written to disk

in large chunks in order to seek as little as possible. In the second phase, each logical partition is read into an in-memory buffer, that buffer is sorted, and the sorted buffer is written to disk. This scheme bypasses the seek limits of the earlier mergesort-based approach. Also, by appropriately choosing the value of L , we can ensure that logical partitions can be read, sorted and written in parallel in the second phase. Since our testbed nodes have 24GB of RAM, to ensure this condition we set the number of logical partitions per node to 2520 so that each logical partition contains less than 1GB of records when we sort 100 TB on 52 nodes. We explain this architecture in more detail in the context of our implementation in the next section.

4.3 Design and Implementation

TritonSort is a distributed, staged, pipeline-oriented dataflow processing system. In this section, we describe TritonSort’s design and motivate our design decisions for each stage in its processing pipeline.

4.3.1 Architecture Overview

Figures 4.2 and 4.7 show the stages of a TritonSort program. See Chapter 3 for details on how TritonSort’s stages operate.

In the process of executing its *run()* method, a worker can get buffers from and return buffers to a shared pool of buffers. This buffer pool can be shared among the workers of a single stage, but is typically shared between workers in pairs of stages with the upstream stage getting buffers from the pool and the downstream stage putting them back. When getting a buffer from a pool, a stage can specify whether or not it wants to block waiting for a buffer to become available if the pool is empty.

4.3.2 Sort Architecture

We implement sort in two phases. First, we perform distribution sort to partition the input data across L logical partitions evenly distributed across all nodes in the cluster. Each logical partition is stored in its own *logical disk*. All logical disks are of identical maximum size $size_{LD}$ and consist of files on the local file system.

The value of $size_{LD}$ is chosen such that logical disks from each physical disk can be read, sorted and written in parallel in the second phase, ensuring maximum resource utilization. Therefore, if the size of the input data is $size_{input}$, there are $L = \frac{size_{input}}{size_{LD}}$ logical disks in the system. In phase two, the records in each logical disk get sorted locally and written to an output file. This implementation satisfies our design goal of reading and writing each record twice.

To determine which logical disk holds which records, we logically partition the 10-byte key space into L even divisions. We logically order the logical disks such that the k^{th} logical disk holds records in the k^{th} division. Sorting each logical disk produces a collection of output files, each of which contains sorted records in a given partition. Hence, the ordered collection of output files represents the sorted version of the data. In this paper, we assume that records' keys are distributed uniformly over the key range which ensures that each logical disk is approximately the same size; we discuss how to handle non-uniform key ranges in Chapter 5.

To ensure that we can utilize as much read/write bandwidth as possible on each disk, we partition the disks on each node into two groups of 8 disks each. One group of disks holds input and output files; we refer to these disks as the input disks in phase one and as the output disks in phase two. The other group holds intermediate files; we refer to these disks as the intermediate disks. In phase one, input files are read from the input disks and intermediate files are written to the intermediate disks. In phase two,

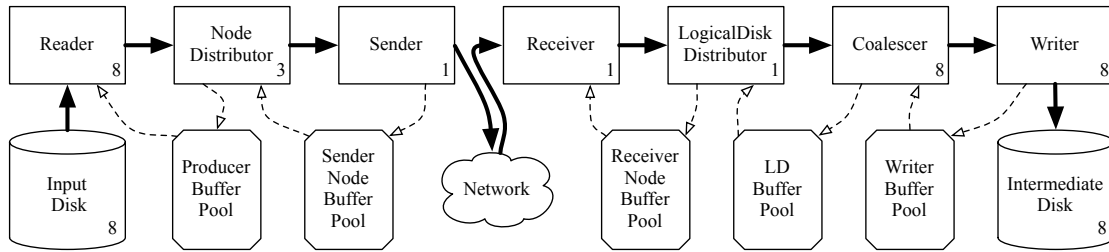


Figure 4.2. Block diagram of TritonSort’s phase one architecture. The number of workers for a stage is indicated in the lower-right corner of that stage’s block, and the number of disks of each type is indicated in the lower-right corner of that disk’s block.

intermediate files are read from the intermediate disks and output files are written to the output disks. Thus, the same disk is never concurrently read from and written to, which prevents unnecessary seeking.

4.3.3 TritonSort Architecture: Phase One

Phase one of TritonSort, diagrammed in Figure 4.2, is responsible for reading input records off of the input disks, distributing those records over to the network to the nodes on which they belong, and storing them into the logical disks in which they belong.

Reader: Each Reader is assigned an input disk and is responsible for reading input data off of that disk. It does this by filling 80 MB ProducerBuffers with input data. We chose this size because it is large enough to obtain near sequential throughput from the disk.

NodeDistributor: A NodeDistributor (shown in Figure 4.3) receives a ProducerBuffer from a Reader and is responsible for partitioning the records in that buffer across the machines in the cluster. It maintains an internal data structure called a *NodeBuffer table*, which is an array of NodeBuffers, one for each of the nodes in the cluster. A NodeBuffer contains records belonging to the same destination machine. Its size was chosen to be the size of the ProducerBuffer divided by the number of nodes, and is approximately 1.6

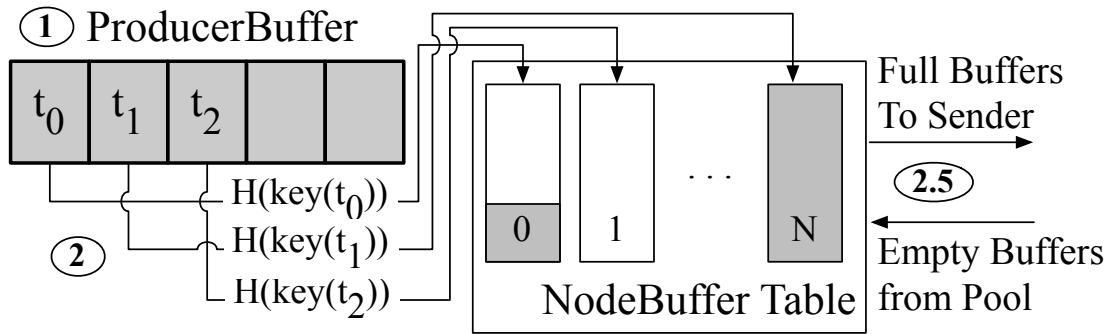


Figure 4.3. The NodeDistributor stage, responsible for partitioning records by destination node.

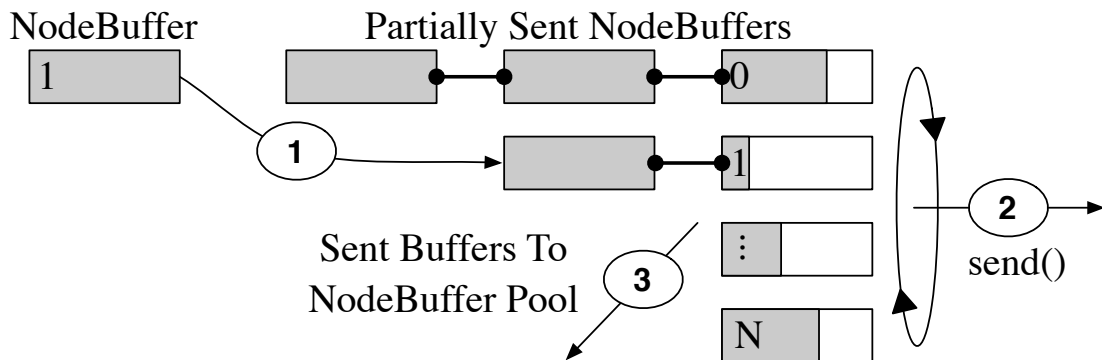


Figure 4.4. The Sender stage, responsible for sending data to other nodes.

MB in size for the scales we consider in this paper.

The NodeDistributor scans the ProducerBuffer record by record. For each record, it computes a hash function $H(k)$ over the record's key k that maps the record to a unique host in the range $[0, N - 1]$. It uses the NodeBuffer table to select a NodeBuffer corresponding to host $H(k)$ and appends the record to the end of that buffer. If that append operation causes the buffer to become full, the NodeDistributor removes the NodeBuffer from the NodeBuffer table and sends it downstream to the Sender stage. It then gets a new NodeBuffer from the NodeBuffer pool and inserts that buffer into the newly empty slot in the NodeBuffer table. Once the NodeDistributor is finished processing a ProducerBuffer, it returns that buffer back to the ProducerBuffer pool.

Sender: The Sender stage (shown in Figure 4.4) is responsible for taking NodeBuffers from the upstream NodeDistributor stage and transmitting them over the network to each of the other nodes in the cluster. Each Sender maintains a separate TCP socket per peer node in the cluster. The Sender stage can be implemented in a multi-threaded or a single-threaded manner. In the multi-threaded case, N Sender workers are instantiated in their own threads, one for each destination node. Each Sender worker simply issues a blocking *send()* call on each NodeBuffer it receives from the upstream NodeDistributor stage, sending records in the buffer to the appropriate destination node over the socket open to that node. When all the records in a buffer have been sent, the NodeBuffer is returned to its pool, and the next one is processed. For reasons described in Section 4.4.1, we choose a single-threaded Sender implementation instead. Here, the Sender interleaves the sending of data across all the destination nodes in small non-blocking chunks, so as to avoid the overhead of having to activate and deactivate individual threads for each send operation to each peer.

Unlike most other stages, which process a single unit of work during each invocation of their *run()* method, the Sender continuously processes NodeBuffers as it runs, receiving new work as it becomes available from the NodeDistributor stage. This is because the Sender must remain active to alternate between two tasks: accepting incoming NodeBuffers from upstream NodeDistributors, and sending data from accepted NodeBuffers downstream. To facilitate accepting incoming NodeBuffers, each Sender maintains a set of NodeBuffer lists, one for each destination host. Initially these lists are empty. The Sender appends each NodeBuffer it receives onto the list of NodeBuffers corresponding to the incoming NodeBuffer's destination node.

To send data across the network, the Sender loops through the elements in the set of NodeBuffer lists. If the list is non-empty, the Sender accesses the NodeBuffer at the head of the list, and sends a fixed-sized amount of data to the appropriate destination host

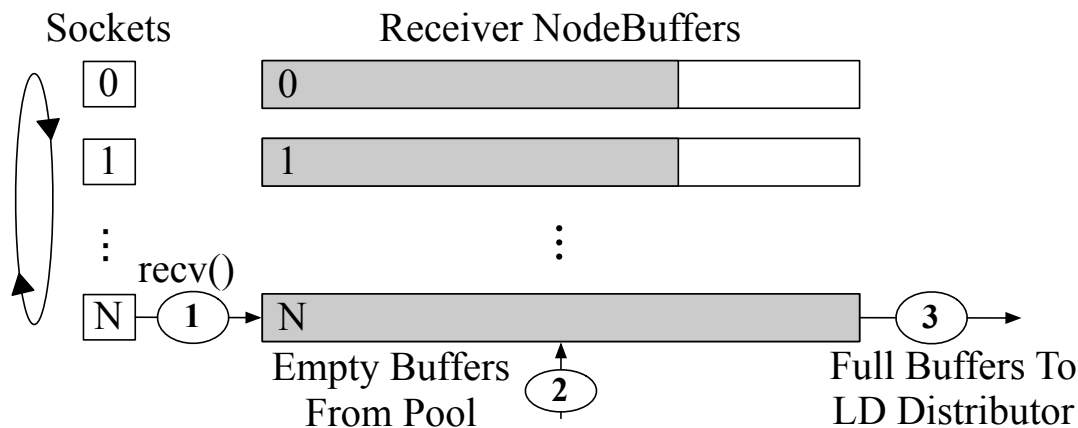


Figure 4.5. The Receiver stage, responsible for receiving data from other nodes' Sender stages.

using a non-blocking *send()* call. If the call succeeds and some amount of data was sent, then the NodeBuffer at the head of the list is updated to note the amount of its contents that have been successfully sent so far. If the *send()* call fails, because the TCP send buffer for that socket is full, that buffer is simply skipped and the Sender moves on to the next destination host. When all of the data from a particular NodeBuffer is successfully sent, the Sender returns that buffer back to its pool.

Receiver: The Receiver stage, shown in Figure 4.5, is responsible for receiving data from other nodes in the cluster, appending that data onto a set of NodeBuffers, and passing those NodeBuffers downstream to the LogicalDiskDistributor stage. In TritonSort, the Receiver stage is instantiated with a single worker. On starting up, the Receiver opens a server socket and accepts incoming connections from Sender workers on remote nodes. Its *run()* method begins by getting a set of NodeBuffers from a pool of such buffers, one for each source node. The Receiver then loops through each of the open sockets, reading up to 16KB of data at a time into the NodeBuffer for that source node using a non-blocking *recv()* call. This small socket read size is due to the rate-limiting fix that we explain in Section 4.4.1. If data is returned by that call, it is appended to the end of

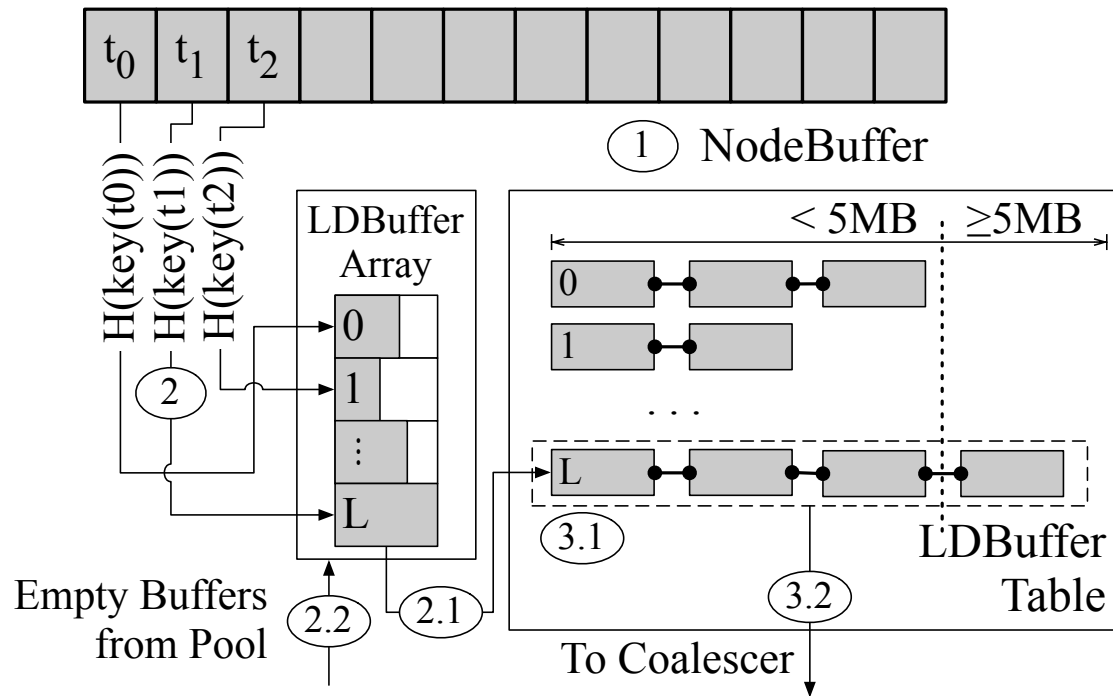


Figure 4.6. The LogicalDiskDistributor stage, which is responsible for distributing records across logical disks and buffering sufficient data to allow for large writes.

the NodeBuffer. If the append would exceed the size of the NodeBuffer, that buffer is sent downstream to the LogicalDiskDistributor stage, and a new NodeBuffer is retrieved from the pool to replace the NodeBuffer that was sent.

LogicalDiskDistributor: The LogicalDiskDistributor stage, shown in Figure 4.6, receives NodeBuffers from the Receiver that contain records destined for logical disks on its node. LogicalDiskDistributors are responsible for distributing records to appropriate logical disks and sending groups of records destined for the same logical disk to the downstream Writer stage.

The LogicalDiskDistributor's design is driven by the need to buffer enough data to issue large writes and thereby minimize disk seeks and achieve high bandwidth. Internal to the LogicalDiskDistributor are two data structures: an array of LDBuffers, one per logical disk, and an LDBufferTable. An LDBuffer is a buffer of records destined to the same

logical disk. Each LDBuffer is 12,800 bytes long, which is the least common multiple of the record size (100 bytes) and the direct I/O write size (512 bytes). The LDBufferTable is an array of LDBuffer lists, one list per logical disk. Additionally, LogicalDiskDistributor maintains a pool of LDBuffers, containing 1.25 million LDBuffers, accounting for 20 of each machine’s 24 GB of memory.

Algorithm 1. The LogicalDiskDistributor stage

```

1: NodeBuffer  $\leftarrow$  getNewWork()
2: {Drain NodeBuffer into the LDBufferArray}
3: for all records  $r$  in NodeBuffer do
4:    $dst = H(\text{key}(r))$ 
5:   LDBufferArray[dst].append( $r$ )
6:   if LDBufferArray[dst].isFull() then
7:     LDTable.insert(LDBufferArray[dst])
8:     LDBufferArray[dst] = getEmptyLDBuffer()
9:   end if
10: end for
11: {Send full LDBufferLists to the Coalescer}
12: for all physical disks  $d$  do
13:   while LDTable.sizeOfLongestList( $d$ )  $\geq$  5MB do
14:      $ld \leftarrow$  LDTable.getLongestList( $d$ )
15:     Coalescer.pushNewWork( $ld$ )
16:   end while
17: end for

```

The operation of a LogicalDiskDistributor worker is described in Algorithm 1. In Line 1, a full NodeBuffer is pushed to the LogicalDiskDistributor by the Receiver. Lines 3-10 are responsible for draining that NodeBuffer record by record into an array of LDBuffers, indexed by the logical disk to which the record belongs. Lines 12-17 examine the LDBufferTable, looking for logical disk lists that have accumulated enough data to write out to disk. We buffer at least 5 MB of data for each logical disk before flushing that data to disk to prevent many small write requests from being issued if the pipeline temporarily stalls. When the minimum threshold of 5 MB is met for any particular physical disk, the longest LDBuffer list for that disk is passed to the Coalescer stage on

Line 15.

The original design of the LogicalDiskDistributor only used the LDBuffer array described above and used much larger LDBuffers (~10MB each) rather than many small LDBuffers. The Coalescer stage (described below) did not exist; instead, the LogicalDiskDistributor transferred the larger LDBuffers directly to the Writer stage.

This design was abandoned due to its inefficient use of memory. Temporary imbalances in input distribution could cause LDBuffers for different logical disks to fill at different rates. This, in turn, could cause an LDBuffer to become full when many other LDBuffers in the array are only partially full. If an LDBuffer is not available to replace the full buffer, the system must block (either immediately or when an input record is destined for that buffer's logical disk) until an LDBuffer becomes available. One obvious solution to this problem is to allow partially full LDBuffers to be sent to the Writers at the cost of lower Writer throughput. This scheme introduced the further problem that the unused portions of the LDBuffers waiting to be written could not be used by the LogicalDiskDistributor. In an effort to reduce the amount of memory wasted in this way, we migrated to the current architecture, which allows small LDBuffers to be dynamically reallocated to different logical disks as the need arises. This comes at the cost of additional computational overhead and memory copies, but we deem this cost to be acceptable due to the small cost of memory copies relative to disk seeks.

Coalescer: The operation of the Coalescer stage is simple. A Coalescer will copy records from each LDBuffer in its input LDBuffer list into a WriterBuffer and pass that WriterBuffer to the Writer stage. It then returns the LDBuffers in the list to the LDBuffer pool.

Originally, the LogicalDiskDistributor stage did the work of the Coalescer stage. While optimizing the system, however, we realized that the non-trivial amount of time

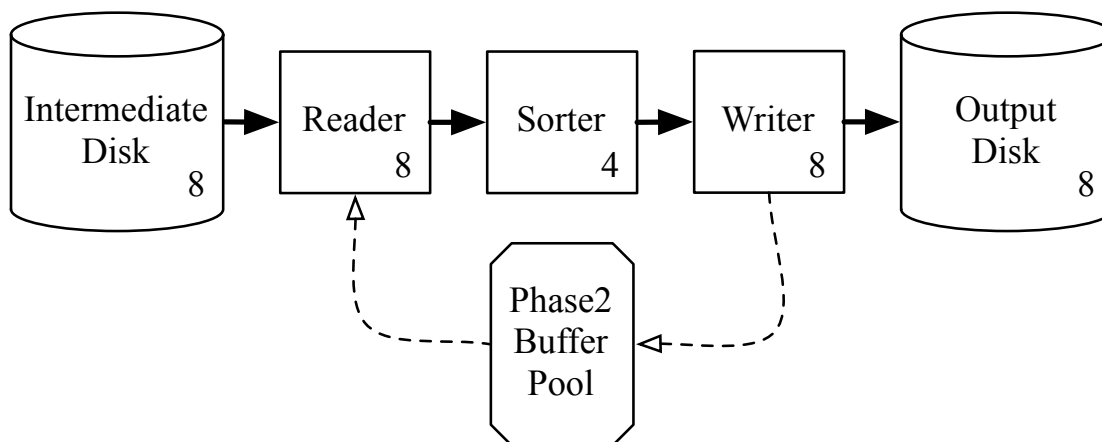


Figure 4.7. Block diagram of TritonSort’s phase two architecture. The number of workers for a stage is indicated in the lower-right corner of that stage’s block, and the number of disks of each type is indicated in the lower-right corner of that disk’s block.

spent merging LDBuffers into a single WriterBuffer could be better spent processing additional NodeBuffers.

Writer: The operation of the Writer stage is also quite simple. When a Coalescer pushes a WriterBuffer to it, the Writer worker will determine the logical disk corresponding to that WriterBuffer and write out the data using a blocking *write()* system call. When the write completes, the WriterBuffer is returned to the pool.

4.3.4 TritonSort Architecture: Phase Two

Once phase one completes, all of the records from the input dataset are stored in appropriate logical disks across the cluster’s intermediate disks. In phase two, each of these unsorted logical disks is read into memory, sorted, and written out to an output disk. The pipeline is straightforward: Reader and Writer workers issue sequential, streaming I/O requests to the appropriate disk, and Sorter workers operate entirely in memory.

Reader: The phase two Reader stage is identical to the phase one Reader stage, except that it reads into a PhaseTwoBuffer, which is the size of a logical disk.

Sorter: The Sorter stage performs an in-memory sort on a PhaseTwoBuffer. A variety of sort algorithms can be used to implement this stage, however we selected the use of radix sort due to its speed. Radix sort requires additional memory overhead compared to an in-place sort like QuickSort, and so the sizes of our logical disks have to be sized appropriately so that enough Reader–Sorter–Writer pipelines can operate in parallel. Our version of radix sort first scans the buffer, constructing a set of structures containing a pointer to each record’s key and a pointer to the record itself. These structures are then sorted by key. Once the structures have been sorted, they are used to rearrange the records in the buffer in-place. This reduces the memory overhead for each Sorter substantially at the cost of additional memory copies.

Writer: The phase two Writer writes a PhaseTwoBuffer sequentially to a file on an output disk. As in phase one, each Writer is responsible for writes to a single output disk.

Because the phase two pipeline operates at the granularity of a logical disk, we can operate several of these pipelines in parallel, limited by either the number of cores in each system (we can’t have more pipelines than cores without sacrificing performance because the Sorter is CPU-bound), the amount of memory in the system (each pipeline requires at least three times the size of a logical disk to be able to read, sort, and write in parallel), or the throughput of the disks. In our case, the limiting factor is the output disk bandwidth. To host one phase two pipeline per input disk requires storing 24 logical disks in memory at a time. To accomplish this, we set *size_{LD}* to 850 MB, using most of the 24 GB of RAM available on each node and allowing for additional memory required by the operating system. To sort 850 MB logical disks fast enough to not block the Reader and Writer stages, we find that four Sorters suffice.

Table 4.1. Median stage runtimes for a 52-node, 100TB sort, excluding the amount of time spent waiting for buffers.

Worker Type	Size Of Input (MB)	Runtime (ms)	# Workers	Throughput (in MBps)	Total Throughput (in MBps)
Reader	81.92	958.48	8	85	683
NodeDistributor	81.92	263.54	3	310	932
LogicalDiskDistributor	1.65	2.42	1	683	683
Coalescer	10.60	4.56	8	2,324	18,593
Writer	10.60	141.07	8	75	601
Phase two Reader	762.95	8,238	8	92	740
Phase two Sorter	762.95	2,802	4	272	1089
Phase two Writer	762.95	8,512	8	89	717

4.3.5 Stage and Buffer Sizing

One of the major requirements for operating TritonSort at near disk speed is ensuring cross-stage balance. Each stage has an intrinsic execution time, either based on the speed of the device to which it interfaces (e.g., disks or network links), or based on the amount of CPU time it requires to process a work unit. Table 4.1 shows the speed and performance of each stage in the pipeline. In our implementation, we are limited by the speed of the Writer stage in both phases one and two.

4.4 Optimizations

In implementing TritonSort, we learned that several non-obvious optimizations were necessary to meet our desired disk bandwidth goals. Here, we present the key takeaways from our experience.

4.4.1 Network

For TritonSort to operate at the aggregate sequential streaming bandwidth of all of its disks, the network must be able to sustain the read throughput of eight disks while data is being shuffled among nodes in the first phase. Since the 7.2k-RPM disks we use deliver at most 100 MBps of sequential read throughput (Table 3.1), the network must be

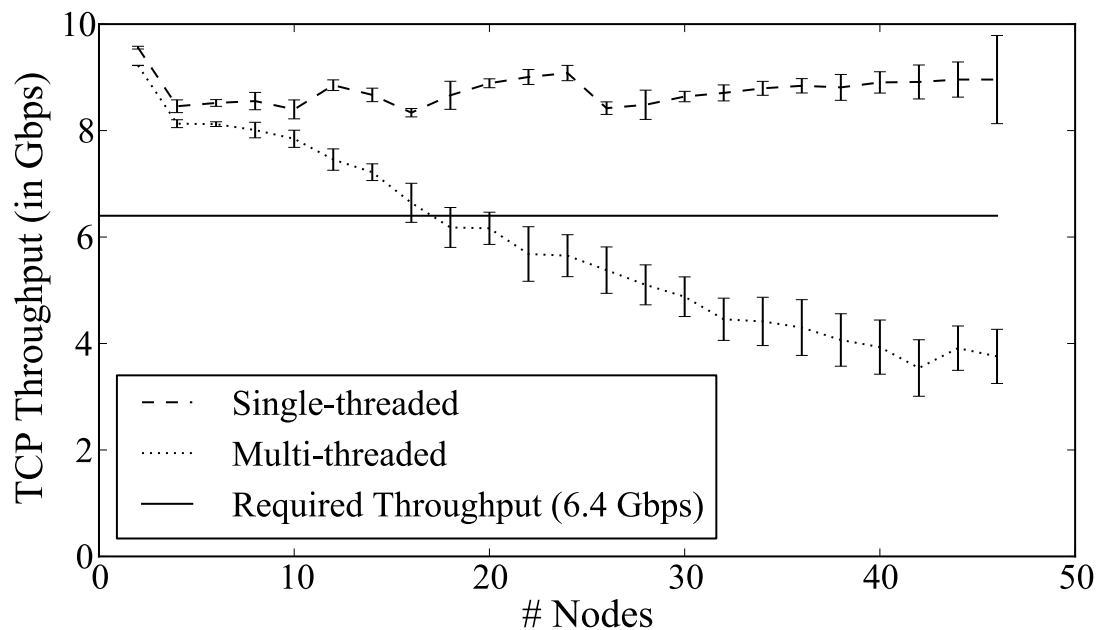


Figure 4.8. Comparing the scalability of single-threaded and multi-threaded Receiver implementations.

able to sustain 6.4 Gbps of all-pairs bandwidth, irrespective of the number of nodes in the cluster.

It is well-known that sustaining high-bandwidth flows in datacenter networks, especially all-to-all patterns, is a significant challenge. Reasons for this include commodity datacenter network hardware, in-cast, queue buildup, and buffer pressure[3]. Since we could not employ a strategy like that presented in [3] to provide fair but high bandwidth flow rates among the senders, we chose instead to artificially rate limit each flow at the Sender stage to its calculated fair share by forcing the sockets to be receive window limited. This works for TritonSort because 1) each machine sends and receives at approximately the same rate, 2) all the nodes share the same RTT since they are interconnected by a single switch, and 3) our switch does not impose an oversubscription factor. In this case, each Sender should ideally send at a rate of $(6.4/N)$ Gbps, or 123 Mbps with a cluster of 52 nodes. Given that our network offers approximately $100\mu\text{sec}$

RTTs, a receiver window size of 8 – 16 KB ensures that the flows will not impose queue buildup or buffer pressure on other flows.

Initially, we chose a straightforward multi-threaded design for the Sender and Receiver stages in which there were N Senders and N Receivers, one for each TritonSort node. In this design, each Sender issues blocking *send()* calls on a NodeBuffer until it is sent. Likewise, on the destination node, each Receiver repeatedly issues blocking *recv()* calls until a NodeBuffer has been received. Because the number of CPU hyperthreads on each of our nodes is typically much smaller than $2N$, we pinned all Senders' threads to a single hyperthread and all Receivers' threads to a single separate hyperthread.

Figure 4.8 shows that this multi-threaded approach does not scale well with the number of nodes, dropping below 4 Gbps at scale. This poor performance is due to thread scheduling overheads at the end hosts. 16 KB TCP receive buffers fill up much faster than connections that are not window-limited. At the rate of 123 MBps, a 16 KB buffer will fill up in just over 1 ms, causing the Sender to stop sending. Thus, the Receiver stage must clear out each of its buffers at that rate. Since there are 52 such buffers, a Receiver must visit and clear a receive buffer in just over 20 μ s. A Receiver worker thread cannot drain the socket, block, go to sleep, and get woken up again fast enough to service buffers at this rate.

To circumvent this problem we implemented a single-threaded, non-blocking receiver that scans through each socket in round-robin order, copying out any available data and storing it in a NodeBuffer during each pass through the array of open sockets. This implementation is able to clear each socket's receiver buffer faster than the arrival rate of incoming data. Figure 4.8 shows that this design scales well as the cluster grows.

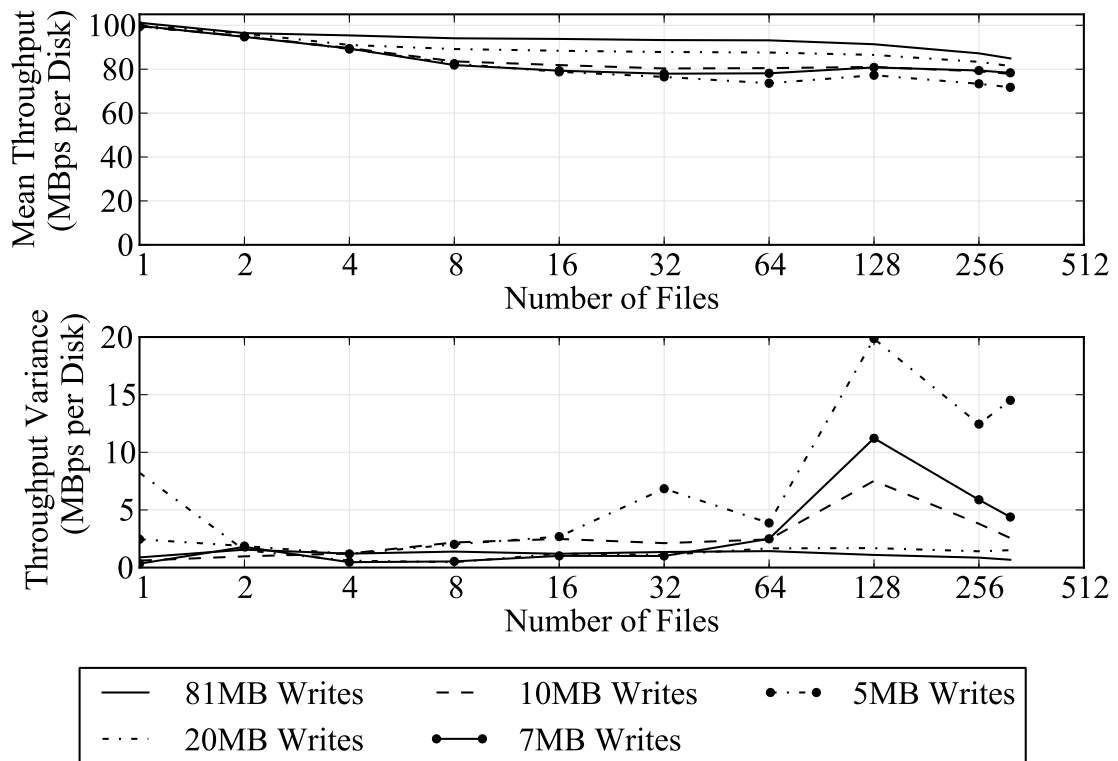


Figure 4.9. Microbenchmark indicating the ideal disk throughput as a function of write size.

4.4.2 Minimizing Disk Seeks

Key to making the TritonSort pipeline efficient is minimizing the total amount of time spent performing disk seeks, both while writing data in phase one, and while reading that data in phase two. As individual write sizes get smaller, write throughput drops, since the disk must occasionally seek between individual write operations. Figure 4.9 shows disk write throughput measured by a synthetic workload generator writing to a configurable set of files with different write sizes. Ideally, the Writer would receive WriterBuffers large enough that it can write them out at close to the sequential rate of the disk. However, the amount of available memory limits TritonSort's write sizes. Since the record space is uniformly distributed across the logical disks, the LogicalDiskDistributor will fill its LDBuffers at approximately a uniform rate. Buffering 80 MB worth of records for a given logical disk before writing to disk would cause the buffers associated with all of the other logical disks to become approximately as full. This would mandate significantly higher memory requirements than what is available in our hardware architecture. Hence, the LogicalDiskDistributor stage must emit smaller WriterBuffers, and it must interleave writes to different logical disks.

4.4.3 The Importance of File Layout

The physical layout of individual logical disk files plays a strong role in trading off performance between the phase one Writer and the phase two Reader. One strategy is to append to the logical disk files in a log-structured manner, in which a WriterBuffer for one logical disk is immediately appended after the WriterBuffer for a different logical disk. This is possible if the logical disks' blocks are allocated on demand. It has the advantage of making the phase one Writer highly performant, since it minimizes seeks and leads to near-sequential write performance. On the other hand, when a phase two Reader begins reading a particular logical disk, the underlying physical disk will need to

seek frequently to read each of the WriterBuffers making up the logical disk.

An alternative approach is to greedily allocate all of the blocks for each of the logical disks at start time, ensuring that all of a logical disk's blocks are physically contiguous on the underlying disk. This can be accomplished with the `fallocate()` system call, which provides a hint to the file system to pre-allocate blocks. In this scheme, interleaved writes of WriterBuffers for different logical disks will require seeking, since two subsequent writes to different logical disks will need to write to different regions on the disk. However, in phase two, the Reader will be able to sequentially read an entire logical disk with minimal seeking. We also use `fallocate()` on input and output files so that phase one Readers and phase two Writers seek as little as possible.

The location of output files on the output disks also has a dramatic effect on phase two's performance. If we do not delete the input files before starting phase two, the output files are allocated space on the interior cylinders of the disk. When evaluating phase two's performance on a 100 TB sort, we found that we could write to the interior cylinders of the disk at an average rate of 64 MBps. When we deleted the input files before phase two began, ensuring that the output files would be written to the exterior cylinders of the disk, this rate jumped to 84 MBps. For the evaluations in Section 4.7, we delete the input files before starting phase two. For reference, the fastest we have been able to write to the disks in microbenchmark has been approximately 90 MBps.

4.4.4 CPU Scheduling

Modern operating systems support a wide variety of static and dynamic CPU scheduling approaches, and there has been considerable research into scheduling disciplines for data processing systems. We put a significant amount of effort into isolating stages from one another by setting the processor affinities of worker threads explicitly, but we eventually discovered that using the default Linux scheduler results in a steady-state

performance that is only about 5% worse than any custom scheduling policy we devised. In our evaluation, we use our custom scheduling policy unless otherwise specified.

4.4.5 Pipeline Demand Feedback

Initially, TritonSort was entirely “push”-based, meaning that a worker only processed work when it was pushed to it from a preceding stage. While simple to design, certain stages perform sub-optimally when they are unable to send feedback back in the pipeline as to what work they are capable of doing. For example, the throughput of the Writer stage in phase one is limited by the latency of writes to the intermediate disks, which is governed by the sizes of WriterBuffers sent to it as well as the physical layout of logical disks (due to the effects of seek and rotational delay). In its naïve implementation, the LogicalDiskDistributor sends work to the Writer stage based on which of its LDBuffer lists is longest with no regard to how lightly or heavily loaded the Writers themselves are. This can result in an imbalance of work across Writers, with some Writers idle and others struggling to process a long queue of work. This imbalance can destabilize the whole pipeline and lower total throughput.

To address this problem, we must effectively communicate information about the sizes of Writers’ work queues to upstream stages. We do this by creating a pool of *write tokens*. Every write token is assigned a single “parent” Writer. We assign parent Writers in round-robin order to tokens as the tokens are created and create a number of tokens equal to the number of WriterBuffers. When the LogicalDiskDistributor has buffered enough LDBuffers so that one or more of its logical disks is above the minimum write threshold (5MB), the LogicalDiskDistributor will query the write token pool, passing it a set of Writers for which it has enough data. If a write token is available for one of the specified Writers in the set, the pool will return that token; otherwise, it will signal that no tokens are available. The LogicalDiskDistributor is required to pass a

token for the target Writer along with its LDBuffer list to the next stage, This simple mechanism prevents any Writer's work queue from growing longer than its "fair share" of the available WriterBuffers and provides reverse feedback in the pipeline without adding any new architectural features.

4.4.6 System Call Behavior

In the construction of any large system, there are always idiosyncrasies in performance that must be identified and corrected. For example, we noticed that the sizes of arguments to Linux `write()` system calls had a dramatic impact on their latency; issuing many small writes per buffer often yielded more performance than issuing a single large write. One would imagine that providing more information about the application's intended behavior to the operating system would result in better management of underlying resources and latency but in this case, the opposite seems to be true. While we are still unsure of the cause of this behavior, it illustrates that the performance characteristics of operating system services can be unpredictable and counter-intuitive.

4.5 MinuteSort: An In-Memory Sort Implementation

For the MinuteSort benchmark, we modified our architecture as follows. In the first phase, as before, we read the input data and distribute records across machines based on the logical disk to which the record maps. However, logical disks are maintained in memory instead of being written to disk immediately. In phase two (once all input records have been transferred to their appropriate logical disks), the in-memory logical disks are directly passed to workers that sort them. These sorters pass sorted logical disks to writers to be written to disk. Hence, logical disks are still written to disk, but are not written until after they have been sorted. This enabled us to make use of 16 workers in the Reader and Writer stages, since we can separate reads and writes to disk temporally

(versus separating those operations by partitioning the disks into input and intermediate disks in the case of out-of-memory sorting). The goal of MinuteSort is to sort as much data as possible in under one minute, and thus the evaluation metric is “GB sorted.”

We ran TritonSort in its MinuteSort configuration on 66 nodes with 20.5 GB of data per node, for a total of 1353 GB of data. We performed 15 consecutive trials. For these trials, TritonSort’s median elapsed time was 59.2 seconds, with a maximum time of 61.7 seconds, a minimum time of 57.7 seconds, and an average time of 59.2 seconds. All times were rounded to the nearest tenth of a second. Only 3 of the 15 consecutive trials had completion times longer than 60 seconds. Although MinuteSort and JouleSort (described in the following section) test against a different number of nodes than the other forms of sorting we evaluate, their results can be qualitatively compared, given that the scalability we have observed is nearly linear across the range of nodes against which we test.

4.6 Measuring TritonSort’s Energy Efficiency

A potential benefit of improved per-node efficiency is lower the amount of energy required to complete a given task. In this section, we describe a quantitative study of TritonSort’s memory usage performed while measuring TritonSort’s performance for the JouleSort benchmark. JouleSort measures the energy efficiency of a large-scale sort, and its evaluation metric is “records sorted per Joule.”

When measuring the energy consumed by the testbed during the run, we measure the combined energy used by the experiment nodes, the experiment head node, and the 10Gbps switch that connects the machines together. We present JouleSort measurements for both TritonSort and an early prototype of Themis, the final implementation of which is described in Chapter 5.

4.6.1 Measuring the Switch

To measure the energy used by our Cisco 5596UP datacenter switch, we plugged the switch into an Avocent PM 3000V PDU during our sorting runs. The PDU tracks maximum, minimum and “present” power draw on a per-port basis. To determine the total amount of energy used by the switch throughout the run, we multiplied the maximum power draw from the switch (in watts) as measured by the PDU by the duration of the run in seconds. This overestimates the energy used by the switch, but makes our calculations easier. The power drawn by the switch measured in this way is 566 watts.

4.6.2 Measuring the Nodes

We measured the power consumed by the cluster machines (both experimental nodes and head node) using two different power meters. The first meter is available on each machine, but does not meet the accuracy standards required by the sort benchmark’s guidelines. The second can only be attached to one machine at a time, but meets the required accuracy standards. As we will show in later sections, the two meters’ power measurements are very similar. We describe each meter and the methodology for measuring power from it below.

One danger when measuring power on many machines is that the clocks on those machines may become out of sync and cause the aggregate power measurements from multiple nodes (that should be correlated by time but aren’t) to be inaccurate. To prevent this from being a problem, we issue all power meter queries from a single machine and timestamp the power meter measurements when they are received. Further, we issue the measurements from the experiment head node so that the timestamps recorded when the sort starts and stops (see above) are taken from the same clock as the timestamps for the power measurements.

All power measurements are performed by simple Python scripts. The content

of the script varies depending on the power monitoring system being queried. In cases where multiple machines are to be monitored at once, the script spawns a thread per monitored machine and each thread runs independently. We start the power monitor scripts manually several minutes before starting the sort run to allow them to “warm up” and make sure everything is working properly, and stop them manually several minutes after the sort run ends. The scripts dump power measurements to a file as they run, and these files are analyzed after the run to determine total energy usage.

HP ILO Power Meters

The first meter we used was the power measurement subsystem of HP’s Integrated Lights-Out (ILO) management tool. Each of our DL380G6 machines comes equipped with an on-board service processor running version 1.82 of ILO2.

We query the ILO power meter using the Remote Board Insight Command Language (RIBCL). RIBCL allows operators to issue commands to ILO by sending an XML document to the ILO system over an SSL-encrypted TCP session and receive an XML response. The power monitoring script repeatedly opens an SSL connection to the ILO system, issues a power monitoring command, retrieves a response, and closes the connection.

RIBCL’s power measurement reports four numbers: maximum, minimum and average power over the past 24 hours, and “present” power, which measures the number of watts for the most recent 0.5 second sample. We use present power as our power measurement for each sample.

Unfortunately, RIBCL requires that only a single XML document “command” be sent per connection. We found in practice that we could not reliably issue RIBCL commands to the ILO system more than once every 15 seconds because the on-board service processor is quite slow and the high overhead of establishing an SSL session

must be incurred once per measurement.

WattsUp? Power Meter

To provide once-per-second measurements of our machines' power consumption, we attached a power meter that could provide once-per-second power measurements to a representative node in the cluster. The particular meter that we used was the IEC 320 universal outlet (UO) version of the WattsUp? Pro/ES/.Net power monitor. We refer to this meter as the WattsUp meter for brevity for the remainder of the text. We chose this meter because of its ready availability and known reliability; several other research projects at UCSD have used this meter to measure server power successfully.

The WattsUp meter has a simple serial-over-USB interface. The client opens a TCP connection to the meter and sends the meter a request for data and a data collection interval. The meter responds by sending the requested data once per interval until it's told to stop or the client closes the TCP connection. Our power measurement script sends the meter a request for power information at an interval of one second. The script then receives and parses the response (by issuing a blocking read call to the socket, which consistently unblocks with a new response once per second) and appends the parsed response to a file.

During the first four runs of each benchmark type, we used the WattsUp meter to measure the power on a random experiment node. On the fifth run, we used it to measure the experimental head node. Since the head node is not doing anything particularly intensive (monitoring power on each machine and recording experiment time), we found that its power consumption was relatively low. Through measurements on both types of power meters, we found that the average draw for the head node was 134 watts with a deviation of about 2 watts. Because of this, we assume that the experiment head node's power draw is a constant 134 watts for the duration of the sort run.

Resolving Discrepancies Between Meters

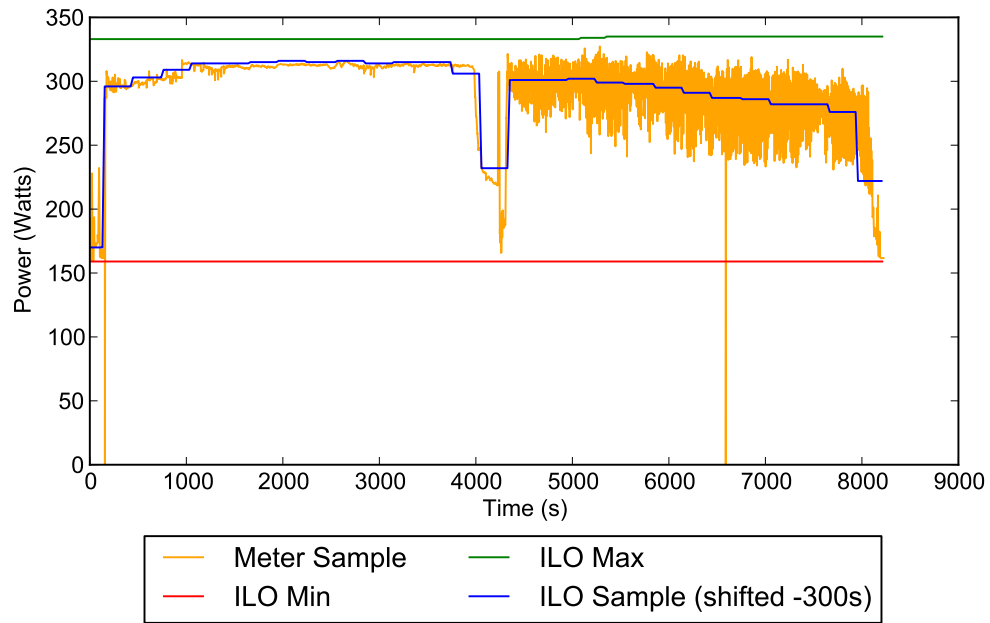
We found that the power measured by the ILO system lags that measured by the WattsUp meter by exactly five minutes. Figure 4.10 shows both the maximum, minimum and “present” power reported by the ILO and the power reported by the WattsUp meter during a JouleSort run, with the ILO measurements appropriately time-shifted. When calculating power with the ILO meters, we time-shifted all samples by 5 minutes to compensate for this observation and allowed the power collection scripts to run for several minutes after the sort run finished to collect sufficient additional samples to cover the entirety of the sort run.

In these runs you can see that there is a sharp reduction in power usage about halfway through the sort run. This is a result of the barrier between phases one and two. Due to the natural variation in node performance, some nodes finish phase one earlier than others, and so their power usage is reduced. However, none of the nodes can start phase two until all nodes are done with phase one, which results in the gap visible in Figure 4.10.

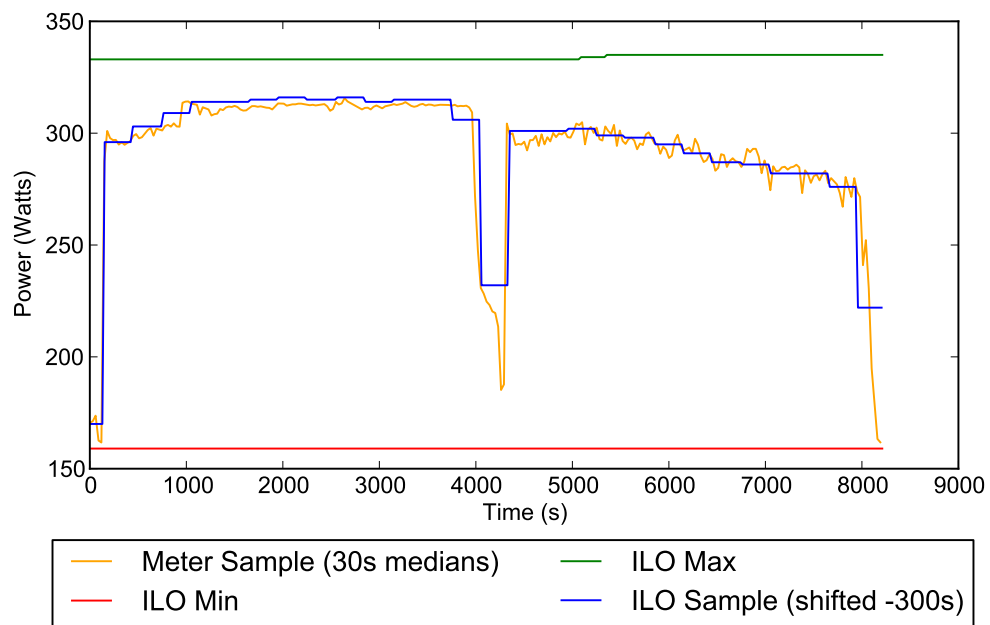
The WattsUp meter’s data is more variable during phase two; we suspect that this is due to the fact that the CPU is far more active during phase two than it is during the other phases. However, if we look at the median power reported by the WattsUp meter during each 30 second interval throughout the run, we notice that the WattsUp meter’s measurements track the ILO’s measurements quite closely.

4.6.3 Calculating Energy

To estimate energy used by the experiment head node and the switch, we multiply their estimated instantaneous power draws (134 watts and 566 watts, respectively) by the duration of the sort run in seconds. Call the energy used by the head node and the switch E_{head} and E_{switch} respectively.



(a) Raw WattsUp meter data



(b) Median of each 30 seconds of WattsUp data

Figure 4.10. Power consumed by a representative node during a JouleSort run, comparing the results of the two power meters used.

Table 4.2. Average power consumed by a node throughout a sort benchmark run for the first four trials of our JouleSort experiments.

System	Trial	Avg. Server Power
TritonSort	1	287 Watts
TritonSort	2	285 Watts
TritonSort	3	309 Watts
TritonSort	4	297 Watts
Themis Prototype	1	290 Watts
Themis Prototype	2	285 Watts
Themis Prototype	3	293 Watts
Themis Prototype	4	306 Watts

All power measurements reported by our meters are reported in watts. To obtain an energy measurement from this collection of instantaneous power measurements, we start by filtering the set of measurements so that we only consider those measurements that were taken on or after the sort run’s start timestamp and on or before the sort run’s end timestamp. The subsequent power calculation varies depending on the meter being used. We refer to the energy used by the experiment nodes as E_{nodes} .

When calculating power based on measurements gathered from the ILO meters, we start by sorting measurements in ascending order by timestamp. We then compute the total energy for a node in the following way. For each measurement (W_i, T_i) , we consider the previous measurement (W_{i-1}, T_{i-1}) and add $W_i * (T_i - T_{i-1})$ to the total energy. In cases where the measurement abuts the start or end of the run, we use the start and end timestamps of the sort run as T_i and T_{i-1} as appropriate to “fill in the gaps” at the beginning and end of the run. We compute the total energy for each node in this way and sum the energy from each node to compute E_{nodes} .

When using the WattsUp meter, we have once-per-second measurements and can produce power estimates in line with the sort benchmark guidelines. To do this, we compute that average (mean) power for the representative node. For the first four trials (where an experimental node is being measured), this data is derived by taking the

Table 4.3. Total energy measured for each 100TB trial by both WattsUp and ILO meters.

Benchmark	Trial	Energy (Joules)		Records per Joule	
		WattsUp	ILO	WattsUp	ILO
TritonSort	1	103,180,896	108,054,648	9,692	9,255
TritonSort	2	99,312,480	105,333,939	10,069	9,494
TritonSort	3	109,495,040	105,425,639	9,133	9,485
TritonSort	4	102,724,272	105,523,992	9,735	9,477
TritonSort	5	101,108,112	103,656,684	9,890	9,647
Themis Prototype	1	129,774,720	136,098,976	7,706	7,348
Themis Prototype	2	127,434,720	135,998,793	7,847	7,353
Themis Prototype	3	132,077,568	136,851,456	7,571	7,307
Themis Prototype	4	137,082,224	136,259,721	7,295	7,339
Themis Prototype	5	132,380,352	135,332,800	7,554	7,389

average of all measurements taken from the WattsUp meter during the sort run. For the fifth trial (where the head node is being measured), the average power is assumed to be the average of the previous four trials.

We believe that this assumption is reasonable because the average power consumed by a node does not vary much; we provide the average power drawn by a node in the first four trials in Table 4.2. The standard deviation for the first four measurements is 11 watts for TritonSort and 9 watts for the early Themis prototype, 3.7% and 3.0% of the mean, respectively.

Once we have computed the average power for a representative node, we multiply that average power by the length of the run in seconds to yield the total energy consumption for a node, and multiply that number by the number of nodes (52 in our experiments) to yield E_{nodes} .

Once we have computed E_{nodes} , E_{head} and E_{switch} , we compute total energy E_{tot} as $E_{nodes} + E_{head} + E_{switch}$.

Table 4.4. Statistics for the energy measurements presented in Table 4.3.

Benchmark	Meter	Energy (Joules)			
		Median	Mean (Average)	Std. Dev.	Std. Err
TritonSort	ILO	105,425,639	105,598,980	3,170,018	1,417,675
TritonSort	WattsUp	102,724,272	103,164,160	736,610	329,422
Themis Prototype	ILO	136,098,976	136,108,349	4,086,316	1,827,456
Themis Prototype	WattsUp	132,077,568	131,749,917	941,356	420,987

4.6.4 Measurement Results

We ran five trials each of a 100TB sort in both TritonSort and the Themis prototype. The raw energy measurements for these trials are given in Table 4.3 and statistics concerning the total energy measurements are given in Table 4.4. TritonSort sorted an average of 9,704 records per Joule. The Themis Prototype sorted an average of 7,595 records per Joule.

Deriving Standard Deviation and Standard Error

When calculating standard deviation and standard error in Table 4.4, we assume that the WattsUp meters are accurate to $\pm 2\%$ and the ILO meters are accurate to $\pm 10\%$. We were unable to obtain any data about the accuracy of Avocent’s PDUs, and so we assume somewhat pessimistically that the PDUs are accurate to $\pm 5\%$.

We obtained standard deviation in the following way. First, we derived the mean power drawn by each server, the head node, and the switch. When using the WattsUp meter’s measurements, we simply used the mean of all power measurements logged by the meter. When using the ILO meter’s measurements, we derived the mean power draw for a node by dividing the total amount of energy consumed by the node by the trial’s runtime. Call the mean power produced by server X P_{N_x} , the mean power produced by the head node P_H and the mean power produced by the switch P_S .

We then multiplied each mean power value by its respective meter’s accuracy

to yield the uncertainty $U(P_{N_x})$, $U(P_H)$ and $U(P_S)$ of each power measurement. We then multiplied these uncertainties by the trial runtime to yield the uncertainty $U(E_{N_x})$, $U(E_H)$ and $U(E_S)$ of each energy measurement. Once these values were derived, we used error propagation to yield the total energy measurement uncertainty for the trial using the following formula:

$$U(E_{trial}) = \sqrt{\left(\sum_{X=0}^{51} U(E_{N_x})^2\right) + U(E_H)^2 + U(E_S)^2}$$

Once $U(E_{trial})$ was calculated for each trial, we performed a further round of error propagation across trials to yield total uncertainty, i.e. standard deviation.

$$U(E_{total}) = \sqrt{\sum_{T=1}^5 U(E_{trialT})^2}$$

Standard error is derived by dividing standard deviation by $\sqrt{5}$.

4.7 Evaluation

We now evaluate TritonSort’s performance and scalability under various hardware configurations.

4.7.1 Evaluation Environment

We evaluated TritonSort on 52 nodes of the cluster described in Section 3.3. Each XFS partition is configured with a single allocation group to prevent file fragmentation across allocation groups, and is mounted with the `noatime`, `attr2`, `nobarrier`, and `noquota` flags set. For this evaluation, the servers were running Linux 2.6.35.1. Our implementation of TritonSort is written in C++.

4.7.2 Comparison to Alternatives

The 100TB Indy GraySort benchmark was introduced in 2009, and hence there are few systems against which we can compare TritonSort’s performance. The most recent holder of the Indy GraySort benchmark, DEMSort [67], sorted slightly over 100TB of data on 195 nodes at a rate of 564 GB per minute. TritonSort currently sorts 100TB of data on 52 nodes at a rate of 916 GB per minute, a factor of six improvement in per-node efficiency.

4.7.3 Examining Changes in Balance

We next examine the effect of changing the cluster’s configuration to support more memory or faster disks. Due to budgetary constraints, we could not evaluate these hardware configurations at scale. Evaluating the performance benefits of SSDs is the subject of future work.

In the first experiment, we replaced the 500GB, 7200RPM disks that are used as the intermediate disks in phase one and the input disks in phase two with 146GB, 15000RPM disks. The reduced capacity of the drives necessitated running an experiment with a smaller input data set. To allow space for the logical disks to be pre-allocated on the intermediate disks without overrunning the disks’ capacity, we decreased the number of logical disks per physical disk by a factor of two. This doubles the amount of data in each logical disk, but the experiment’s input data set is small enough that the amount of data per logical disk does not overflow the logical disk’s maximum size.

Phase one throughput in these experiments is slightly lower than in subsequent experiments because the 30-35 seconds it takes to write the last few bytes of each logical disk at the end of the phase is roughly 10% of the total runtime due to the relatively small dataset size.

The results of this experiment are shown in Table 4.5. We first examine the effect

Table 4.5. Effect of increasing speed of intermediate disks on a two node, 500GB sort.

Intermediate Disk Speed (RPM)	Logical Disks Per Physical Disk	Phase 1 Throughput (MBps)	Phase 1 Bottleneck Stage	Average Write Size (MB)
7200	315	69.81	Writer	12.6
7200	158	77.89	Writer	14.0
15000	158	79.73	LogicalDiskDistributor	5.02

Table 4.6. Effect of increasing the amount of memory per node on a two node, 2TB sort.

RAM Per Node (GB)	Phase 1 Throughput (MBps)	Average Write Size (MB)
24	73.53	12.43
48	76.45	19.21

of decreasing the number of logical disks without increasing disk speed. Decreasing the number of logical disks increases the average length of LDBuffer chains formed by the LogicalDiskDistributor; note that most of the time, full WriterBuffers (14MB) are written to the disks. In addition, halving the number of logical disks decreases the number of external cylinders that the logical disks occupy, decreasing maximal seek latency. These two factors combine together to net a significant (11%) increase in phase one throughput.

The performance gained by writing to 15000 RPM disks in phase one is much less pronounced. The main reason for this is that the increase in write speed causes the Writers to become fast enough that the LogicalDiskDistributor exposes itself as the bottleneck stage. One side-effect of this is that the LogicalDiskDistributor cannot populate WriterBuffers as fast as they become available, so it reverts to a pathological case in which it always is able to successfully retrieve a write token and hence continuously writes minimally-filled (5MB) buffers. Creating a LogicalDiskDistributor stage that dynamically adjusts its write size based on write token retrieval success rate is the subject of future work.

In the next experiment, we doubled the RAM in two of the machines in our cluster and adjusted TritonSort's memory allocation by doubling the size of each WriterBuffer (from 14MB to 28MB) and using the remaining memory (22GB) to create additional

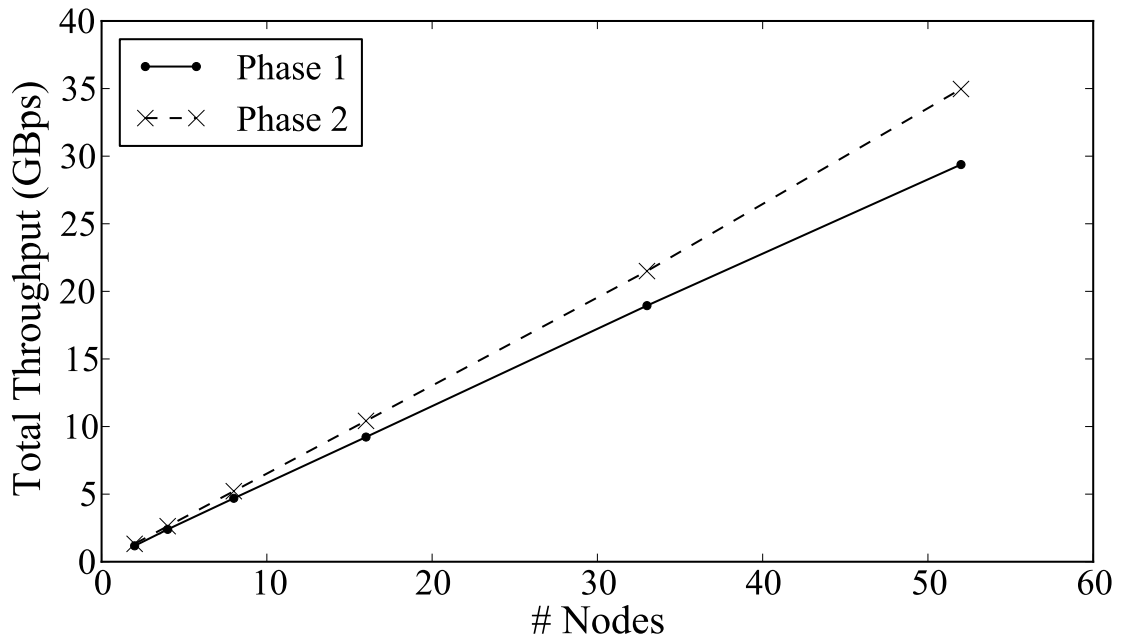


Figure 4.11. Throughput when sorting 1 TB per node as the number of nodes increases.

LDBuffers. As shown in Table 4.6, increasing the amount of memory allows for the creation of longer chains of LDBuffers in the LogicalDiskDistributor, which in turn causes write sizes to increase. The increase in write size is not linear in the amount of RAM added; this is likely because we are approaching the point past which larger writes will not dramatically improve write throughput.

4.7.4 TritonSort Scalability

Figure 4.11 shows TritonSort’s total throughput when sorting 1 TB per node as the number of nodes increases from 2 to 48. Phase two exhibits practically linear scaling, which is expected since each node performs phase two in isolation. Phase one’s scalability is also nearly linear; the slight degradation in its performance at large scales is likely due to network variance that becomes more pronounced as the number of nodes increases.

4.8 Conclusions

In this work, we describe the hardware and software architecture necessary to build TritonSort, a highly efficient, pipelined, stage-driven sorting system designed to sort tens to hundreds of TB of data. Through careful management of system resources to ensure cross-resource balance, we are able to sort tens of GB of data per node per minute, resulting in 916 GB/min across only 52 nodes. We believe the work holds a number of lessons for balanced system design and for scale-out architectures in general and will help inform the construction of more balanced data processing systems that will bridge the gap between scalability and per-node efficiency.

4.9 Acknowledgments

This project was supported by NSF's Center for Integrated Access Networks and NSF MRI #CNS-0923523. We'd like to thank Cisco Systems for their support of this work. We'd like to acknowledge Stefan Savage for providing valuable feedback concerning network optimizations, and thank our shepherd Andrew Birrell and the anonymous reviewers for their feedback and suggestions.

Chapter 4 contains material as it appears in the Proceedings of the USENIX Symposium on Networked Systems Design and Implementation (NSDI) 2011. Rasmussen, Alexander; Porter, George; Conley, Michael; Madhyastha, Harsha; Niranjan Mysore, Radhika; Pucher, Alexander; Vahdat, Amin. The dissertation author was the primary investigator and author of this paper.

Chapter 5

Themis: I/O-Efficient MapReduce

This chapter presents Themis, an I/O-efficient MapReduce system derived from TritonSort. Themis is named after the Titan in Greek mythology who is tasked with creating balance, order and harmony.

Many MapReduce jobs are I/O-bound, and so minimizing the number of I/O operations is critical to improving their performance. Themis reads and writes data records to disk exactly twice, which is the minimum amount possible for data sets that cannot fit in memory.

In order to minimize I/O, Themis makes fundamentally different design decisions from previous MapReduce implementations. Themis performs a wide variety of MapReduce jobs – including click log analysis, short-read sequence alignment, and PageRank – at nearly the speed of TritonSort’s record-setting sort performance.

5.1 Introduction

Our experience building TritonSort shows that an appropriately balanced implementation can realize orders of magnitude improvement in throughput and efficiency. Translating these types of gains to more general-purpose data processing systems will help close the efficiency gap present in modern large-scale data processing systems, allowing more work to be performed with the same hardware, or the same amount of work

to be performed with less hardware. This improved efficiency will result in substantially lowered system cost, energy usage, and management complexity.

Given that many MapReduce jobs are I/O-bound, an efficient MapReduce system must aim to minimize the number of I/O operations it performs. Fundamentally, every MapReduce system must perform at least two I/O operations per record when the amount of data exceeds the amount of memory in the cluster [1]. We refer to a system that meets this lower-bound as having the “2-IO” property. Any data processing system that does not have this property is doing more I/O than it needs to. Existing MapReduce systems incur additional I/O operations in exchange for simpler and more fine-grained fault tolerance.

Themis is an implementation of MapReduce designed to have the 2-IO property. Themis accommodates the flexibility of the MapReduce programming model while simultaneously delivering high efficiency. It does this by considering fundamentally different points in the design space than existing MapReduce implementations:

1. Eliminating task-level fault tolerance: At the scale of tens of thousands of servers, failures are common, and so MapReduce was designed with a strong task-level fault tolerance model. However, more aggressive fault tolerance gains finer-grained restart at the expense of lower overall performance. Interestingly, many Hadoop users report cluster sizes of under 100 nodes [36], much smaller than those deployed by MapReduce’s early adopters. In 2011, Cloudera’s VP of Technology Solutions stated that the mean size of their clients’ Hadoop clusters is 200 nodes, with the median size closer to 30 [55]. At this moderate scale, failures are much less common, and aggressive fault tolerance is wasteful in the common case. Foregoing task-level fault tolerance permits a design that achieves the 2-IO property. When a job experiences a failure, Themis simply re-executes it. This optimistic approach to fault tolerance enables Themis to aggressively pipeline record processing without unnecessarily materializing intermediate results to disk. As we

will show in Chapter 6, for moderate cluster sizes this approach has the counter-intuitive effect of improving performance despite the occasional job re-execution.

2. Dynamic, adaptive memory allocation: To maintain the 2-IO property, Themis must process a record completely once it is read from disk. This prevents Themis from putting records back on disk in response to memory pressure through swapping or writing spill files. Themis implements a policy-based, application-level memory manager that provides fine-grained sharing of memory between operators processing semi-structured, variably-sized records. This allows it to support datasets with as much as a factor of 10^7 skew between record sizes while maintaining the 2-IO property.

3. Central management of shuffle and disk I/O: Themis uses a centralized, per-node disk scheduler that ensures that records from multiple sources are written to disk in large batches to reduce disk seeks. Themis delivers nearly sequential disk I/O across a variety of MapReduce jobs, even for workloads that far exceed the size of main memory.

To validate our design, we have written a number of MapReduce programs on Themis, including a web user session tracking application, PageRank, n-gram counting, and a DNA read sequence alignment application. We found that Themis processes these jobs at nearly the per-node performance of TritonSort's record-setting sort run and nearly the maximum sequential speed of the underlying disks.

5.2 The Challenge of Skew

One of MapReduce's attractive properties is its ability to handle semi-structured and variably-sized data. This variability makes maintaining the 2-IO property a challenge. In this section, we describe two sources of variability and the resulting requirements they place on our design.

An input dataset can exhibit several different kinds of *skew*, which simply refers to variability in its structure and content. These include:

Record Size Skew: In systems with semi-structured or unstructured data, some records may be much larger than others. This is called *record size skew*. In extreme cases, a single record may be gigabytes in size.

Partitioning Skew: Data that is not uniformly distributed across its keyspace exhibits *partitioning skew*. This can cause some nodes to process much more data than others if the data is naïvely partitioned across nodes, creating stragglers [24]. Handling skew in MapReduce is complicated by the fact that the distribution of keys in the data produced by a map function is often not known in advance. Existing MapReduce implementations handle partitioning skew by spilling records to disk that cannot fit into memory.

Computational Skew: In a dataset exhibiting *computational skew*, some records take much longer than average to process. Much of the work on mitigating computational skew in MapReduce involves exploiting the nature of the particular problem and relying on a degree of user guidance [46] or proactively re-partitioning the input data for a task [47]. As the focus of our work is I/O-bound jobs, we do not consider computational skew in this work.

Performance Heterogeneity: The performance of a population of identical machines can vary significantly; the reasons for this heterogeneity are explored in [73]. In addition, clusters are rarely made up of a homogeneous collection of machines, due both to machine failures and planned incremental upgrades. While we believe that the techniques presented in this work can be applied to heterogeneous clusters, we have not evaluated Themis in such a setting.

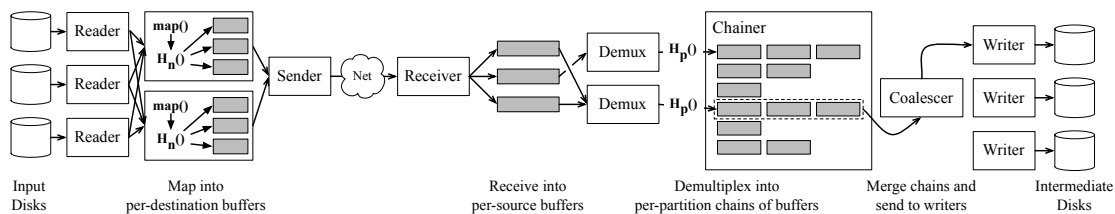


Figure 5.1. Stages of Phase One (Map/Shuffle) in Themis.

To handle record skew, Themis dynamically controls its memory usage, which we describe in Section 5.4. Themis adopts a sampling-based skew mitigation technique to minimize the effects of partitioning skew. We discuss this mitigation technique in Section 5.5.

5.3 System Architecture

In this section, we describe the design of Themis.

5.3.1 Core Architecture

Themis reuses several core runtime components that were used to build TritonSort. Like TritonSort, Themis is written as a sequence of *phases*, each of which consists of a directed dataflow graph of *stages* connected by FIFO queues. Each stage consists of a number of *workers*, each running as a separate thread.

5.3.2 MapReduce Overview

Unlike existing MapReduce systems, which executes map and reduce tasks concurrently in waves, Themis implements the MapReduce programming model in three phases of operation, summarized in Table 5.1. Phase zero, described in Section 5.5, is responsible for sampling input data to determine the distribution of record sizes as well as the distribution of keys. These distributions are used by subsequent phases to minimize partitioning skew. Phase one, described in Section 5.3.3, is responsible for applying the

Table 5.1. Themis’s three phase architecture.

Phase	Description	Required?
0	Skew Mitigation	Optional
1	map() and shuffle	Required
2	sort and reduce()	Required

map function to each input record, and routing its output to an appropriate partition in the cluster. This is the equivalent of existing systems’ map and shuffle phases. Phase two, described in Section 5.3.4, is responsible for sorting and applying the reduce function to each of the intermediate partitions produced in phase one. At the end of phase two, the MapReduce job is complete.

Phase one reads each input record and writes each intermediate record exactly once. Phase two reads each intermediate partition and writes its corresponding output partition exactly once. Thus, Themis has the 2-IO property.

5.3.3 Phase One: Map and Shuffle

Phase one is responsible for implementing both the map operation as well as shuffling records to their appropriate intermediate partition. Each node in parallel implements the stage graph pipeline shown in Figure 5.1.

The **Reader** stage reads records from an input disk and sends them to the **Mapper** stage, which applies the map function to each record. As the map function produces intermediate records, each record’s key is hashed to determine the node to which it should be sent and placed in a per-destination buffer that is given to the Sender when it is full. The **Sender** sends data to remote nodes using a round-robin loop of short, non-blocking send() calls. We call the Reader to Sender part of the pipeline the “producer-side” pipeline.

The **Receiver** stage receives records from remote nodes over TCP using a round-robin loop of short, non-blocking recv() calls. We implemented a version of this stage

that uses `select()` to avoid unnecessary polling, but found that its performance was too unpredictable to reliably receive all-to-all traffic at 10Gbps. The Receiver places incoming records into a set of small per-source buffers, and sends those buffers to the Demux stage when they become full.

The **Demux** stage is responsible for assigning records to partitions. It hashes each record’s key to determine the partition to which it should be written, and appends the record to a small per-partition buffer. When that buffer becomes full, it is emitted to the **Chainer** stage, which links buffers for each partition into separate *chains*. When chains exceed a pre-configured length, which we set to 4.5 MB to avoid doing small writes, it emits them to the **Coalescer** stage. The **Coalescer** stage merges chains together into a single large buffer that it sends to the **Writer** stage, which appends buffers to the appropriate partition file. The combination of the Chainer and Coalescer stages allows buffer memory in front of the Writer stage to be allocated to partitions in a highly dynamic and fine-grained way. We call the Receiver to Writer part of the pipeline the “consumer-side” pipeline.

A key requirement of the consumer-side pipeline is to perform large, contiguous writes to disk to minimize seeks and provide high disk bandwidth. Themis uses the same node-wide, application-driven disk scheduler used in TritonSort to ensure that writes are large. We refer the reader to Section 4.4.5 for details on the disk scheduler’s implementation.

5.3.4 Phase Two: Sort and Reduce

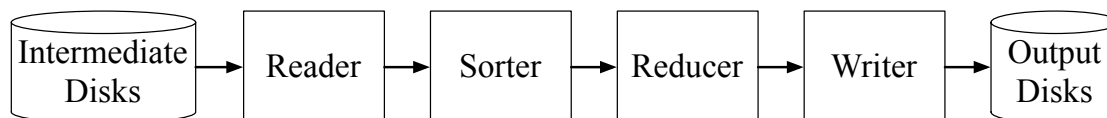


Figure 5.2. Stages of Phase Two (Sort/Reduce) in Themis.

By the end of phase one, the map function has been applied to each input record, and the records have been grouped into partitions and stored on the appropriate node so that all records with the same key are stored in a single partition. In phase two, each partition must be sorted by key, and the reduce function must be applied to groups of records with the same key. The stages that implement phase two are shown in Figure 5.2.

There is no network communication in phase two, so nodes process their partitions independently. Entire partitions are read into memory at once by the **Reader** stage. A **Sorter** stage sorts these partitions by key, keeping the result in memory. The **Reducer** stage applies the reduce function to all records sharing a key. Reduced records are sent to the **Writer**, which writes them to disk.

All records with a single key must be stored in the same partition for the reduce function to produce correct output. As a result, partitioning skew can cause some partitions to be significantly larger than others. Themis's memory management system allows phase two to process partitions that approach the size of main memory, and its optional skew mitigation phase can reduce partitioning skew without user intervention. We describe these systems in Sections 5.4 and 5.5, respectively.

A key feature of Themis's Sorter stage is that it can select which sort algorithm is used to sort a buffer on a buffer-by-buffer basis. There is a pluggable *sort strategy* interface that lets developers use different sorting algorithms; currently quicksort and radix sort are implemented. Each sort strategy calculates the amount of scratch space it needs to sort the given buffer, depending on the buffer's contents and the sort algorithm's space complexity. For both quicksort and radix sort, this computation is deterministic. In Themis, radix sort is chosen if the keys are all the same size and the required scratch space is under a configurable threshold; otherwise, quicksort is used.

Table 5.2. A comparison of Themis’s memory allocator implementations.

	TritonSort	Themis	Used in Phase			Subject to deadlock?
			0	1	2	
Pool	✓	✓	✓	✓		
Quota		✓	✓	✓		
Constraint		✓			✓	✓

Table 5.3. A summary of the Themis memory allocator API.

Function	Description
CallerID registerCaller(Worker worker)	Register worker with the allocator
void* allocate(CallerID caller, uint64_t size)	allocate a memory region of size bytes for caller
void deallocate(void* memory)	deallocate memory that was allocated by this allocator

5.4 Memory Management and Flow Control

Themis relies on a dynamic and flexible memory management system to partition memory between operators. Themis’s memory manager actually serves two distinct purposes: (1) it enables resource sharing between operators, and (2) it supports enforcing back-pressure and flow control. In the first case, Themis requires flexible use of memory given our desire to support large amounts of record size skew while maintaining the 2-IO property. In the second case, individual stages in the Themis pipeline naturally run at different speeds (e.g., the network is 10 Gbps, whereas the disk subsystem only supports writing at approximately 5.5 Gbps), and so back-pressure and flow control are needed to prevent faster stages from starving slower stages for resources.

Themis supports a single memory allocation interface with pluggable memory policies. We first describe the memory allocator’s interface, and then describe the three policies that we have implemented.

5.4.1 Memory Allocation Interface

Worker stages in Themis allocate space for buffers and other necessary scratch space using a unified and simple memory allocator interface, shown in Table 5.3.

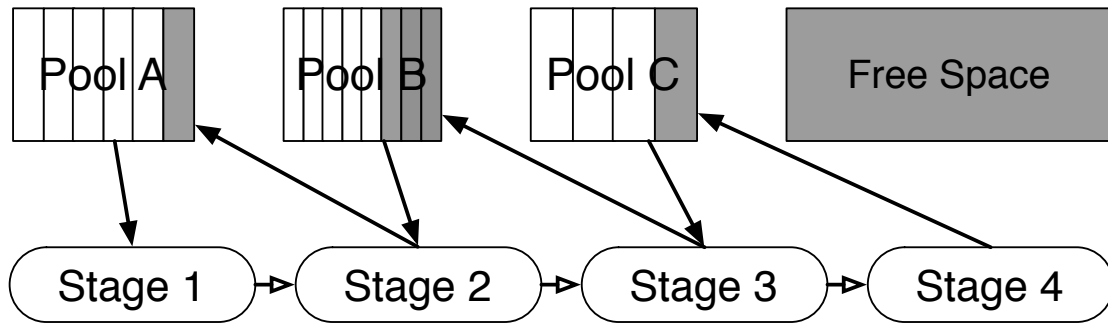


Figure 5.3. A diagrammatic overview of pool-based memory management. Note that memory in each pool is divided into fixed-size regions, and that any memory not allocated to pools cannot be utilized by stages.

Memory allocators can be assigned on a stage-by-stage basis, but in the current implementation we assume that memory regions are allocated and deallocated by the same allocator. The `allocate` call blocks until the underlying memory allocation policy satisfies the allocation, which can be an unbounded amount of time. As we will see, this simple mechanism, paired with one of three memory policies, provides for both resource sharing as well as flow control. We now examine each of these policies.

5.4.2 Policy 1: Pool-Based Management

The first policy we consider is a “pool” memory policy, which is inherited from TritonSort [70]. A memory pool is a set of pre-allocated buffers that is filled during startup. Buffers can be checked out from a pool, and returned when they are finished being used as illustrated in Figure 5.3. When a worker tries to check out a buffer from an empty pool, it blocks until another worker returns a buffer to that pool. The pool memory policy has the advantage that all memory allocation is done at startup, avoiding allocation during runtime. Through efficient implementation, the overhead of checking out buffers can be very small. This is especially useful for stages that require obtaining buffers with very low latency, such as the Receiver stage, which obtains buffers to use in receiving data from the network. The Receiver receives uninterpreted bytes from network sockets

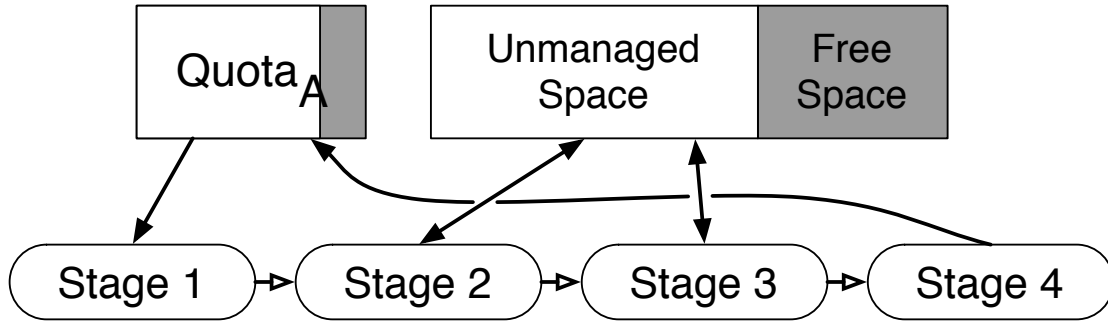


Figure 5.4. A diagrammatic overview of quota-based memory management. In this figure, $Quota_A$ provides a memory quota between Stage 1 and Stage 4. Stages 2 and 3 use unmanaged memory created with standard `malloc` and `free` syscalls.

into small, fixed-size byte buffers. These buffers are passed to a subsequent stage, which converts them into buffers containing complete records. For this reason, the Receiver can use pool-based management while still supporting record-size skew.

Pools can be used to provide resource sharing between workers by giving each of those workers a reference to a single pool. The producer-consumer relationship between pairs of stages also provides a form of flow control; the upstream stage checking out buffers can only produce work at the rate at which the downstream stage can return them to the pool. However, pools have several disadvantages. First, the buffers in a pool are all fixed-size, and so the pool memory policy supports very limited amounts of data skew. By carving memory up into fixed-size pools, the maximum record size supported by this policy is limited to the size of the smallest pool. Additionally, buffer pools reserve a fixed amount of memory for a particular pair of stages. One consequence of this is a loss of flexibility; if one stage temporarily needs more memory than usual (e.g., if it is handling a large record), it cannot “borrow” that memory from another stage due to the static partitioning of memory across pools.

5.4.3 Policy 2: Quota-Based Management

While the pool memory policy is simple, it is quite inflexible, and does not handle skewed record sizes very well. The quota-based memory policy is designed to support more flexible memory allocation while still providing flow control. At a high level, the quota policy ensures that stages producing records do not overwhelm stages that eventually consume them. For example, most of our evaluation is Writer limited, and so we want to ensure that the Receiver stage, which produces records received from the network, does not overwhelm the Writer stage, which is the bottleneck.

Themis has three such producer-consumer pairs: between the Reader and the mapper (with the mapper acting as the consumer), between the mapper and the Sender (with the mapper acting as the producer), and between the Receiver and the Writer. The mapper acts as both a consumer and a producer, since it is the only stage in the phase one pipeline that creates records as directed by the map function that were not read by the Reader.

Quotas are enforced by the queues between stages. A quota can be viewed as the amount of memory that the pipeline between a producer and a consumer can use. When a producer stage pushes a buffer into the pipeline, the size of that buffer is debited from the quota. When a consumer stage consumes that buffer, the buffer's size is added back to the quota. If a producer is about to exceed the quota, then it blocks until the consumer has consumed sufficient memory. Quota-based allocation is illustrated in Figure 5.4.

Quota-based memory management dramatically reduces the number of variables that need to be tuned relative to the pool-based memory policy. One need only adjust the quota allocations present between pairs of stages, rather than the capacity of a much larger number of buffer pools. Additionally, stages that are not producers and consumers do not need to do any form of coordination, which makes their memory allocations very

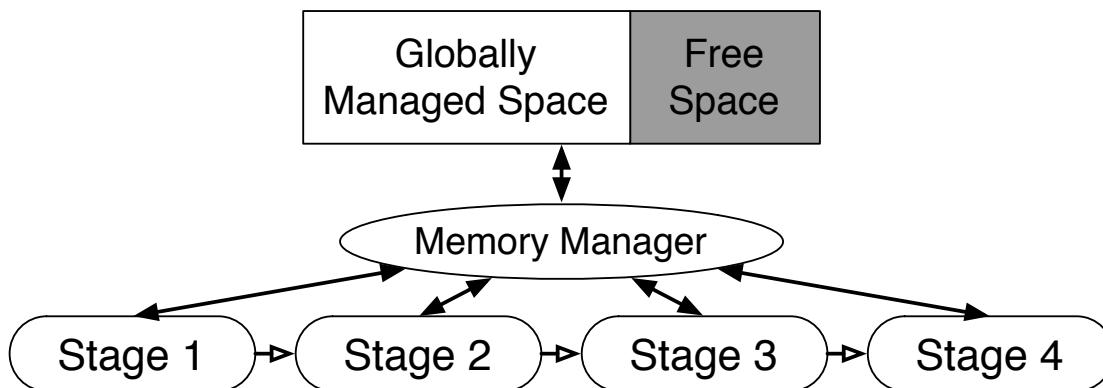


Figure 5.5. A diagrammatic overview of constraint-based memory management. All stages' memory requests are satisfied by a central memory manager that schedules these requests according to the stage graph's structure.

fast.

Quota-based management assumes that any scratch space or additional memory needed by stages between the producer and consumer is accounted for in the quota. This is to prevent intermediate stages from exceeding the total amount of memory, since their memory accesses are not tracked. It also tacitly assumes that the size of a buffer being produced cannot exceed the size of the quota. This is much less restrictive than a pool-based approach, as quotas are typically several gigabytes.

5.4.4 Policy 3: Constraint-Based Management

In situations where the amount of memory used by stages to process records cannot be determined in advance, quota-based systems are not ideal for providing flow control. In these situations, Themis uses a more heavyweight, constraint-based memory management policy.

In the constraint-based memory policy, the total amount of memory in use by workers is tracked centrally in the memory allocator. If a worker requests memory, and enough memory is available, that request is granted immediately. Otherwise, the worker's request is added to a per-worker queue of outstanding requests and the worker sleeps

on a condition variable until the request can be satisfied. Constraint-based allocation is illustrated in Figure 5.5.

When multiple workers have outstanding unsatisfied allocation requests, the memory allocator prioritizes worker requests based on a worker's distance in the stage graph to a stage that consumes records. The producer-side pipeline measures distance to the Sender stage, and the consumer-side pipeline measures distance to the Writer stage. The rationale behind this decision is that records that are being processed should be completely processed before more work is admitted. This decision is inspired by work on live-lock prevention in routers [54]. In this way, the constraint-based allocator implements flow control based on the structure of the dataflow graph.

While this system places precise upper bounds on the amount of memory present in the system, it requires a great deal of coordination between workers, which requires significant lock contention in our implementation. In effect, the reliance on keeping the amount of available memory consistent requires that all allocation and deallocation requests are processed serially. Hence, constraint-based memory allocation is useful for situations where the number of allocation requests being made is relatively small, but the probability of exceeding available memory in common-case operation is high. Phase two in Themis uses constraint-based memory management for precisely these reasons.

In the constraint-based policy, it is possible that certain allocation interleavings can trigger deadlock. Predicting whether a general dataflow system will deadlock is undecidable [56], and deadlock prevention requires knowledge of data dependencies between stages that we deemed too heavyweight. To address the problem of deadlocks, Themis provides a deadlock detector. The deadlock detector periodically probes workers to see if they are waiting for a memory allocation request to complete. If multiple probe cycles pass in which all workers are waiting for an allocation or are idle, the deadlock detector informs the memory allocator that a deadlock has occurred. We have

not experienced deadlock using the policy choices described in Table 5.2 in any of the MapReduce jobs we have evaluated. Efficient ways of handling deadlock is the subject of ongoing work.

In summary, Themis provides a pluggable, policy-driven memory allocation subsystem that provides for flexible resource sharing between stages and workers to handle record size skew while also enabling flow control.

5.5 Skew Mitigation

To satisfy the 2-IO property, Themis must ensure that every partition can be sorted in memory, since an out-of-core sort would induce additional I/Os. In addition, to support parallelism, partitions must be small enough that several partitions can be processed in parallel. Phase zero is responsible for choosing the number of partitions, and selecting a partitioning function to keep each partition roughly the same size. This task is complicated by the fact that the data to be partitioned is generated by the map function. Thus, even if the distribution of input data is known, the distribution of intermediate data may not be known. This phase is optional: if the user has knowledge of the intermediate data's distribution, they can specify a custom partitioning function, similar to techniques used in Hadoop.

Phase zero approximates the distribution of intermediate data by applying the map function to a subset of the input. If the data is homoscedastic, then a small prefix of the input is sufficient to approximate the intermediate distribution. Otherwise, more input data will need to be sampled, or phase two's performance will decrease. DeWitt et al. [26] formalize the number of samples needed to achieve a given skew with high probability; typically we sample 1 GB per node of input data for nodes supporting 8 TB of input. The correctness of phase two only depends on partitions being smaller than main memory. Since our target partition size is less than 5% of main memory, this means

that a substantial sampling error would have to occur to cause job failure. So although sampling does impose additional I/O over the 2-IO limit, we note that it is a small and constant overhead.

Once each node is done sampling, it transmits its sample information to a central coordinator. The coordinator uses these samples to generate a partition function, which is then re-distributed back to each node.

5.5.1 Mechanism

On each node, Themis applies the map operation to a prefix of the records in each input file stored on that node. As the map function produces records, the node records information about the intermediate data, such as how much larger or smaller it is than the input and the number of records generated. It also stores information about each intermediate key and the associated record's size. This information varies based on the sampling policy. Once the node is done sampling, it sends that metadata to the coordinator.

The coordinator merges the metadata from each of the nodes to estimate the intermediate data size. It then uses this size, and the desired partition size, to compute the number of partitions. Then, it performs a streaming merge-sort on the samples from each node. Once all the sampled data is sorted, partition boundaries are calculated based on the desired partition sizes. The result is a list of “boundary keys” that define the edges of each partition. This list is broadcast back to each node, and forms the basis of the partitioning function used in phase one.

The choice of sampling policy depends on requirements from the user, and we now describe each policy.

5.5.2 Sampling Policies

Themis supports the following sampling policies:

(1) Range partitioning: For MapReduce jobs in which the ultimate output of all the reducers must be totally ordered (e.g., sort), Themis employs a range partitioning sampling policy. In this policy, the entire key for each sampled record is sent to the coordinator. A downside of this policy is that very large keys can limit the amount of data that can be sampled because there is only a limited amount of space to buffer sampled records.

(2) Hash partitioning: For situations in which total ordering of reduce function output is not required, Themis employs hash partitioning. In this scheme, a hash of the key is sampled, instead of the keys themselves. This has the advantage of supporting very large keys, and allowing Themis to use reservoir sampling [82], which samples data in constant space in one pass over its input. This enables more data to be sampled with a fixed amount of buffer. This approach also works well for input data that is already partially or completely sorted because adjacent keys are likely to be placed in different partitions, which spreads the data across the cluster.

5.6 Evaluation

We evaluate Themis through benchmarks of several different MapReduce jobs on both synthetic and real-world data sets. A summary of our results are as follows:

- Themis is highly performant on a wide variety of MapReduce jobs, and outperforms Hadoop by 3x - 16x on a variety of common jobs.

Table 5.4. A description and table of abbreviations for the MapReduce jobs evaluated in this section. Data sizes take into account 8 bytes of metadata per record for key and value sizes.

Job Name	Description	Data Size		
		Input	Intermediate	Output
Sort-100G	Uniformly-random sort, 100GB per node	2.16TB	2.16TB	2.16TB
Sort-500G	Uniformly-random sort, 500GB per node	10.8TB	10.8TB	10.8TB
Sort-1T	Uniformly-random sort, 1TB per node	21.6TB	21.6TB	21.6TB
Sort-1.75T	Uniformly-random sort, 1.75TB per node	37.8TB	37.8TB	37.8TB
Pareto-1M	Sort with Pareto-distributed key/value sizes, $\alpha = 1.5$, $x_0 = 100$ (1MB max key/value size)	10TB	10TB	10TB
Pareto-100M	Sort with Pareto-distributed key/value sizes, $\alpha = 1.5$, $x_0 = 100$ (100MB max key/value size)	10TB	10TB	10TB
Pareto-500M	Sort with Pareto-distributed key/value sizes, $\alpha = 1.5$, $x_0 = 100$ (500MB max key/value size)	10TB	10TB	10TB
CloudBurst	CloudBurst (two nodes, performing alignment on lakewash_combined_v2.genes.nucleotide)	971.3MB	68.98GB	517.9MB
PageRank-U	PageRank (synthetic uniform graph, 25M vertices, 50K random edges per vertex)	1TB	4TB	1TB
PageRank-PL	PageRank (synthetic graph with power-law vertex in-degree, 250M vertices)	934.7GB	3.715TB	934.7GB
PageRank-WEX	PageRank on WEX page graph	1.585GB	5.824GB	2.349GB
WordCount	Count words in text of WEX	8.22GB	27.74GB	812MB
n-Gram	Count 5-grams in text of WEX	8.22GB	68.63GB	49.72GB
Click-Sessions	Session extraction from 2TB of synthetic click logs	2TB	2TB	8.948GB

- Themis can achieve nearly the sequential speed of the disks for I/O-bound jobs, which is approximately the same rate as TritonSort’s record-setting performance.
- Themis’s memory subsystem is flexible, and is able to handle large amounts of data skew while ensuring efficient operation.

5.6.1 Workloads and Evaluation Overview

We evaluate Themis on the cluster described in Section 3.3. Each XFS partition is configured with a single allocation group to prevent file fragmentation across allocation groups, and is mounted with the `noatime` flag set. For this evaluation, all servers were running Linux 2.6.32. Our implementation of Themis is written in C++ and is compiled with g++ 4.6.2.

To evaluate Themis at scale, we often have to rely on large synthetically-generated data sets, due to the logistics of obtaining and storing freely-available, large data sets. All synthetic data sets are evaluated on 20 cluster nodes. Non-synthetic data sets are small enough to be evaluated on a single node.

All input and output data is stored on local disks without using any distributed filesystem and without replication. We explore Themis's interaction with distributed storage in Chapter 6.

We evaluate Themis's performance on several different MapReduce jobs. A summary of these jobs is given in Table 5.4, and each job is described in more detail below.

Sort

Large-scale sorting is a useful measurement of the performance of MapReduce and of data processing systems in general. During a sort job, all cluster nodes are reading from disks, writing to disks, and doing an all-to-all network transfer simultaneously. Sorting also measures the performance of MapReduce independent of the computational complexity of the map and reduce functions themselves, since both map and reduce functions are effectively no-ops. We study the effects of both increased data density and skew on the system using sort due to the convenience with which input data that meets desired specifications can be generated. We generate skewed data with a Pareto distribution. The record size in generated datasets is limited by a fixed maximum, which is a parameter given to the job.

WordCount

Word count is a canonical MapReduce job. Given a collection of words, word count's map function emits $\langle \text{word}, 1 \rangle$ records for each word. Word count's reduce function sums the occurrences of each word and emits a single $\langle \text{word}, N \rangle$ record, where

N is the number of times the word occurred in the original collection.

We evaluate WordCount on the 2012-05-05 version of the Freebase Wikipedia Extraction (WEX) [85], a processed dump of the English version of Wikipedia. The complete WEX dump is approximately 62GB uncompressed, and contains both XML and text versions of each page. We run word count on the text portion of the WEX data set, which is approximately 8.2GB uncompressed.

n-Gram Count

An extension of word count, n -gram count counts the number of times each group of n words appears in a text corpus. For example, given “The quick brown fox jumped over the lazy dog”, 3-gram count would count the number of occurrences of “The quick brown”, “quick brown fox”, “brown fox jumped”, etc. We also evaluate n -gram count on the text portion of the WEX data set.

PageRank

PageRank is a graph algorithm that is widely used by search engines to rank web pages. Each node in the graph is given an initial rank. Rank propagates through the graph by each vertex contributing a fraction of its rank evenly to each of its neighbors.

PageRank’s map function is given a record for each vertex in the graph whose key is the vertex’s ID and whose value is a concatenation of the vertex’s adjacency list and its initial rank. The map function emits `<adjacent vertex ID, rank contribution>` pairs for each adjacent vertex ID, and also re-emits the adjacency list so that the graph can be reconstructed. PageRank’s reduce function adds the rank contributions for each vertex to compute that vertex’s rank, and emits the vertex’s existing adjacency list and new rank.

We evaluate PageRank with three different kinds of graphs. The first (PageRank-U) is a 25M vertex synthetically-generated graph where each vertex has an edge to every

other vertex with a small, constant probability. Each vertex has an expected degree of 5,000. The second (PageRank-PL) is a 250M vertex synthetically-generated graph where vertex in-degree follows a power law distribution with values between 100 and 10,000. This simulates a more realistic page graph where a relatively small number of pages are linked to frequently. The third (PageRank-WEX) is a graph derived from page links in the XML portion of the WEX data set; it is approximately 1.5GB uncompressed and has 5.3M vertices.

CloudBurst

CloudBurst [53] is a MapReduce implementation of the RMAP [79] algorithm for short-read gene alignment, which aligns a large collection of small “query” DNA sequences called *reads* with a known “reference” genome. CloudBurst performs this alignment using a standard technique called *seed-and-extend*. Both query and reference sequences are passed to the map function and emitted as a series of fixed-size *seeds*. The map function emits seeds as sequence of <seed, seed metadata> pairs, where the seed metadata contains information such as the seed’s location in its parent sequence, whether that parent sequence was a query or a reference, and the characters in the sequence immediately before and after the seed.

CloudBurst’s reduce function examines pairs of query and reference strings with the same seed. For each pair, it computes a similarity score of the DNA characters on either side of the seed using the Landau-Vishkin algorithm for approximate string matching. The reduce function emits all query/reference pairs with a similarity score above a configured threshold.

We evaluate CloudBurst on the lakewash_combined_v2 data set from University of Washington [39], which we pre-process using a slightly modified version of the CloudBurst input loader used in Hadoop.

Click Log Analysis

Another popular MapReduce job is analysis of click logs. Abstractly, click logs can be viewed as a collection of `<user ID, timestamp|URL>` pairs (where the `|` symbol denotes the concatenation of logical fields as part of the value) indicating which page a user loaded at which time. We chose to evaluate one particular type of log analysis task, *session tracking*. In this task, we seek to identify disjoint ranges of timestamps at least some number of seconds apart. For each such range of timestamps, we output `<user ID, start timestamp|end timestamp|start URL|end URL>` pairs.

The map function is a pass-through; it simply groups records by user ID. The reduce function does a linear scan through records for a given user ID and reconstructs sessions. For efficiency, it assumes that these records are sorted in ascending order by timestamp. We describe the implications of this assumption in the next section.

5.6.2 Job Implementation Details

In this section, we briefly describe some of the implementation details necessary for running our collection of example jobs at maximum efficiency.

Combiners

A common technique for improving the performance of MapReduce jobs is employing a *combiner*. For example, word count can emit a single `<word, k>` pair instead of k `<word, 1>` pairs. Themis supports the use of combiner functions. We opted to implement combiners within the mapper stage on a job-by-job basis rather than adding an additional stage. Despite what conventional wisdom would suggest, we found that combiners actually decreased our performance in many cases because the computational overhead of manipulating large data structures was enough to make the mapper compute-bound. The large size of these data structures is partially due to our

decision to run the combiner over an entire job's intermediate data rather than a small portion thereof to maximize its effectiveness.

In some cases, however, a small data structure that takes advantage of the semantics of the data provides a significant performance increase. For example, our word count MapReduce job uses a combiner that maintains a counter for the top 25 words in the English language. The combiner updates the appropriate counter whenever it encounters one of these words rather than creating an intermediate record for it. At the end of phase one, intermediate records are created for each of these popular words based on the counter values.

Improving Performance for Small Records

The map functions in our first implementations of word count and n-gram count emitted `<word/n-gram, 1>` pairs. Our implementations of these map functions emit `<hash(word), 1|word>` pairs instead because the resulting intermediate partitions are easier to sort quickly because the keys are all small and the same size.

Secondary Keys

A naïve implementation of the session extraction job sorts records for a given user ID by timestamp in the reduce function. We avoid performing two sorts by allowing the Sorter stage to use the first few bytes of the value, called a *secondary key*, to break ties when sorting. For example, in the session extraction job the secondary key is the record's timestamp.

5.6.3 Performance

We evaluate the performance of Themis in two ways. First, we compare performance of the benchmark applications to the cluster's hardware limits. Second, we compare the performance of Themis to that of Hadoop on two benchmark applications.

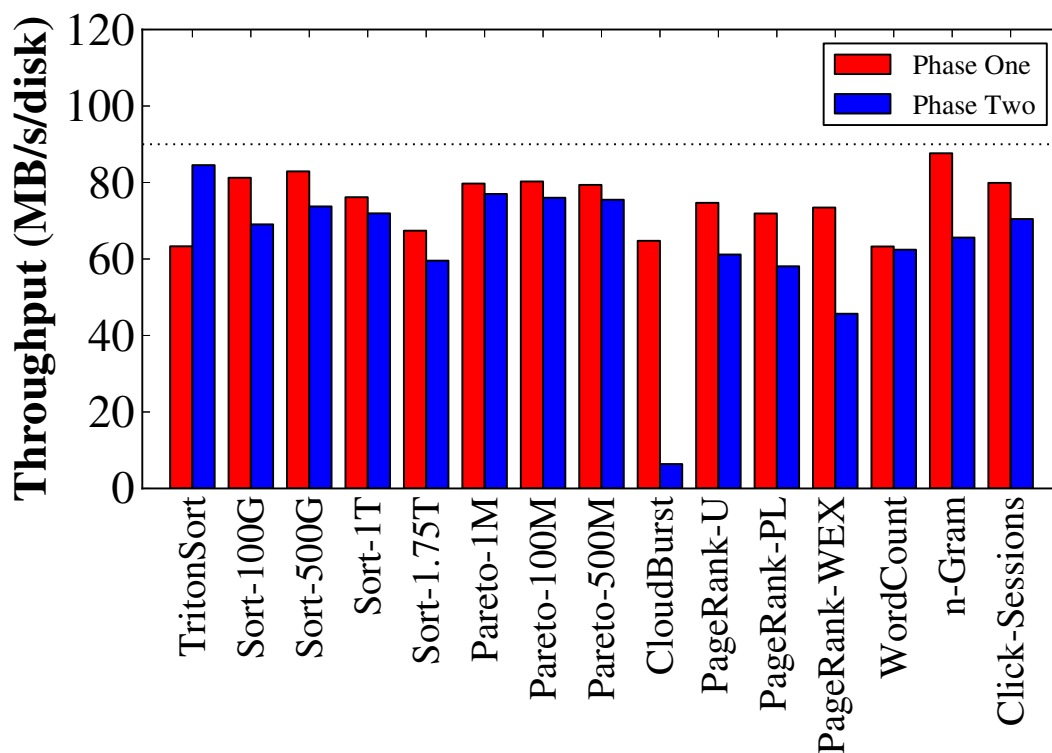


Figure 5.6. Performance of evaluated MapReduce jobs. Maximum sequential disk throughput of approximately 90 MB/s is shown as a dotted line. Our TritonSort record from 2011 is shown on the left for comparison.

Performance Relative to Disk Speeds

The performance of Themis on the benchmark MapReduce jobs is shown in Figure 5.6. Performance is measured in terms of *MB/s/disk* in order to provide a relative comparison to the hardware limitations of the cluster. The 7200 RPM drives in the cluster are capable of approximately 90 MB/s/disk of sequential write bandwidth, which is shown as a dotted line in the figure. A job running at 90 MB/s/disk is processing data as fast as it can be written to the disks.

Most of the benchmark applications run at near maximum speed in both phases. CloudBurst's poor performance in phase two is due to the computationally intensive nature of its reduce function, which is unable to process records fast enough to saturate

Table 5.5. Performance comparison of Hadoop and Themis.

Application	Running Time		Improvement
	Hadoop	Themis	
Sort-500G	28881s	1789s	16.14x
CloudBurst	2878s	944s	3.05x

the disks. More CPU cores are needed to drive computationally intensive applications such as CloudBurst at maximum speed in both phases. Notice however that CloudBurst is still able to take advantage of our architecture in phase one.

We have included TritonSort’s performance on the Indy 100TB sort benchmark for reference. TritonSort’s 2011 Indy variant runs a much simpler code base than Themis. We highlight the fact that Themis’s additional complexity and flexibility does not impact its ability to perform well on a variety of workloads. Our improved performance in phase one relative to TritonSort at scale is due to a variety of internal improvements and optimizations made to the codebase in the intervening period, as well as the improved memory utilization provided by moving from buffer pools to dynamic memory management. Performance degradation in phase two relative to TritonSort is mainly due to additional CPU and memory pressure introduced by the Reducer stage.

Comparison with Hadoop

We evaluate Hadoop version 1.0.3 on the Sort-500G and CloudBurst applications. We started with a configuration based on the configuration used by Yahoo! for their 2009 Hadoop sort record [80]. We optimized Hadoop as best we could, but found it difficult to get it to run many large parallel transfers without having our nodes blacklisted for running out of memory.

The total running times for both Hadoop and Themis are given in Table 5.5. I/O-bound jobs such as sort are able to take full advantage of our architecture, which explains why Themis is more than a factor of 16 faster. As explained above, CloudBurst

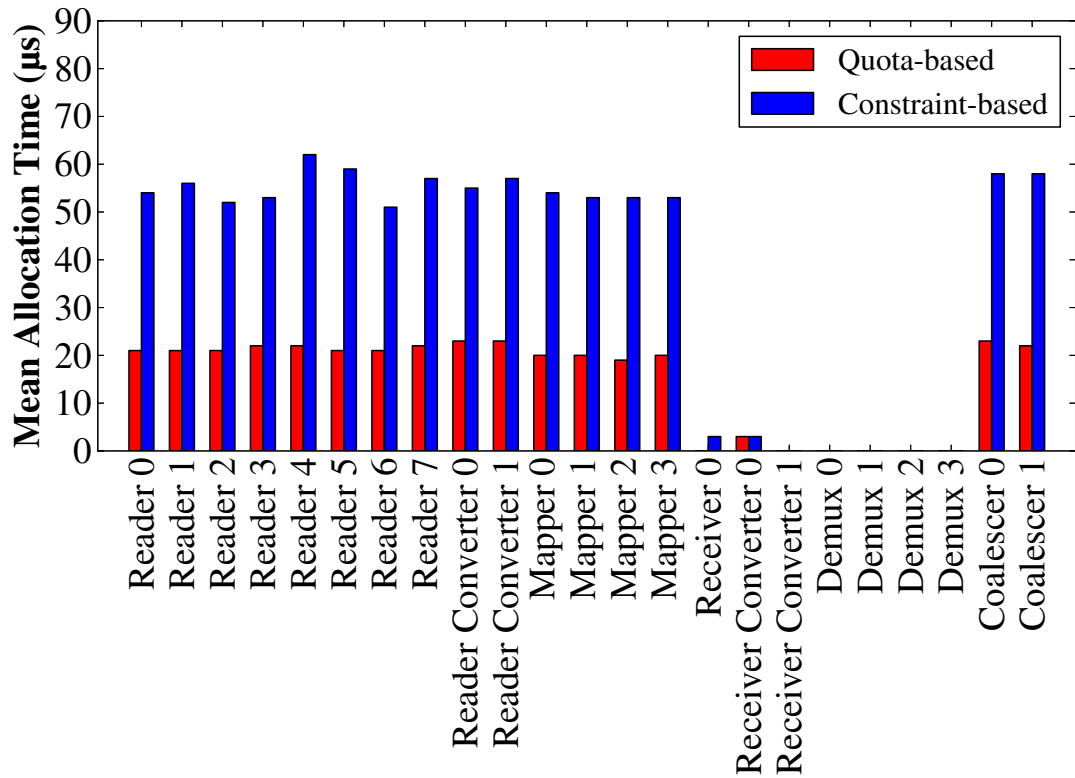


Figure 5.7. Effects of allocation policy on mean allocation times across workers.

is fundamentally compute-bound, but the performance benefits of the 2-IO property allow the Themis implementation of CloudBurst to outperform the Hadoop implementation by a factor of 3.

5.6.4 Memory Management

In this section, we evaluate the performance of our different memory allocation policies. We also show that our allocation system is robust in the face of transient changes in individual stage throughputs.

Memory Allocator Performance

We examine both the individual allocation times of our different memory allocation policies and their end-to-end performance. We evaluate the performance on

Table 5.6. Performance of allocation policies.

Allocation Policy	Phase One Throughput
Constraint-Based	84.90 MBps/disk
Quota-Based	83.11 MBps/disk

phase one of a 200GB, 1-node sort job. Table 5.6 shows that phase one’s throughput is essentially unaffected by the choice of allocator policy in this particular instance. These performance numbers can be explained by looking at the mean allocation time for each worker in the system. Figure 5.7 shows that while the constraint-based allocator is more than twice as slow as the quota-based allocator, the absolute allocation times are both measured in tens of microseconds, which is negligible compared to time taken to actually do useful work.

However, the results above only hold in the case where the constraint-based allocator does not deadlock. While we never experienced deadlock in phase two, we found it was quite easy to construct situations in which phase one deadlocked. For example, the exact same experiment conducted on a slightly larger data set causes deadlock in phase one with the constraint-based allocator.

The performance results in Figure 5.6 demonstrate the constraint-based allocation policy performs well in phase two. Because phase two handles entire intermediate partitions in memory, its allocations are orders of magnitude larger than those in phase one. This dramatically increases the likelihood that a single memory request is larger than one of the phase’s quotas.

Robustness of the Quota-Based Memory Allocation Policy

We evaluate the robustness of the quota-based memory allocator by artificially slowing down the network for a period of time. We observe the effect on the total quota usage of a stage in the pipeline. Figure 5.8 shows that the Reader Converter’s quota usage

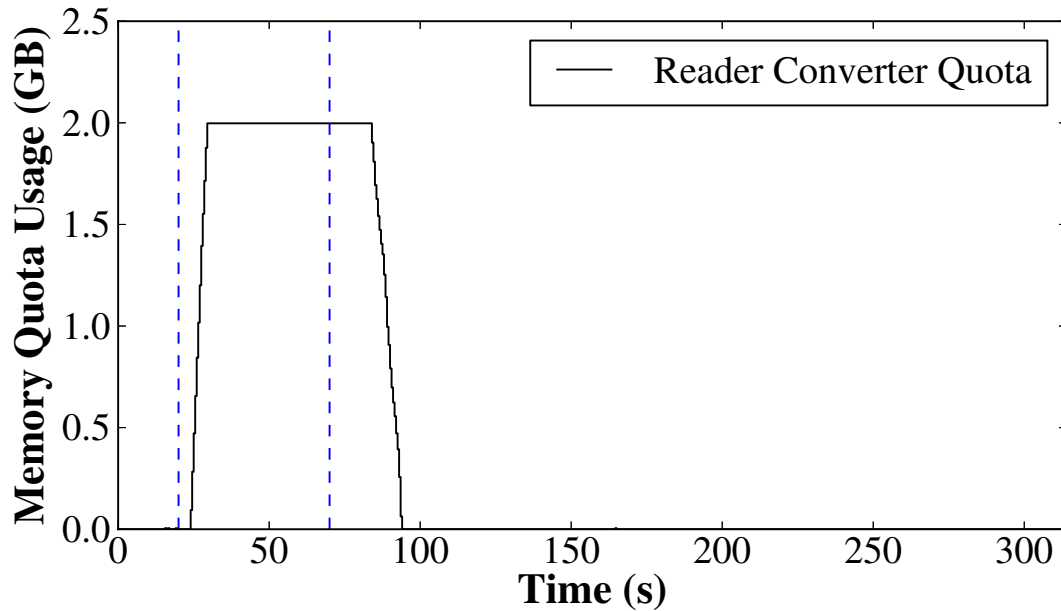


Figure 5.8. Memory quota usage of the Reader Converter stage. The network was made artificially slow in the time period designated by the dashed lines.

spikes up to its limit of 2GB in response to a slow network and then returns back to a steady state of near 0. A slow network means that stages upstream of the network are producing data faster than the network can transmit data. This imbalance leads to data backing up in front of the network. In the absence of the quota allocation policy, this data backlog grows unbounded.

5.6.5 Skew Mitigation

Next, we evaluate Themis’s ability to handle skew by observing the sizes of the intermediate data partitions created in phase one. Figure 5.9 shows the partition sizes produced by Themis on the evaluated applications. The error bars denoting the 95% confidence intervals are small, indicating that all partitions are nearly equal in size. This is unsurprising for applications with uniform data, such as sort. However, Themis also achieves even partitioning on very skewed data sets, such as Pareto-distributed sort,

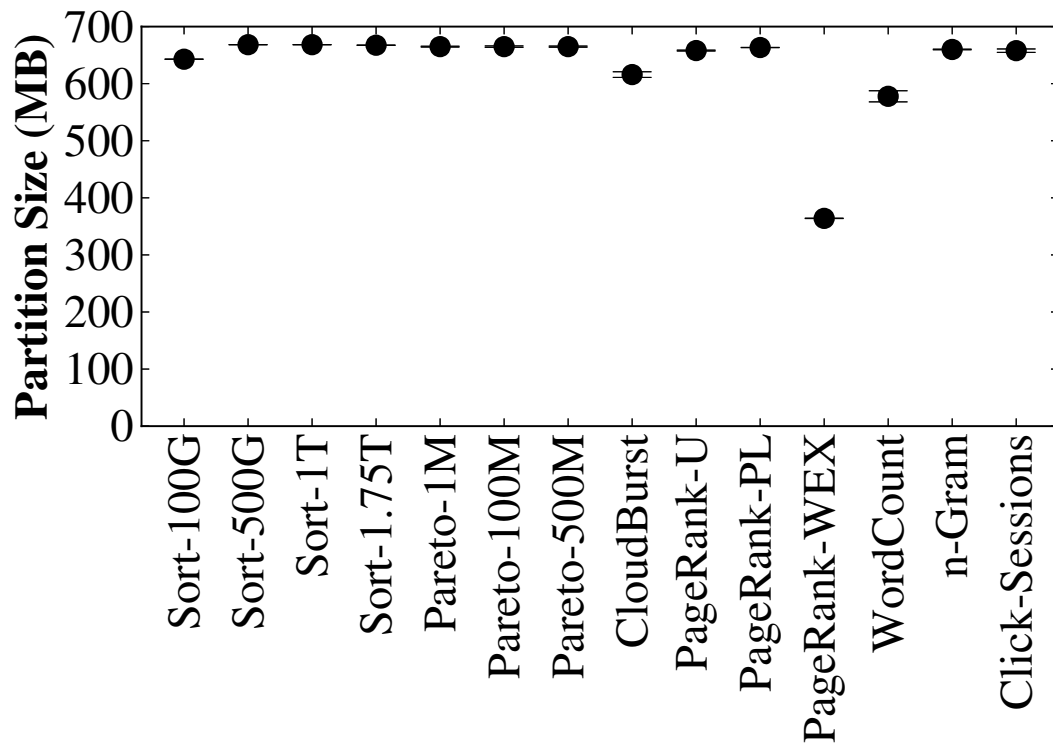


Figure 5.9. Partition sizes for various Themis jobs. Error bars denoting the 95% confidence intervals are hard to see due to even partitioning.

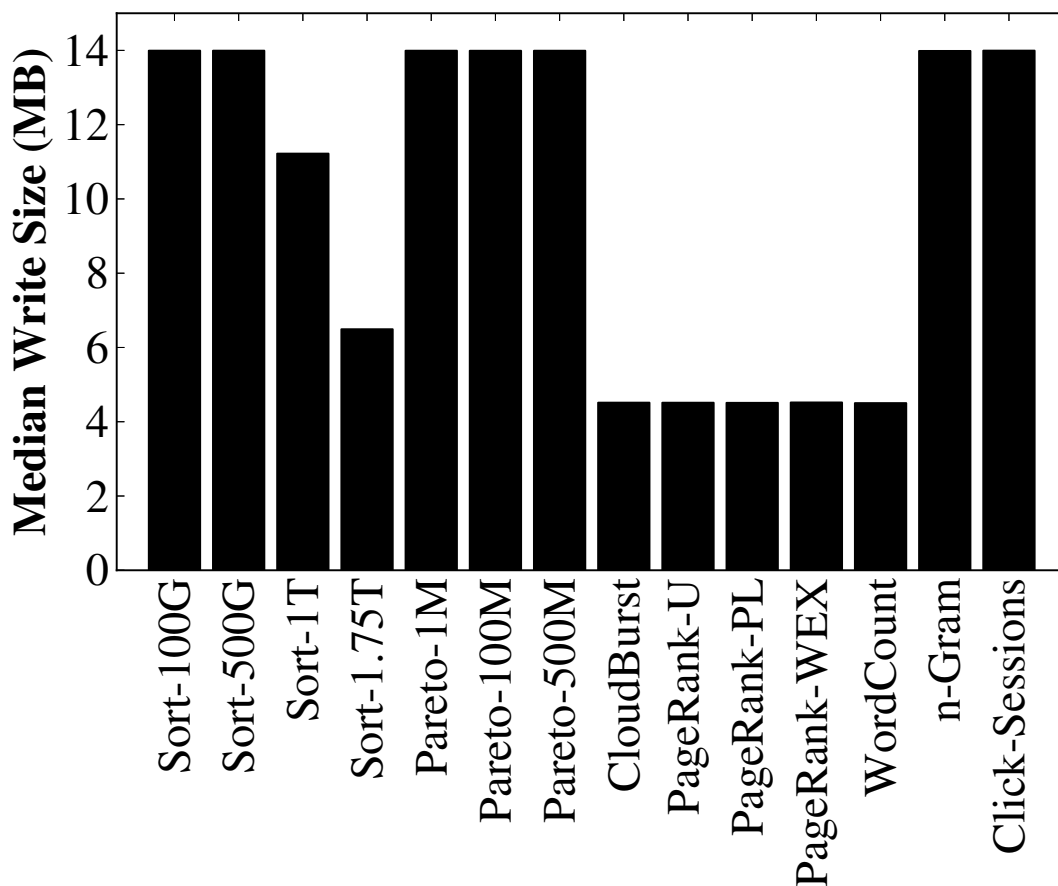


Figure 5.10. Median write sizes for various Themis jobs.

PageRank, and WordCount. PageRank-WEX has fairly small partitions relative to the other jobs because its intermediate data size is not large enough for phase zero to create an integer number of partitions with the desired size.

5.6.6 Write Sizes

One of primary goals of phase one is to do large writes to each partition to avoid unnecessary disk seeks. Figure 5.10 shows the median write sizes of the various jobs we evaluated. For jobs like Sort and n-Gram where the map function is extremely simple and mappers can map data as fast as Readers can read it, data buffers up in the Chainer stage and all writes are large. As the amount of intermediate data per node grows, the

size of a chain that can be buffered for a given partition decreases, which fundamentally limits the size of a write. For example, Sort-1.75T writes data to 2832 partitions, which means that its average chain length is not expected to be longer than about 5 MB given a Receiver memory quota of 14GB; note, however, that the mean write size is above this minimum value, indicating that the Writer is able to take advantage of temporary burstiness in activity for certain partitions. If the stages before the Writer stage cannot quite saturate it (such as in WordCount, CloudBurst and PageRank), chains remain fairly small. Here the minimum chain size of 4.5 MB ensures that writes are still reasonably large. In the case of PageRank-WEX, the data size is too small to cause the chains to ever become very large.

5.7 Conclusions

Many MapReduce jobs are I/O-bound, and so minimizing the number of I/O operations is critical to improving their performance. In this work, we present Themis, a MapReduce implementation that meets the 2-IO property, meaning that it issues the minimum number of I/O operations for jobs large enough to exceed memory. To avoid materializing intermediate results, Themis foregoes task-level fault tolerance, relying instead on job-level fault tolerance. Since the 2-IO property prohibits it from spilling records to disk, Themis must manage memory dynamically and adaptively. To ensure that writes to disk are large, Themis adopts a centralized, per-node disk scheduler that batches records produced by different mappers.

There exist a large and growing number of clusters that can process petabyte-scale jobs, yet are small enough to experience a qualitatively lower failure rate than warehouse-scale clusters. We argue that these deployments are ideal candidates to adopt more efficient implementations of MapReduce, which result in higher overall performance than more pessimistic implementations. Themis has been able to implement a wide variety of

MapReduce jobs at nearly the sequential speed of the underlying storage layer, and is on par with TritonSort’s record sorting performance.

5.8 Acknowledgments

The authors wish to thank Kenneth Yocum for his valuable input, as well as Mehul Shah and Chris Nyberg for their input on Themis’s approach to sampling. This work was sponsored in part by NSF Grants CSR-1116079 and MRI CNS-0923523, as well as through donations by Cisco Systems and a NetApp Faculty Fellowship.

Chapter 5 contains material as it appears in the Proceedings of the ACM Symposium on Cloud Computing (SoCC) 2012. “Themis: An I/O-Efficient MapReduce”. Rasmussen, Alexander; Conley, Michael; Kapoor, Rishi; Lam, Vinh The; Porter, George; Vahdat, Amin. The dissertation author was the primary investigator and author of this paper.

Chapter 6

I/O-Efficient Fault Tolerance

A key requirement when building scale-out data processing architectures is allowing them to recover from failures in a manner that is transparent to the end user. Traditional MapReduce implementations provide fault tolerance by materializing intermediate data to disk on both sides of a network transfer. This increases the amount of disk I/O that each MapReduce job must perform, which fundamentally limits the performance of I/O-bound workloads.

In this chapter, we argue that small and medium clusters – on which MapReduce is commonly deployed, and where the likelihood of a failure during a job is low relative to large-scale clusters – can benefit from more optimistic forms of fault tolerance for which the common-case overhead is far lower than traditional approaches. In particular, we explore the implications of the job-level fault tolerance approach adopted by Themis in the previous chapter, and describe an alternative fault tolerance method for Themis that leverages prior work in scan sharing and eager record-level provenance.

6.1 Introduction

A key requirement and challenge in building scale-out data processing architectures is allowing them to recover from failures without burdening the programmer. MapReduce traditionally provides fault tolerance by splitting the execution of the map

and reduce functions into a collection of idempotent *tasks*. Each map task operates over a portion of the input, while each reduce task operates over records produced by the map function with a particular set of keys. When a task fails, it is simply re-executed. We refer to this method of fault tolerance as *task-level fault tolerance*.

A key benefit of this fault tolerance technique is that it is *proportional*. Generally speaking, this means that the amount of additional work required to recover from a failure is proportional to the size of that failure. Proportional fault tolerance techniques work extremely well on clusters containing thousands of nodes, because failures in those environments are extremely common and the relative size of each individual failure is small [21].

In MapReduce’s case, however, proportional fault tolerance comes with a significant cost; map tasks must materialize their output to their local disks before transferring that output to reduce tasks. These materializations are required because, in general, each reduce task needs some of the records produced by every map task in order to run. Were map tasks to send their outputs to reduce tasks directly, the loss of the node on which a reduce task runs would require that map tasks re-compute all data sent to that task. In I/O-bound applications, the extra materializations required by task-level fault tolerance can negatively affect performance.

Many modern MapReduce clusters are “dense”, in the sense that they pack a large amount of storage, compute, and network bandwidth into a small number of racks of servers. In this chapter, we show that in these “dense” clusters, the additional I/O necessitated by task-level fault tolerance often leads to lower overall job throughput than simply re-running a job if a failure occurs.

The more optimistic *job-level fault tolerance* employed by Themis in the previous chapter allows Themis to perform much more aggressive operator pipelining than task-level fault tolerance can achieve while still maintaining the 2-IO property. However,

job-level fault tolerance precludes running jobs that take longer than the cluster MTTF to complete, preventing large clusters (or unusually failure-prone small ones) from running some jobs. To mitigate this problem, we present a fault tolerance approach that provides proportional recovery without imposing additional intermediate data materialization during failure-free execution. Our main goal in designing this fault tolerance scheme is to perform as little additional I/O as possible both in common case operation and during recovery from failure.

Our contributions are as follows:

1. We explore the tradeoffs of different levels of fault tolerance in “dense” clusters.
2. We modify Themis to allow it to run multiple jobs concurrently, using scan sharing [61, 75, 83] to reduce the amount of I/O required for each job.
3. Leveraging this multi-tenant capability, we present a fault tolerance mechanism that composes previously known techniques to reduce the amount of additional I/O needed for recovery at the expense of additional redundant computation.
4. We show how this fault tolerance mechanism can be used to provide proportional recovery both from failures of a single disk and an entire node. When scan sharing, an eight-node Themis cluster can recover from a disk failure with under 5% overhead.
5. We compare this approach to approaches based on record-based provenance information.

6.2 Motivation

In this section, we summarize the argument for replacing task-level fault tolerance as MapReduce’s fault tolerance scheme for “dense” clusters. We then provide an overview

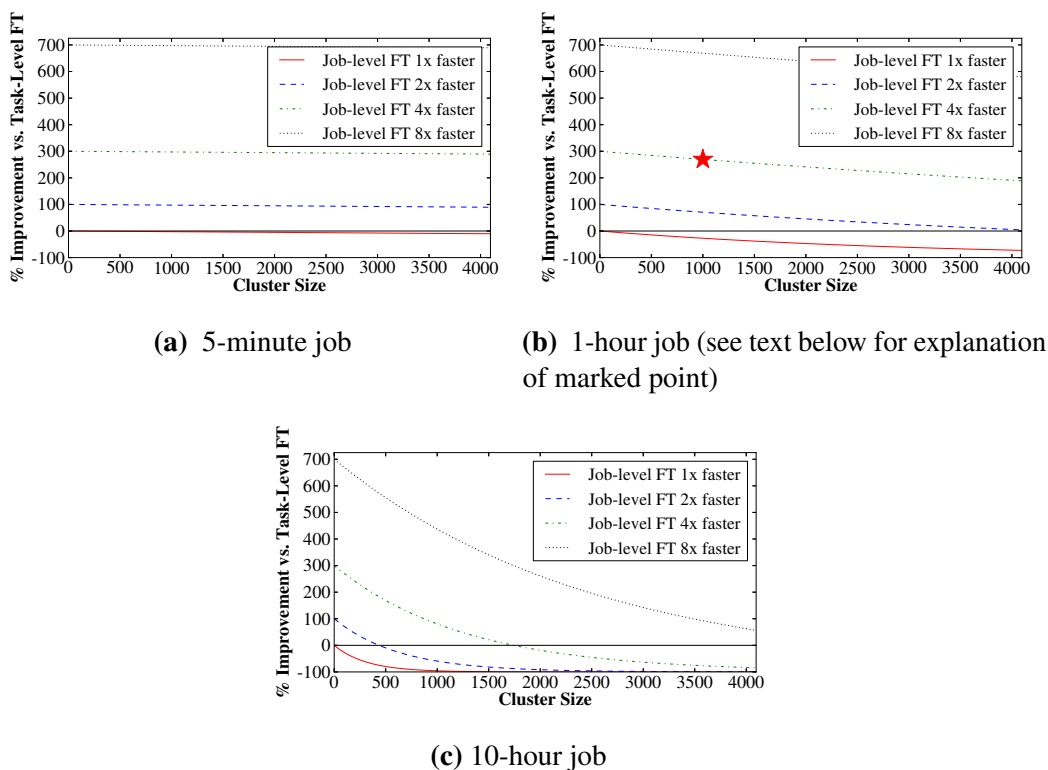


Figure 6.1. A lower-bound of the expected benefit of job-level fault tolerance for varying cluster sizes, given that an error-free execution of a job with task-level fault tolerance takes five minutes (a), an hour (b), or ten hours (c) to complete.

of alternative fault approaches used by current data processing systems.

6.2.1 Fault Tolerance for “Dense” Clusters

Much of MapReduce’s architecture is based on the assumption that it is running on a very large cluster of unreliable machines. However, a large number of “Big Data” clusters do not approach the size of warehouse-scale data centers like those at Google and Microsoft because moderately-sized clusters (10s of racks or fewer) are increasingly able to support important real-world problem sizes. The storage capacity and number of CPU cores in commodity servers are both increasing rapidly. In Cludera’s reference system design [18], in which each node has 16 or more disks, a petabyte worth of 1TB drives fits into just over three racks, or about 60 nodes. Coupled with the emergence

Table 6.1. Component-level failure rates observed in a Google data center as reported in [30].

Component	Failure rates
Node	4.3 months
Disk	2-4% annualized
Rack	10.2 years

of affordable 10 Gbps Ethernet at the end host and increasing bus speeds, data can be packed more densely than ever before while keeping disk I/O as the bottleneck resource. This implies that fewer servers are required for processing large amounts of data for I/O-bound workloads. We now consider the implications of this increased density on fault tolerance.

Job-level fault tolerance allows for much more aggressive operator pipelining than task-level fault tolerance can achieve while still maintaining the 2-IO property. However, it is not self-evident that the overhead of re-executing failed jobs does not cancel any performance gained by this aggressive pipelining. In this section, we show not only that job-level fault tolerance is a feasible approach for moderately-sized clusters, but also that there are significant potential performance benefits for using job-level fault tolerance in these environments.

Understanding the expected impact of failures is critical to choosing the appropriate fault tolerance model. MapReduce was designed for clusters of many thousands of machines running inexpensive, failure-prone commodity hardware [22]. For example, Table 6.1 shows component-level mean-time to failure (MTTF) statistics in one of Google’s data centers [30]. Google’s failure statistics are corroborated by similar studies of hard drive [66, 77] and node [57, 76] failure rates.

6.2.2 Modeling Node Failure Rates

At massive scale, there is a high probability that some portion of the cluster will fail during the course of a job. To understand this probability, we employ a simple model [12], shown in Equation 6.1, to compute the likelihood that a node in a cluster of a particular size will experience a failure during a job:

$$P(N, t, MTTF) = 1 - e^{-N \cdot t / MTTF} \quad (6.1)$$

The probability of a failure occurring in the next t seconds is a function of (1) the number of nodes in the cluster, N , (2) t , and (3) the mean time to failure of each node, $MTTF$, taken from the node-level failure rates in Table 6.1. This model assumes that nodes fail with exponential (Pareto) probability, and we simplify our analysis by considering node failures only. We do this because disk failures can be made rare by using node-level mechanisms (i.e., RAID), and correlated rack failures are likely to cripple the performance of a cluster with only a few racks.

Based on the above model, in a 100,000 node data center, there is a 93% chance that a node will fail during any five-minute period. On the other hand, in a moderately-sized cluster (e.g., 200 nodes, the average Hadoop cluster size as reported by Cloudera), there is only a 0.53% chance of encountering a node failure during a five-minute window, assuming the $MTTF$ rates in Table 6.1.

This leads to the question of whether smaller deployments benefit from job-level fault tolerance, where if any node running a job fails the entire job restarts. Intuitively, this scheme will be more efficient overall when failures are rare and/or jobs are short.

6.2.3 Modeling Expected Job Completion Time

Let T be the job's duration and $MTTF$ be the mean time to failure of the cluster. In our model, failure occurs as a Poisson process. We compute the expected running time of a failed job (denoted T_F) as follows:

$$\begin{aligned}
 T_F &= \int_0^T t \cdot \frac{1}{MTTF} e^{-\frac{t}{MTTF}} dt \\
 &= \left[-te^{-\frac{t}{MTTF}} - MTTF \cdot e^{-\frac{t}{MTTF}} \right]_{t=0}^{t=T} \\
 &= MTTF - (T + MTTF)e^{-\frac{T}{MTTF}}
 \end{aligned} \tag{6.2}$$

Therefore, if the job duration T is much larger than the MTTF of the cluster ($T \gg MTTF$), Equation 6.2 implies that $T_F \approx MTTF$, and we expect the job to fail. On the other hand, if $T \ll MTTF$, Equation 6.2 implies that $T_F \approx T$, and we expect the job to succeed.

Having modeled the running time of a failed job, we can now derive a model for overall job completion time. Let p denote the probability of failure in a single Themis job. Let T denote the running time of the job when there are no failures.

Consider a situation in which the job fails during the first $(n - 1)$ trials and completes in the n^{th} trial. The probability of this event is $p^{n-1}(1 - p)$. Note that a successful trial takes time T and a failed trial takes time T_F . To simplify our notation, let $\alpha = T_F/T$ be the fraction of its successful runtime the failed job spent running. Then the total running time in this case is

$$(n - 1)\alpha T + T = ((n - 1)\alpha + 1)T.$$

By considering such an event for all possible values of n , we get the expected

running time to completion for the job:

$$\begin{aligned}
S(p, T) &= \sum_{n=1}^{\infty} ((n-1)\alpha + 1)T \cdot p^{n-1}(1-p) \\
&= T(1-p) \sum_{n=1}^{\infty} (\alpha n p^{n-1} + (1-\alpha)p^{n-1}) \\
&= T(1-p) \left(\alpha \sum_{n=1}^{\infty} n p^{n-1} + (1-\alpha) \sum_{n=1}^{\infty} p^{n-1} \right) \\
&= T(1-p) \left(\alpha \frac{1}{(1-p)^2} + (1-\alpha) \frac{1}{1-p} \right) \\
&= T \left(\alpha \frac{p}{1-p} + 1 \right) \tag{6.3}
\end{aligned}$$

Hence, we can model the expected completion time of a job $S(p, T)$ as:

$$S(p, T) = T \left(\frac{p}{1-p} + 1 \right) \tag{6.4}$$

where p is the probability of a node in the cluster failing, and T is the runtime of the job. This estimate is pessimistic, in that it assumes that jobs fail just before the end of their execution.

By combining equations 6.1 and 6.4, we can compute the expected benefit—or penalty—that we get by moving to job-level fault tolerance. Modeling the expected runtime of a job with task-level fault tolerance is non-trivial, so we instead compare to an error-free baseline in which the system's performance is not affected by node failure. This comparison underestimates the benefit of job-level fault tolerance.

Figure 6.1 shows the expected performance benefits of job-level fault tolerance compared to the error-free baseline. More formally, we measure performance benefit as $S(P(\cdot), T_{job})/T_{task}$, where T_{job} is the time a job on an error-free cluster takes to execute with job-level fault tolerance and T_{task} is the time the same job takes to execute with

task-level fault tolerance.

The benefits of job-level fault tolerance increase as the error-free performance improvement made possible by moving to job-level fault tolerance (i.e. T_{task}/T_{job}) increases. For example, if T_{task}/T_{job} is 4, T_{task} is one hour and we run on a cluster of 1,000 nodes, we can expect Themis to complete the job 240% faster than the task-level fault tolerant alternative on average; this scenario is marked with a star in Figure 6.1b. There are also situations in which job-level fault tolerance will significantly under-perform task-level fault tolerance. For example, if T_{task}/T_{job} is 2, Themis will under-perform a system with task-level fault tolerance for clusters bigger than 500 nodes. From this, we make two key observations: for job-level fault tolerance to be advantageous, the cluster has to be moderately-sized, and Themis must significantly outperform the task-level alternative.

6.3 Alternative Fault Tolerance Methods

We now examine a number of alternative fault tolerance schemes and their applicability to “dense” clusters.

6.3.1 Replication

Systems that employ replication for fault tolerance store multiple copies, or replicas, of intermediate data in the system simultaneously. The granularity of this replication can vary: whole files, the blocks that comprise a file, or even individual records may be replicated. To prevent correlated failures from causing data loss, these replicas are often stored in different failure domains; for example, replicas might be stored on different hosts, different racks, or even geographically-separated data centers. If one of the replicas is lost, another replica can be used in its place, either by migrating it or accessing it remotely.

While MapReduce typically relies on some degree of replication in its input and output data for fault tolerance, intermediate data generated by individual map tasks is typically not replicated due to the high overhead both in terms of storage space and bandwidth involved (though Ko et al. explore mitigating these effects in [43]).

6.3.2 Upstream backup

The task-level fault tolerance scheme currently used in MapReduce is an example of a class of fault tolerance called *upstream backup* [11, 91]. In upstream backup, the output of an operator is buffered locally on disk before being sent over the network to subsequent operators. If the downstream operator fails (due to node failure, for example), its inputs can be sent to a replacement instance of the operator without having to re-run the map tasks that generated those inputs. Upstream backup is a restricted form of keeping a bounded history in dataflow systems [11].

6.3.3 Parallel Recovery

A disadvantage of upstream backup is that the recovery latency can be high because recovery of a downstream operator is limited to the speed at which the slowest upstream node can send data to it. In parallel recovery, intermediate data is additionally checkpointed on many separate nodes. When a failure occurs, each of these nodes can contribute a small portion of the recovery data to the new downstream operator. This enables significant parallelism, reducing the time required to recover the data. Spark's D-Streams [92] and RAMCloud [63] both employ parallel recovery.

6.3.4 Process-Pairs

In systems employing process-pairs parallelism [34], two replicas of the same computation are executed simultaneously. In the traditional definition, checkpoints of the primary's execution are periodically sent to the backup and, if the primary fails, the

backup assumes the primary's role and a new backup is instantiated. FLuX [78] applies the process-pairs approach to the continuous query domain, providing process pairs on either side of a network transmission and providing seamless fail-over. While this approach allows the computation to continue in the face of a limited amount of failure, it potentially imposes significant additional network bandwidth and compute overhead.

6.3.5 Provenance and Selective Replay

The above mechanisms work to ensure that data itself is kept fault-tolerant. Fault tolerance mechanisms based on provenance and replay ensure instead that the sequence of steps necessary to reproduce each piece of intermediate data are kept fault tolerant, while the intermediate data itself is volatile. MapReduce employs a limited form of provenance; a map task's output can be recomputed if the function that task was running and the data over which it was running are known, without recomputing anything else.

The storage requirements of maintaining provenance information depend largely on its granularity. For example, the overhead of record-level provenance is a function of the number of intermediate records, which can be quite large at scale. However, provenance can be quite effective when kept at a much coarser-grained level. Spark maintains provenance at the Resilient Distributed Dataset (RDD) level, which requires much less overhead than record-level bookkeeping. However, the Spark authors point out that they perform upstream backup of intermediate records for what they call "wide dependencies", of which MapReduce's all-to-all shuffle is one, "... to simplify fault recovery" [91].

6.3.6 Scan-Sharing

Scan-sharing [75] is a form of multi-query optimization in which the output of a scan of a dataset is used by more than one job at a time. This optimization takes advantage

of the fact that some datasets are much more popular than others. Jobs that share the same data can be co-scheduled and “share” scans of that data, effectively eliminating the I/O overhead for all but one of the jobs. For I/O-bound workloads, this provides a significant reduction in overhead, and does not require any additional storage overhead or maintenance of provenance.

6.4 Design

In this section, we describe our goals in implementing fault tolerance for “dense” MapReduce clusters. We then present an overview of the design of our fault tolerance approach, which incorporates aspects of several of the approaches described in Section 6.3.

6.4.1 Goals

Our goals when designing a fault tolerance scheme for “dense” MapReduce clusters are as follows. First, recovery should be proportional; that is, the amount of additional time taken to recover from a failure should be proportional to the failure’s size. Second, the fault tolerance scheme should impose as little additional disk I/O in failure-free operation as possible, and perform as little additional disk I/O during recovery as possible. Finally, the system should be able to recover from failures of both a disk and an entire node.

6.4.2 Recovery in MapReduce

In this work, we assume that failures are fail-stop with complete loss of state. This means that if a disk fails, all data stored on that disk is lost. If a node fails, all its disks are considered to have failed. Failed disks and nodes must be explicitly recovered by an operator. Recovering from Byzantine faults is beyond the scope of this work.

Fundamentally, recovering from a failure in MapReduce consists of two main tasks. Any intermediate data that was stored on failed disks must be recovered. We call this part of the recovery process *write recovery*, because it ensures that all intermediate records have been written. Also, the system must ensure that all input data was completely processed. If a node was in the middle of processing an input file when it failed, some of that file's records may not have been mapped and transmitted successfully. We call this part of the recovery process *read recovery*, because it ensures that every input record has been read and mapped.

6.4.3 Write Recovery Approach

In order to perform write recovery, the system must regenerate all intermediate data that was supposed to have been stored on the failed disks. Themis uses a technique we call *scan-and-discard* to perform this recovery. In the scan-and-discard approach, the input data set is re-read and each record is re-mapped, but only those records that would have been stored on the failed disks are transmitted to their destination.

One obvious drawback of the scan-and-discard technique is that all input records must be re-read and re-mapped, even though most of those records will not be transmitted. Themis attempts to reduce or eliminate this additional I/O cost through scan sharing.

There is a large body of prior work suggesting both a significant opportunity for and potential benefit from scan sharing in the MapReduce context. Recent traces from industrial MapReduce deployments [17] indicate that there are many opportunities for scan sharing in multi-tenant MapReduce clusters. In these traces, input file access frequency is roughly Zipfian, meaning that most input file accesses are for a small number of "hot" files. In addition, input file access exhibits a large amount of temporal locality. In the traces analyzed in [17], between 60 and 90% of input file re-accesses happen within one hour of the original access. In one particular workload (a Cloudera customer

running a cluster of 100 machines), 70% of input re-accesses occurred within one minute of the original access. Agrawal, Kifer and Olson [2] observe that there are often many concurrent jobs that access a shared set of data files. The authors of Comet [37] achieved a 50% reduction in total I/O in their DryadLINQ cluster using scan sharing. Scan sharing has also been shown to provide a significant improvement in job throughput for Pig and Hive workloads [61, 83, 87].

6.4.4 Read Recovery Approach

Our approach to read recovery is similar to that for write recovery; we re-read any input files that may not have been completely processed and re-map each record. In contrast to our write recovery approach, only records that the failed node would have sent to the remaining live nodes are transmitted to their destinations.

Once the read recovery process has completed, each intermediate record is guaranteed to be present on the cluster's intermediate disks at least once. To maintain correctness, however, the reduce function must not reduce multiple duplicate copies of the same record, since this would likely change the result of the job. Maintaining exactly one copy of each intermediate record is challenging and potentially quite heavyweight, since it involves tracking whether each intermediate record was successfully transmitted by the failed node prior to the failure. We avoid this complication by allowing duplicates and filtering them out on demand in a manner that is transparent to the reduce function.

6.5 Implementation

In this section, we describe the implementation of our fault tolerance strategies as an extension to Themis. Section 6.5.1 provides a brief overview of Themis' architecture, and Section 6.5.2 describes the implementation of our write and read recovery strategies in the context of that architecture. In Section 6.5.3, we describe extensions to Themis

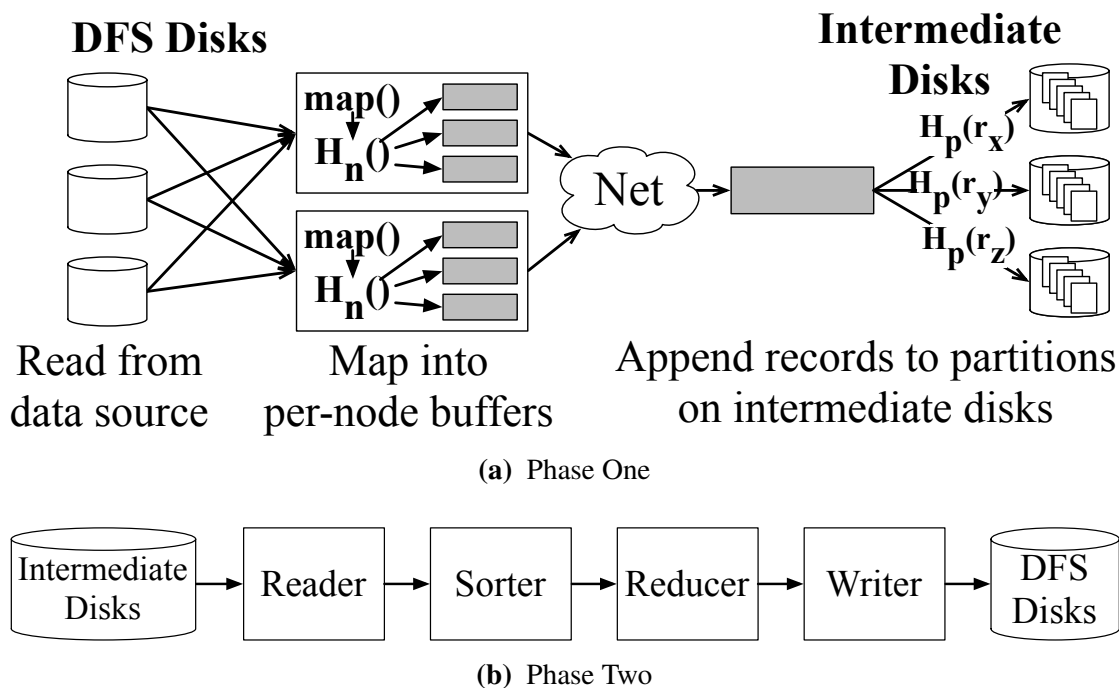


Figure 6.2. A diagrammatic overview of Themis' phases.

to support multi-tenancy. Section 6.5.4 describes the way that jobs are dispatched. Section 6.5.5 describes how files are assigned to nodes, and explores the practical concern of achieving high bandwidth from distributed storage. Section 6.5.6 describes how failures are detected and how nodes respond to failure during a job.

6.5.1 Themis: I/O-Efficient MapReduce

In this section, we present a brief recap of the design of Themis, our highly I/O-efficient MapReduce system. A more detailed description and evaluation of Themis is presented in Chapter 5. We opted to implement our fault tolerance scheme in Themis rather than Hadoop because Themis lacked a proportional fault tolerance mechanism prior to this work, whereas the task-level fault tolerance scheme used by Hadoop is a tightly-integrated part of its design.

Nodes in a Themis cluster each have a collection of *intermediate disks* that store

volatile intermediate data and a disjoint collection of *DFS disks* that store input and output data, and are typically under the control of a distributed file system like HDFS.

Themis runs a MapReduce job in two main *phases*, called *phase one* and *phase two*. In phase one, input records are read in parallel from the cluster's DFS disks. Themis applies the map function to each record, producing a collection of *intermediate records* that are written to intermediate partitions spread across the cluster's intermediate disks. Each intermediate partition holds all records with a certain set of keys. The mapping from keys to intermediate partitions is determined by a *partition function*. Phase one is roughly analogous to Hadoop's map and shuffle phases.

At the end of phase one, all intermediate records have been generated, partitioned and stored across the cluster's intermediate disks. A diagrammatic overview of phase one is given in Figure 6.2a.

In phase two, each intermediate partition is read from the cluster's intermediate disks completely into memory. Once in memory, it is sorted in-core by key, and the reduce function is applied to each group of records in the partition with the same key. This produces a collection of *output records* that are written to files on the DFS disks. Phase two is roughly equivalent to Hadoop's sort and reduce phases. A diagrammatic overview of phase two is given in Figure 6.2b.

Note that phase one requires all-to-all communication among cluster nodes, but that phase two can be executed on each node independently.

Partitioning

In order for phase two to be processed efficiently, partitions should be small enough for several of them to be processed in memory simultaneously. Additionally, they should be as uniformly-sized as possible to prevent stragglers. The partition function is responsible for ensuring both these properties. The user can provide their own partition

function, or it can be derived at runtime through an optional sampling phase called *phase zero*. Phase zero requires a fairly small sample to produce a good partition function, and typically takes under a minute to run.

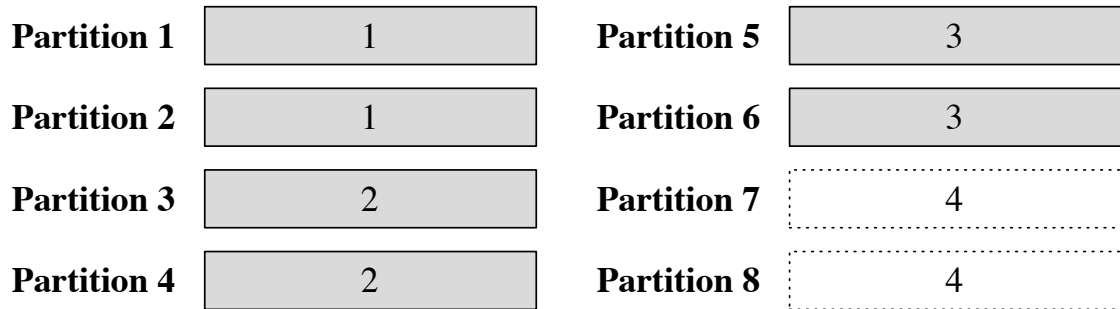
6.5.2 Recovery Mechanism

As described in Section 6.4, recovering from a failure consists of two central actions: write recovery and read recovery. In the case of Themis, write recovery involves recovering partitions on any intermediate disk that failed, while read recovery involves re-generating missing pieces of partitions that a failed node should have produced, but didn't. When a job fails, Themis will recover it by running a *recovery job*, which is treated like a normal MapReduce job but is dedicated to recovery.

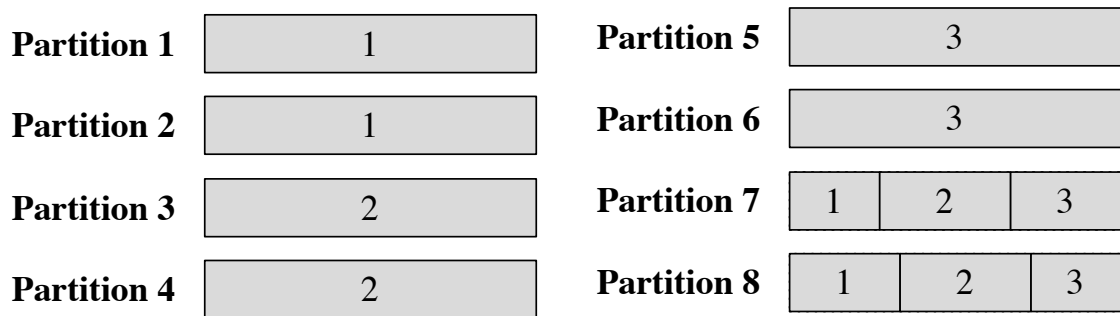
Before we explore the technical details of the implementation, consider the following illustrative example. Suppose that Themis is running on a two-node cluster with two intermediate disks each, storing a total of eight intermediate partitions for a particular job. In Figure 6.3a, disk 4 in this cluster has failed during phase one, causing the loss of partitions 7 and 8. Figure 6.3b shows the state of the intermediate partitions at the end of phase one of the recovery job, when the data for partitions 7 and 8 has been recovered.

Note that the recovered data for partitions 7 and 8 is spread across all the remaining disks roughly evenly; this is highly desirable because it allows as many disks as possible to participate in phase two of the recovery job. It should also be noted that after the failure of disk 4 in phase one, phase two can be run to completion on partitions 1 through 6 without waiting for the recovery job to recover the other partitions.

Figure 6.4a shows the same cluster after experiencing a failure of an entire node. Not only have partitions 5 through 8 been lost, but the remaining partitions are incomplete because the node did not finish producing intermediate data for those partitions before it

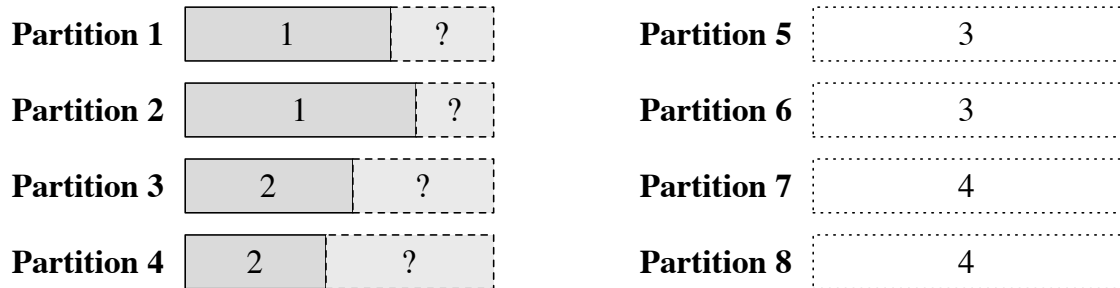


(a) The state of the job's intermediate partitions after the failure of disk 4. All intermediate partitions stored on disk 4 has been lost.

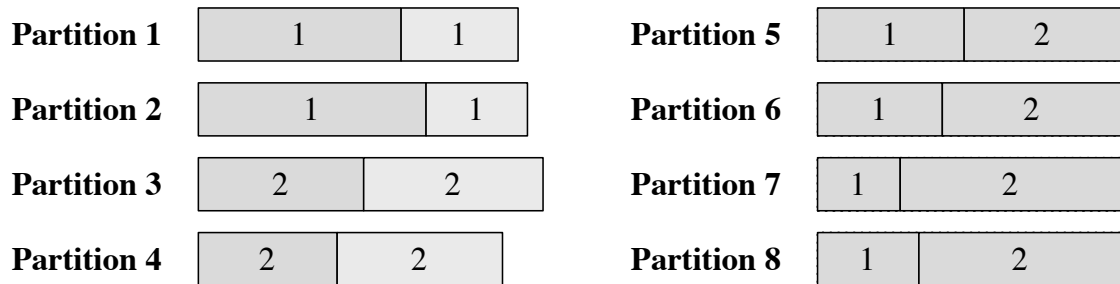


(b) The state of the job's intermediate partitions after recovery from the disk failure. Intermediate data for the partitions on disk 4 have spread across disks 1 through 3.

Figure 6.3. Illustrative example of disk failure and recovery in a two-node cluster with two intermediate disks per node and eight intermediate partitions. The rectangles representing each partition are labeled with the disk or disks on which data for that partition is stored.



(a) The state of the job's intermediate partitions after the failure of node 2. All intermediate data for disks 3 and 4 has been lost, and some data for the remaining partitions may not have been generated.



(b) The state of the job's intermediate partitions after recovery from the node failure. Intermediate data for the partitions on disks 3 and 4 have spread across disks 1 and 2, and data that should have been produced by node 2 has been added to node 1's partitions (although there may be duplicates).

Figure 6.4. Illustrative example of node failure and recovery in a two-node cluster with two intermediate disks per node and eight intermediate partitions. A '?' indicates that it is unknown whether the data has been lost or not.

failed. Once phase one of the recovery job has completed in Figure 6.4b, write recovery has spread the lost data from partitions 5 through 8 across disks 1 and 2, while read recovery has ensured that every record that belongs in partitions 1 through 4 has been written at least once.

In contrast to disk failure, phase two cannot be run after a node failure in phase one because some intermediate partitions may not be complete.

If a disk or node fails in phase two, write recovery must be performed to restore the intermediate data that was lost in the failure, but no read recovery must be performed. Since phase zero is optional and does not produce any output aside from a partition

Table 6.2. Table summarizing Themis’ response to various kinds of failures at different points in the job.

Phase	Failure	Write Recovery	Read Recovery	Run Subsequent Phases?
Zero (Sample)	Any	None	None	Yes
One (Map + Shuffle)	Disk	Failed disk’s partitions	None	Yes
One (Map + Shuffle)	Node	All node’s disks’ partitions	Node’s input files	No
Two (Sort + Reduce)	Disk	Failed disk’s partitions	None	Yes
Two (Sort + Reduce)	Node	All node’s disks’ partitions	None	Yes

function, any failure during phase zero simply requires re-executing it.

The responses to various kinds of failure in each of Themis’ stages is summarized in Table 6.2.

In the following sections, we will describe the mechanisms behind both write and read recovery.

Write Recovery

To perform write recovery, the recovery job must re-map the failed job’s input, discarding any records that were not stored on the intermediate disks that failed. To do this, the recovery job wraps its partition function in a *record filter*. This filter is applied to each record before it is passed to the partition function. Abstractly, a record filter is a function that takes a record as input and returns either “accept” or “reject”. The filter accepts a record if the record belongs to one of the partitions being recovered, and rejects it otherwise.

In practice, Themis accomplishes record filtering in one of two ways. If the failed job was using a user-defined partition function, the record filter applies the failed job’s partition function to the record. If the resulting partition number is outside the range of partitions to be recovered, the filter rejects the record.

If the original job is using a partition function generated by phase zero, the record filter stores a set of boundary key ranges, one per contiguous range of partitions being recovered. The complete list of boundary keys for each partition is stored on distributed

storage at the end of phase zero, and the filter retrieves the appropriate boundary keys when it is constructed.

When an intermediate record is emitted by the map function, the filter first compares each intermediate record's key to the boundaries of each of its ranges; if the record is within any of the filter's ranges, the filter accepts the record.

In order to speed recovery by writing to as many disks in parallel as possible, the intermediate data being recovered is spread across the cluster's remaining intermediate disks. This is done by running phase zero during the recovery job on a filtered sample of the input data, which generates a partition function that spreads data in the filtered partition ranges evenly throughout the cluster.

At the end of phase one of the recovery job, any partitions that were completely lost during a failure have been reconstituted and spread across the cluster's remaining intermediate disks.

Read Recovery

As Table 6.2 illustrates, read recovery is always performed alongside write recovery. We take advantage of this by piggy-backing read recovery on write recovery.

In order to perform read recovery, we must first know the set of files that were not completely processed by the failed node. Themis tracks which files were completely mapped and received using a form of end-to-end acknowledgments [74]. When a node is done reading a file in phase one, it sends an EOF, or "end-of-file", annotation to every node in the cluster indicating that the node will not receive any more data for the file. Special care is taken to ensure that every intermediate record associated with the file is transferred before this annotation. When a node receives an EOF annotation, it adds the file's file ID to a list. At the end of phase one, these lists are merged together to form a list of the nodes that received each file. If every live node received an EOF annotation for

a file, performing read recovery on that file is not necessary. Each input file is checked for this condition when constructing the input file list for a recovery job and files are flagged for read recovery as appropriate.

Once phase one has completed, two sets of intermediate files will exist for the failed job: the partially-complete set of files from the failed job and the set of files generated as a result of read recovery. It is likely that some of the records in these files are duplicates, and any duplicate records must be removed to retain the reduce function's correctness. To distinguish intermediate records from one another, Themis tags each intermediate record with *source metadata* that uniquely identifies the record.

To uniquely identify intermediate records, we leverage the common assumption that the map function is deterministic and, as such, that applying the map function to an input record creates a totally-ordered sequence of intermediate records. We identify an intermediate record by the position of its "parent" input record within the input dataset and its position in the totally-ordered sequence of intermediate records. Specifically, we tag each record with a 64-bit file GUID, a 64-bit offset, and a 32-bit intermediate record ID. For the purposes of evaluation, we store all 20 bytes of metadata even if the metadata could potentially be compressed; note that for records with small offsets and intermediate record IDs, these three pieces of metadata require far less than 20 bytes per record to store.

In phase two, intermediate partitions from the failed and recovery jobs with the same intermediate partition number are concatenated together into an in-memory buffer and sorted as a single intermediate partition. Before the reduce function is called on a set of intermediate records with a given key, that set of records is secondarily sorted by its source metadata. The reduce function's record iterator then skips any records whose source metadata is the same as that of the previous record.

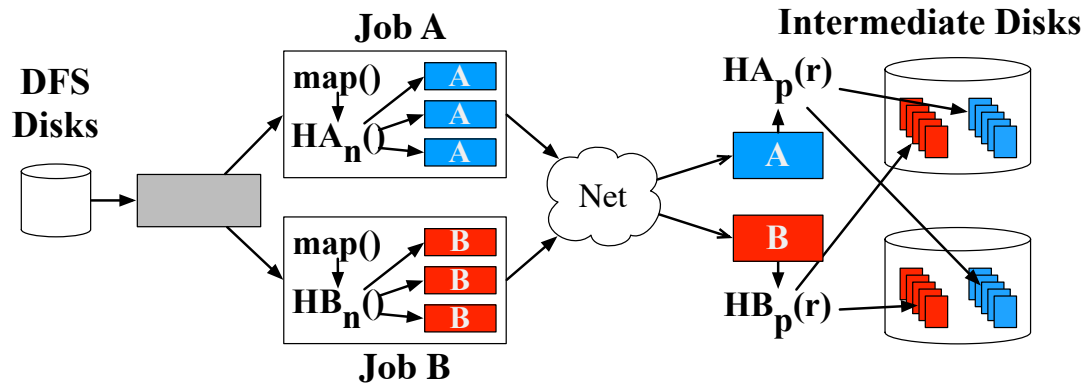


Figure 6.5. An overview of multi-tenancy in Themis. Input records are mapped by both job A and job B's map functions, and intermediate records are routed based on each job's partition function independently.

6.5.3 Multi-Tenancy in Themis

Each Themis node runs as a single process that assumes that it has exclusive access to its intermediate disks and that it will not experience memory pressure from other processes that results in swapping as long as it does not exceed its configured memory limit. Its memory and disk management subsystems (described in detail in [69] and [70]) rely on these assumptions and are the key enablers of Themis' I/O-efficiency and high performance. Hence, running multiple Themis processes on a single node would result in degraded performance since the processes would interfere with one another.

To allow multiple jobs to run simultaneously in Themis with minimal interference, we have modified Themis to support running multiple jobs concurrently within a single process. To allow for this concurrent processing, records read from disk are passed through each job's map function one function at a time, but intermediate records are transferred and written in parallel. Buffers of intermediate records produced by a map function are tagged with the unique ID of that map function's job before being sent to the appropriate destination node. Once a buffer is received, this job ID is used to determine to which set of intermediate partitions the buffer's records will be written. This process

is illustrated in Figure 6.5

A unique feature of our deployment prototype is that it does not co-schedule map and reduce function computation. Instead, it organizes jobs into *batches*, and runs phases one and two for all jobs in a batch simultaneously before processing the next batch. If phase zero needs to be run to compute partition functions for any of these jobs, it is run on each job in the batch individually before phase one starts.

6.5.4 Job Dispatch

The execution of batches of jobs is controlled by a *cluster coordinator*. The cluster coordinator accepts descriptions of batches from clients and coordinates their execution across the cluster's machines. Each machine in the cluster runs a *node coordinator* that is responsible for running a Themis process on its machine and reporting an error if it crashes.

Messages are exchanged between the user, the cluster coordinator and the node coordinators through the manipulation of message queues. Additionally, the coordinators maintain metadata about both themselves and the jobs they run. In our current implementation, the role of message queues and metadata store are both filled by a Redis [72] database. Redis was chosen primarily for convenience; a scalable key-value store like Hyperdex [29] or Cassandra [48] and message queue like Kafka [44] or Kestrel [42] could be substituted.

To run a batch, the user pushes a description of the jobs in the batch to the cluster coordinator's job queue. Upon dequeuing a batch, the cluster coordinator assigns a unique job ID to each job in the batch. It then determines the set of input files that each job will process, and divvies those files out among nodes. We describe this process in more detail in Section 6.5.5.

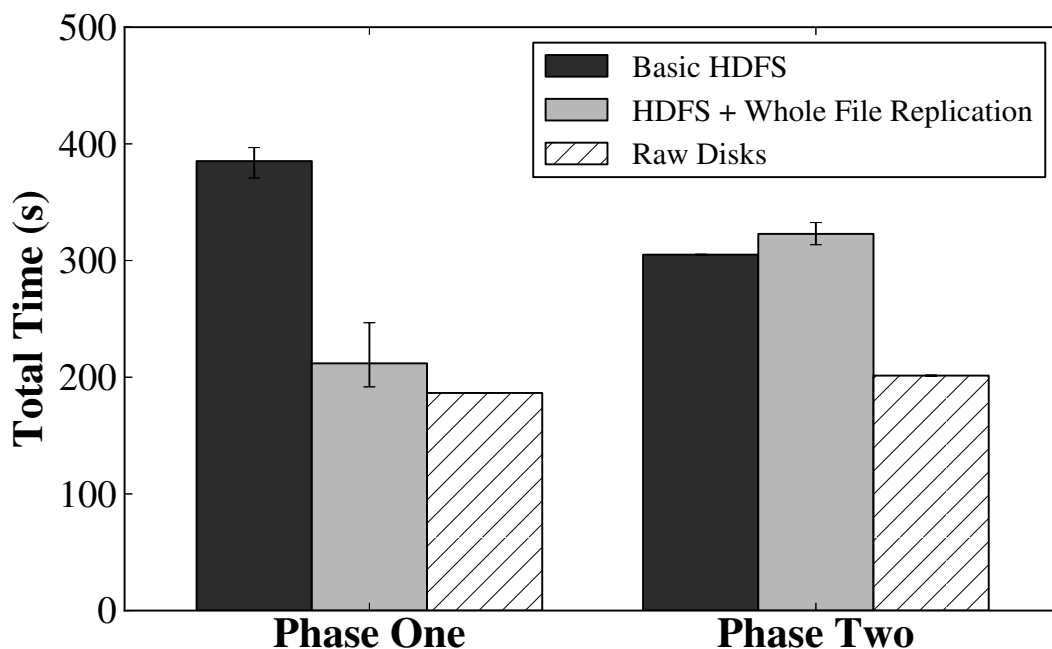


Figure 6.6. Comparing the performance of unmodified HDFS, HDFS with whole file replication for the primary replica, and reading and writing from raw disks.

6.5.5 Input Files and Distributed Storage

The specification of each Themis job includes an input directory; all files in the input directory are processed. Themis can read input files from raw disks or from HDFS [8] using the WebHDFS REST API. We use HDFS exclusively in this work.

Each file is uniquely identified by its URL, which is of the form `<protocol>://<host>:<port>/<path from root>`. Each file is also given a file ID that must be unique within the job. In our implementation, a file's ID is the upper 64 bits of the MD5 hash of its URL.

Our main concern when moving from raw disks to distributed storage was maximizing the amount of bandwidth we could achieve from the storage system. In order to achieve sufficient bandwidth, we found that we needed to change the way HDFS allocates blocks for files. In particular, we modified HDFS so that it performs *whole-file replication*

of the file's primary replica by placing every block on a specific disk in the cluster based on the file's name. For example, a file named `/1.2.3.4/3/<path>` would be stored on the third DFS disk on node `1.2.3.4`. To allow Themis to remain oblivious to this scheme, we implemented a proxy that performs a basic round-robin allocation of primary file replicas to cluster disks and transparently maps between regular and placement-aware paths. The proxy only interposes itself in communication between Themis and HDFS when a file is first opened, and imposes no additional overhead thereafter.

Figure 6.6 compares the performance of an 800GB, 8 node sort with and without these modifications; as a reminder, phase one of Themis reads sequentially from HDFS, while phase two writes sequentially to it. The substantial performance improvement for reads is the result of the elimination of read contention on each node's DFS disks when many files are being read simultaneously. However, the increased rigidity of block allocation imposed by the proxy makes the performance of writes slightly worse than unmodified HDFS.

We found that HDFS' block placement APIs were not sufficient for providing whole-file replication for all of a file's replicas. Hence, blocks for all other replicas are allocated according to HDFS' default policy, and access to non-primary replicas occurs at the speed of unmodified HDFS. The cluster coordinator will assign files to nodes that contain their primary replica whenever possible.

6.5.6 Responding to Failures

As node coordinators run, they refresh a keep-alive key in Redis every few seconds; if a node fails to refresh its keep-alive key, the cluster coordinator presumes that the node has failed. A node notifies the cluster coordinator directly if it finds that it can no longer write to one of its intermediate disks.

Themis attempts to insulate the rest of the cluster from a failure whenever one

occurs so that the healthy portion of the cluster can complete as much work as possible. To avoid the attendant complexity and fragility of coordinating failure notification across nodes, Themis simply discards any data meant for a failed portion of the cluster. When a node fails, all existing TCP sockets to that node will break. Nodes respond to broken sockets by discarding all data meant for that socket for the remainder of the batch. Similarly, when a disk fails, all data that would have been written to the failed disk for the rest of the batch is discarded. Subsequent batches will not use failed disks or nodes until an operator has explicitly marked them as having recovered.

Currently, the user is responsible for issuing a recovery job to recover a failed job. Scheduling recovery jobs to maximize the likelihood of scan sharing is beyond the scope of this work; we examine some related efforts relevant to this problem in Chapter 7.

6.6 Per-Record Replay Proportionality

When examining our options for adding fault tolerance to Themis, we were particularly motivated by the idea of being able to recover by only reading and re-mapping records whose intermediate data contributed to failed intermediate partitions. We recognized that the overhead of storing this information would potentially be quite high; in general, it requires storing information about the lineage and intermediate partition of every intermediate record. Nonetheless, we wanted to gain an understanding of the regimes in which this overhead might be a reasonable tradeoff for a decreased recovery time. In this section, we examine the potential benefits and disadvantages of this approach using a microbenchmark.

To evaluate the potential time savings from selectively reading the subset of input records needed to perform recovery, we created a 13.5 GB file on one of our cluster's disks and compared the time taken to completely scan through the file with the time taken to read a certain percentage of the file's records. The percentage of records

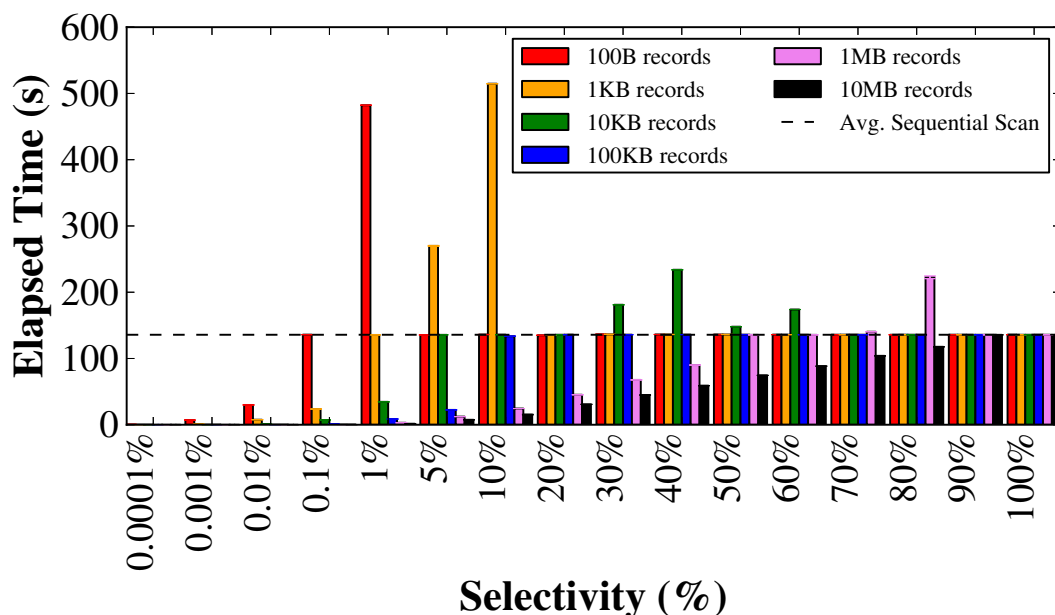
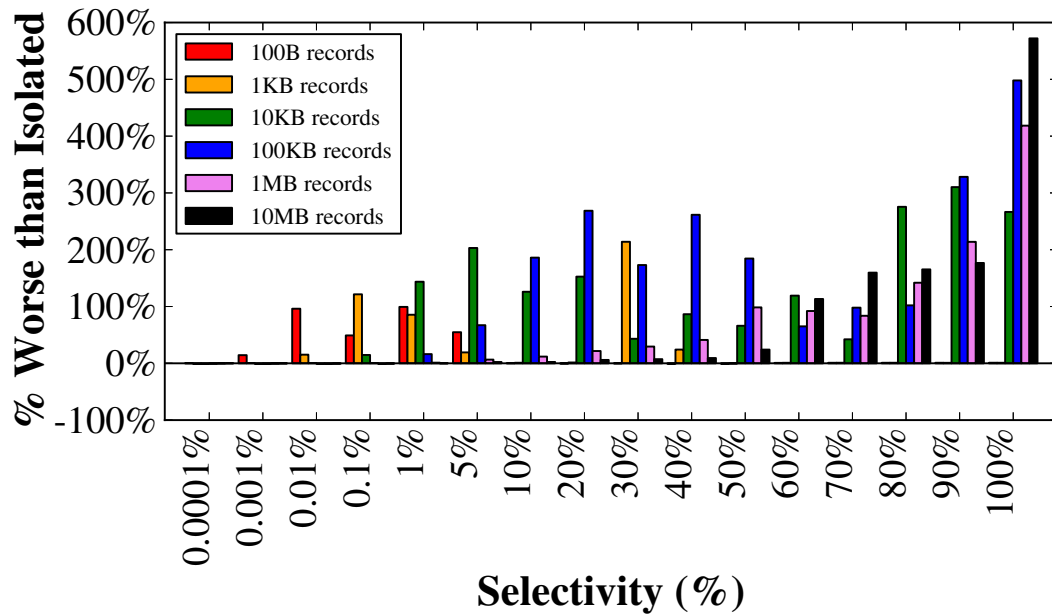


Figure 6.7. Time to sequentially scan a 13.5 GB file vs. selectively reading a percentage of records.

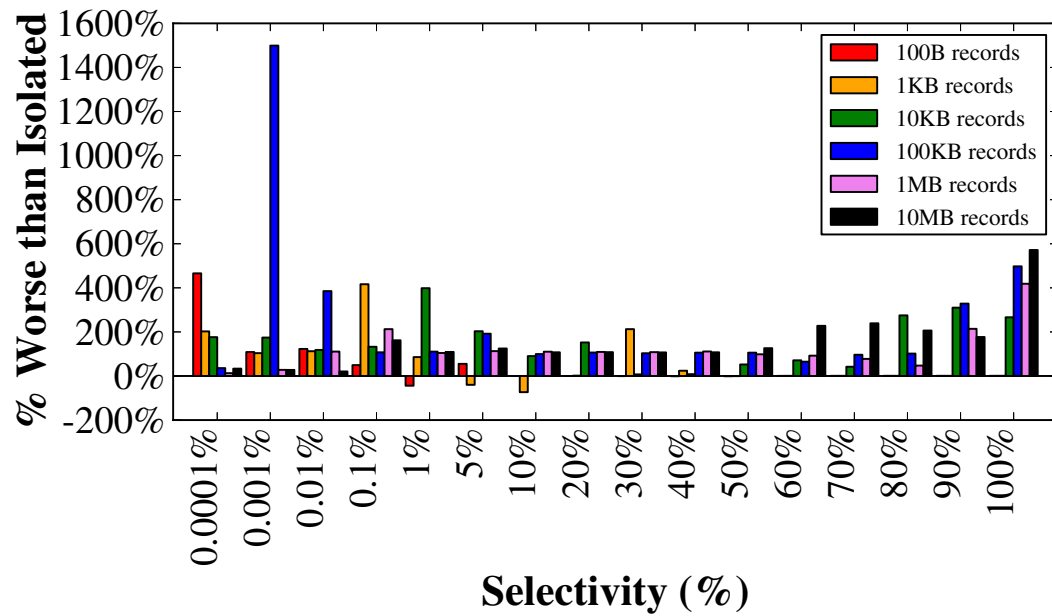
selectively read roughly corresponds to the “selectivity” of the recovery being simulated. For example, if 1% of records are being read, this corresponds to the amount of reading necessary to recover from a lost of 1% of the cluster’s intermediate partitions.

As a simplifying assumption, we assumed that the records are evenly spaced throughout the file. We completely purged the operating system’s file buffer cache and disabled any caching on our disk controllers so that each experiment started from a cold cache.

As Figure 6.7 shows, when the selectivity of recovery is quite small, selective reads can achieve large speedups over a sequential scan. However, selectively reading records is far from proportional. For example, for a file with 1KB records, the cost of sequentially scanning the file is the same as the cost of selectively reading 1% of its records; this means that the loss of more than 1% of the cluster’s intermediate partitions

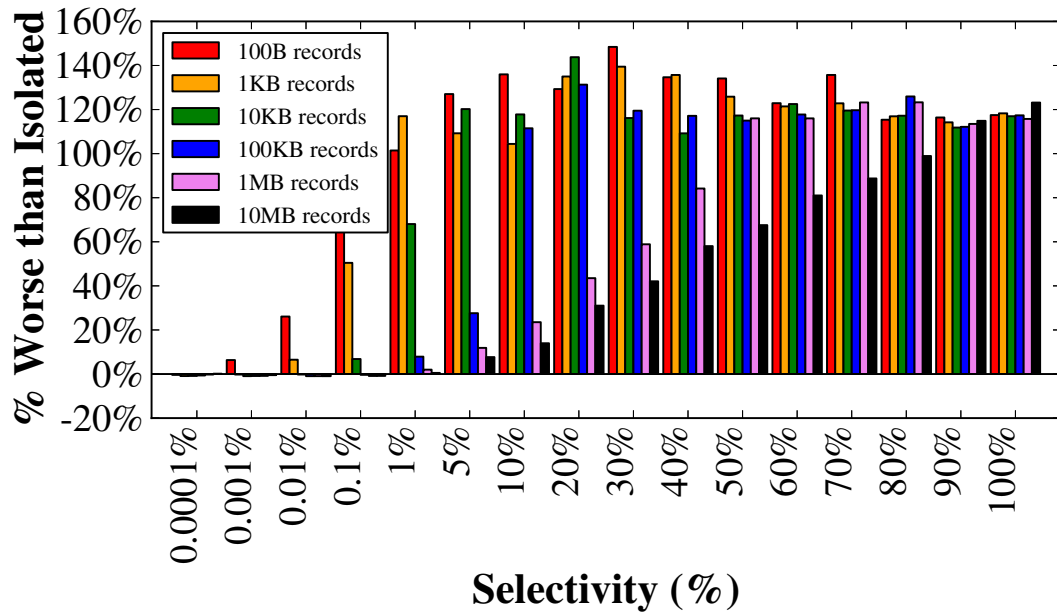


(a) The effect of simultaneity on sequential scans.

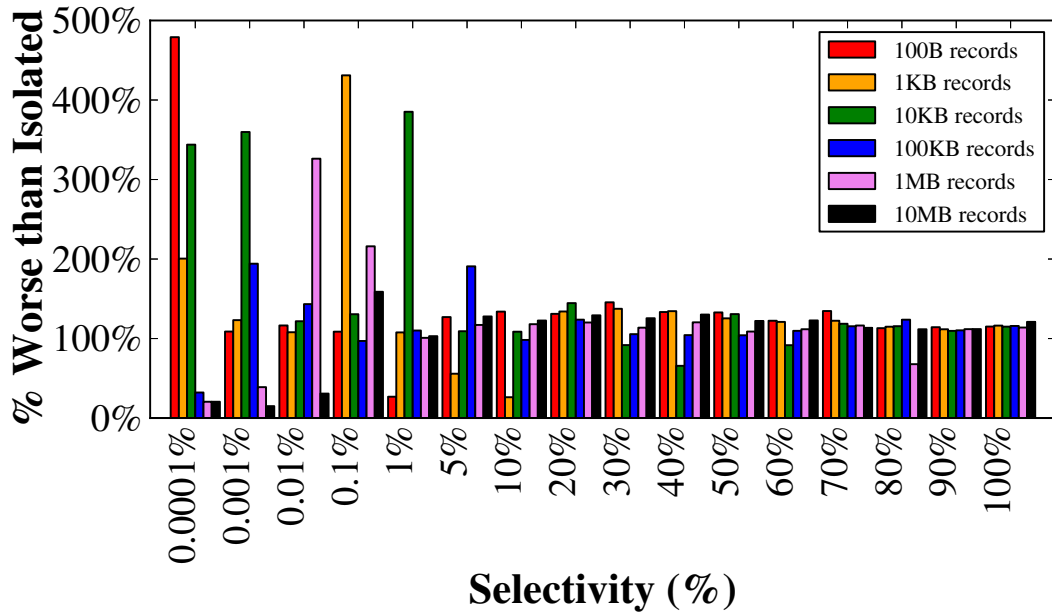


(b) The effect of simultaneity on selective reads.

Figure 6.8. The negative impact of both scanning through and selectively reading from the same file simultaneously.



(a) The effect of simultaneity on sequential scans.



(b) The effect of simultaneity on selective reads.

Figure 6.9. The negative impact of running a scan on one file while selectively reading records from a second file.

can be recovered from just as quickly by scanning input files as it can by selectively reading them for I/O-bound jobs.

We suspect that this non-proportionality is due to a combination of the overhead of seeking between records, the overhead of the relatively many `read()` syscalls needed to retrieve those records, and the behavior of the operating system's buffer cache. Note that for certain record sizes and selectivities, selective reading performs dramatically worse than sequential scanning; this is due mainly to poor interaction between the application and the buffer cache.

In addition to its non-proportionality, selective reads have a negative impact on the performance of other concurrent operations to the same disk. Figure 6.8 shows that selectively reading from a file while scanning through it simultaneously can decrease the speed of the scan by up to 600%. We believe that cache interference between the two writing processes, as well as the mechanical act of disrupting the sequentiality of disk access with seeking, are the source of these overheads.

Figure 6.9 shows the impact of running a scan and a selective read over two different files on the same disk simultaneously. Here the performance decrease for scans is much less drastic; we believe the primary source of this performance decrease to be the overhead imposed on the scan by disk seeks.

These results indicate, somewhat intuitively, that when the selectivity of the recovery is very small (less than 0.01%), it is highly beneficial to perform selective reads. However, selective reads are only a proportional form of fault tolerance if records are relatively large, and they have the potential to interact poorly with other concurrent sequential scans. In addition, a recovery with small selectivity is only likely when the cluster is fairly large, which is a different operating environment from the "dense" clusters on which we focus in this work.

6.7 Evaluation

In Section 6.7.1, we describe our experimental methodology. In Section 6.7.2, we show that recovery from both disk and node failure are proportional, in that the time taken to recover is proportional to the size of the failure. In Section 6.7.3, we show that the overhead imposed by scan sharing a normal job with a recovery job is low.

6.7.1 Methodology

We evaluated our fault tolerance mechanisms on eight of the machines in the cluster described in Section 3.3. Each hard drive is configured with a single XFS partition that is configured with a single allocation group to avoid file fragmentation across allocations groups and is mounted with the `noatime`, `nobarrier` and `noquota` flags set. For this evaluation, all servers were running Linux 2.6.32. Jobs source and sink data to HDFS, configured with 128MB blocks and whole-file replication of the primary replica of each file.

Themis is written in C++ and, in this evaluation, is compiled with g++ 4.7.1. The cluster coordinator, node coordinator and HDFS rewriting proxy are written in Python.

We rely on the sort MapReduce job to evaluate our fault tolerance mechanisms. Since sort corresponds to no-op map and reduce functions, it provides a natural way of evaluating fault tolerance independently of the job being performed. At the same time, sort's large intermediate data set size allowed us to stress-test the system's ability to scale proportionally. Additionally, we have found it logistically difficult to both obtain and store freely-available data sets that are sufficiently large that they do not fit in a single node's memory. The input data set for sort is easy to generate synthetically, which allows us to scale the evaluation beyond a single node.

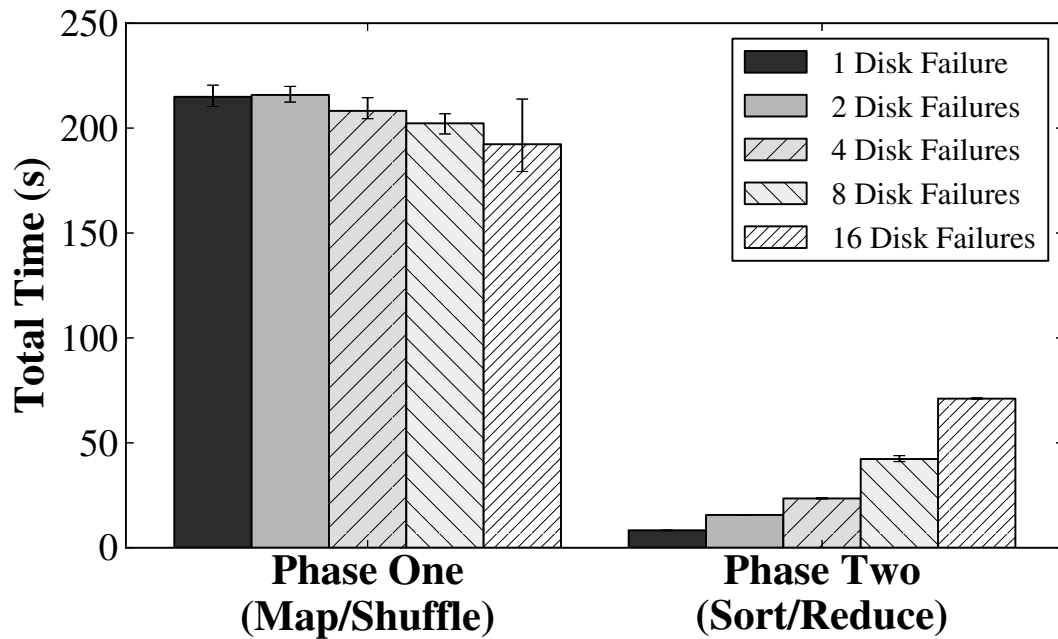


Figure 6.10. Runtime of recovery from a disk failure during an 800GB sort with an increasing number of failed disks.

6.7.2 Proportionality of Recovery

In this section, we explore the proportionality of our recovery process in response to disk and node failures.

Recovering From Disk Failure

To test the proportionality of recovery from a disk failure, we ran an 800GB sort job across our eight-node testbed and failed an increasing number of disks during phase one. Disk failures were injected into the system by making the part of Themis that writes to intermediate disks fail after it had written a certain number of bytes to the disks we wanted to fail. We then ran a recovery job to recover the data from those failed disks. Figure 6.10 shows the elapsed time of both phases for the recovery job.

The elapsed time of the recovery job's phase two increases sub-linearly as the number of disk failures increases. This is because phase two is designed to process

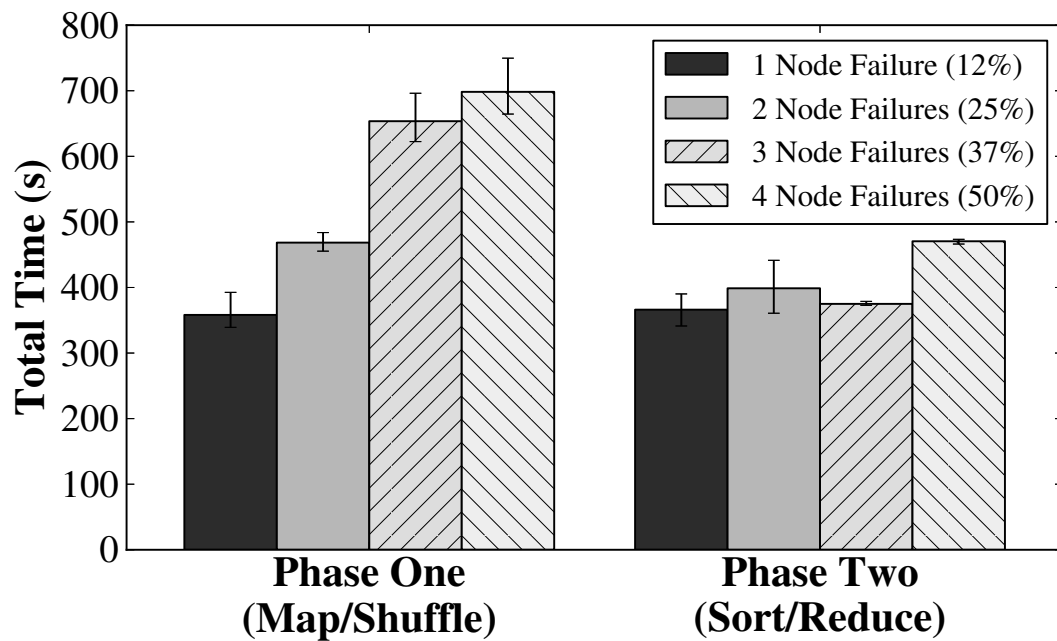


Figure 6.11. Runtime of recovery from node failures during an 800GB sort.

multiple intermediate partitions in parallel and the number of partitions created during recovery is fairly small, so processing twice as many partitions doesn't necessarily take twice as much time. The decrease in phase one's recovery time as the number of disks to recover increases is coincidental and simply reflects the variability of access time provided by HDFS.

Recovering From Node Failure

To test the proportionality of recovery from node failure, we ran the same 800GB sort job as in the disk failure tests, but instead of failing individual disks, we killed all Themis-related processes on a set of nodes approximately 120 seconds after starting the job. Each DFS disk's input consists of ten evenly-sized files, each approximately 1.6GB long. Figure 6.11 shows the elapsed time of both phases of the recovery jobs for these failures.

Phase one's recovery time increases drastically as the number of failures increase.

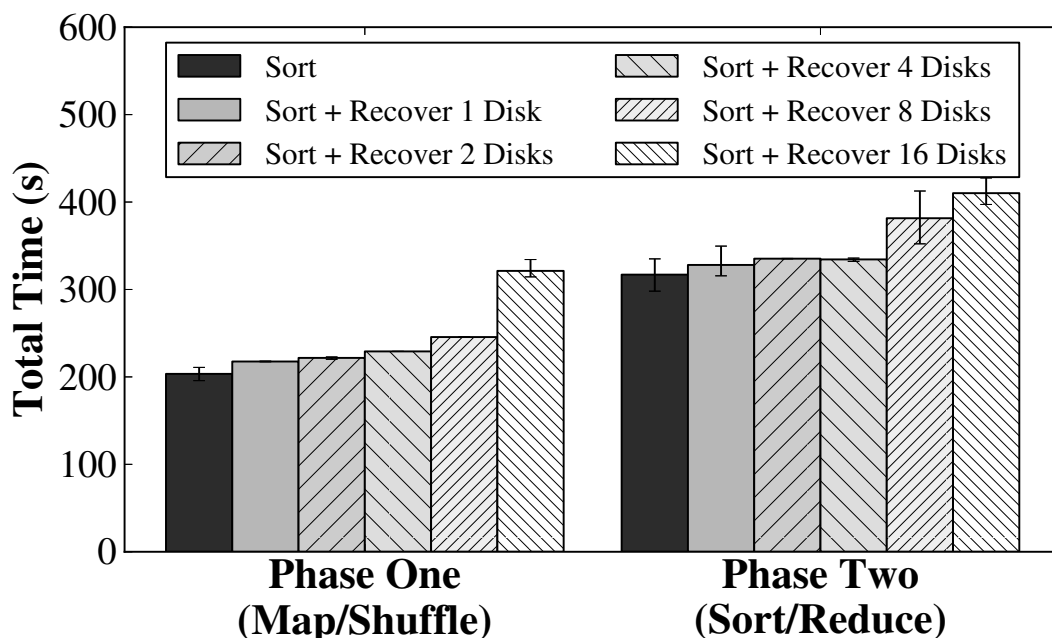


Figure 6.12. Comparing the baseline performance of an 800GB sort with the performance of scan-sharing that sort with disk failure recovery jobs.

The primary reason for this is that the same amount of recovery must be done across an increasingly small number of nodes. Recovery time in phase one is further increased by the fact that nodes are typically not accessing the whole-file-replicated primary replica of the files they are recovering; as a result, read performance degrades to that of unmodified HDFS.

Phase two's recovery time increases sub-linearly for the same architectural reasons that it increases sub-linearly during disk recovery. Due to end-of-file acknowledgments, only a small number of duplicate records are generated. As a result, phase two's node recovery is roughly equivalent to scan-sharing phase two of a normal 800GB sort with a disk recovery for all of the failed nodes' disks.

6.7.3 Scan Sharing Overhead

To evaluate the overhead imposed on a normal job by scan-sharing it with a recovery job, we ran an 800GB sort job scan-shared with the recovery jobs described in Section 6.7.2. In Figure 6.12, we see that phase one’s runtime remains fairly flat until we scan-share the sort job recovery of eight disks. At this point, the system is writing so much intermediate data to the remaining disks that it transitions from being bound by the speed at which it can read from HDFS to being bound by the speed at which it can write to its intermediate disks. At the same time, the amount of intermediate data produced by the recovery job becomes large enough to visibly impact phase two.

6.8 Conclusions

MapReduce’s traditional approach to fault tolerance is proportional, but it imposes the overhead of additional rounds of I/O in common-case operation, which negatively impacts the system’s overall performance. In this work, we have shown that, through leveraging the multi-tenancy typical of a MapReduce cluster and composing previously-known fault tolerance techniques, it is possible to provide proportional fault tolerance without imposing additional rounds of I/O in failure-free operation.

6.9 Acknowledgments

This work was sponsored in part by NSF Grants CSR-1116079 and MRI CNS-0923523, and through donations by Cisco Systems and a NetApp Faculty Fellowship.

Chapter 6 contains material as it appears in the Proceedings of the ACM Symposium on Cloud Computing (SOCC) 2012. Rasmussen, Alexander; Porter, George; Vahdat, Amin. The dissertation author was the primary investigator and author of this paper.

Chapter 6 contains material submitted for publication as “I/O-Efficient Fault Tolerance for MapReduce”. Rasmussen, Alexander; Porter, George; Vahdat, Amin. The dissertation author was the primary investigator and author of this paper.

Chapter 7

Related Work

7.1 Large-Scale Sorting Systems

The Datamation sorting benchmark[7] initially measured the elapsed time to sort one million records from disk to disk. As hardware has improved, the number of records required by the benchmark has grown to its current level of 100TB. Over the years, numerous authors have reported the performance of their sorting systems, and we benefit from their insights[67, 45, 88, 9, 59, 58]. We differ from previous sort benchmark holders in that we focus on maximizing both aggregate throughput and per-node efficiency.

NOWSort[9] was the first of the aforementioned sorting systems to run on a shared-nothing cluster. NOWSort employs a two-phase pipeline that generates multiple sorted runs in the first phase and merges them together in the second phase, a technique shared by DEMSort[67]. An evaluation of NOWSort done in 1998[10] found that its performance was limited by I/O bus bandwidth and poor instruction locality. Modern PCI buses and multi-core processors have largely eliminated these concerns; in practice, TritonSort is bottlenecked by disk bandwidth.

7.2 Achieving Per-Resource Balance

Achieving per-resource balance in a large-scale data processing system is the subject of a large volume of previous research dating back at least as far as 1970. Among the more well-known guidelines for building such systems are the Amdahl/Case rules of thumb for building balanced systems [5] and Gray and Putzolu’s “five-minute rule” [33] for trading off memory and I/O capacity. These guidelines have been re-evaluated and refreshed as hardware capabilities have increased.

7.3 Architectural Influences

The staged, pipelined dataflow architecture used in both TritonSort and Themis is inspired in part by SEDA[84], a staged, event-driven software architecture that decouples worker stages by interposing queues between them. Data-intensive systems like Dryad [40] export a similar model, although Dryad has several capabilities that TritonSort and Themis do not currently implement.

Many of our design decisions are informed by lessons learned from parallel database systems. Gamma[25] was one of the first parallel database systems to be deployed on a shared-nothing cluster. To maximize throughput, Gamma employs horizontal partitioning to allow separable queries to be performed across many nodes in parallel, an approach that is similar in many respects to our use of logical disks. TritonSort’s Sender-Receiver pair is similar to the exchange operator first introduced by Volcano[32] in that it abstracts data partitioning, flow control, parallelism and data distribution from the rest of the system.

7.4 Fault Tolerance Techniques

There is a large continuum of fault tolerance options between task-level and job-level fault tolerance. Percolator [65] provides ACID-compliant transactions with snapshot-isolation semantics on its multi-petabyte document repository. Checkpointing and rollback is another popular form of fault tolerance; we refer the reader to [28] for a survey of different techniques in this space. FLuX [78] uses process-pairs replication to ensure that if one of the two replicas fails, data processing can still continue seamlessly.

Several efforts have been made to increase the resilience of intermediate data without dramatically impacting performance. ISS [43] provides a replicated storage layer that increases the failure resilience of intermediate and output data by asynchronously replicating it. HOP [19] pipelines the transmission of intermediate data from map tasks to reduce tasks with its materialization to local disk, only acting on optimistically transmitted data when it has been “committed” at the source.

Lineage has long been of interest to a wide range of fields, in areas as diverse as ensuring that research results can be reproduced [13], determining which source records contributed to a record in a materialized view [20], and policy enforcement [89]. Spark [91] uses lineage at the RDD level to provide fault tolerance for RDDs.

Recovery-Oriented Computing (ROC) [15, 71] is a research vision that focuses on efficient recovery from failure, rather than focusing exclusively on failure avoidance. This is helpful in environments where failure is inevitable, such as data centers. The design of task-level fault tolerance in existing MapReduce implementations shares similar goals with the ROC project.

7.5 Multi-Query Optimization and Scan Sharing

In the MapReduce context, multi-query optimization typically focuses on reducing the number of I/O operations required to execute a set of jobs. Agrawal, Kifer and Olson [2]’s scheduling approach for MapReduce decides whether to try to delay jobs for possible scan sharing based on a model of job arrival times and input file access patterns. Circumflex [86] builds upon this work by relaxing some of the modeling assumptions. In [94], Zhang proposes a cost function for estimating the savings from scan sharing. MRShare [60] applies multi-query optimization to Hadoop, rewriting jobs that arrive in batches so that they share input data scans.

7.6 Improving MapReduce’s Performance

Several efforts aim to improve MapReduce’s efficiency and performance. Some focus on runtime changes to better handle common patterns like job iteration [14], while others have extended the programming model to handle incremental updates [49, 65]. Work on new MapReduce scheduling disciplines [93] has improved cluster utilization at a map- or reduce-task granularity by minimizing the time that a node waits for work. Tenzing [16], a SQL implementation built atop the MapReduce framework at Google, relaxes or removes the restriction that intermediate data be sorted by key in certain situations to improve performance.

Massively parallel processing (MPP) databases often perform aggregation in memory to eliminate unnecessary I/O if the output of that aggregation does not need to be sorted. Themis could skip an entire read and write pass by pipelining intermediate data through the reduce function directly if the reduce function was known to be commutative and associative. We chose not to do so to keep Themis’s operational model equivalent to the model presented in the original MapReduce paper.

7.7 Skew Mitigation in MapReduce

Characterizing input data in both centralized and distributed contexts has been studied extensively in the database systems community [50, 52, 35], but many of the algorithms studied in this context assume that records have a fixed size and are hence hard to adapt to variably-sized, skewed records. Themis’s skew mitigation techniques bear strong resemblance to techniques used in MPP shared-nothing database systems [24].

The original MapReduce paper [22] acknowledges the role that imbalance can play on overall performance, which can be affected by data skew. SkewReduce [46] alleviates the computational skew problem by allowing users to specify a customized cost function on input records. Partitioning across nodes relies on this cost function to optimize the distribution of data to tasks. SkewTune [47] proposes a more general framework to handle skew transparently, without requiring hints from users. SkewTune is activated when a slot becomes idle in the cluster, and the task with the greatest estimated remaining time is repartitioned to take advantage of that slot. This reallocates the unprocessed input data through range-partitioning, similar to Themis’s phase zero.

Sailfish [68] aims to mitigate partitioning skew in MapReduce by choosing the number of reduce tasks and intermediate data partitioning dynamically at runtime. It chooses these values using an index constructed on intermediate data. Sailfish and Themis represent two design points in a space with the similar goal of improving MapReduce’s performance through more efficient disk I/O.

Chapter 8

Conclusions and Future Directions

Existing large-scale data processing systems scale out quite well, but do not scale up; put another way, they do not utilize their clusters' resources to nearly the extent that they should. In this dissertation, we have presented two systems that illustrate the substantial gain in per-node efficiency that can be realized if a minimal amount of efficiently-performed I/O is considered as a first-class architectural concern.

In this chapter, we summarize the systems presented in this dissertation, and discuss Themis's present limitations and some possible future research directions.

8.1 Summary

With TritonSort, we have shown that a particular representative problem in this space, large-scale sorting, can be performed at close to the maximum throughput of the cluster through careful management of system resources to ensure cross-resource balance. TritonSort's architecture is based on two central, intuitive principles:

- **When possible, write in large, sequential chunks.** The reasoning behind this principle applies mainly to magnetic hard drives, due to these devices' physical characteristics. TritonSort's user-level, global disk management subsystem performs fine-grained, dynamic buffering in front of a node's disks to ensure that

writes are large and sequential even when the performance of a given disk is variable.

- **Read and write as little as possible.** Since secondary storage is likely to remain the bottleneck for large-scale data processing well into the future, it is critical that data processing systems read and write to secondary storage as little as possible. TritonSort’s two phase external sort pipelines records aggressively; it reads and writes each record exactly twice, the theoretical lower bound for external sorting.

With Themis, we showed that TritonSort’s two central principles could be applied to a wider class of data-intensive problems. However, in order to achieve similar performance benefits for general-purpose problems, we had to significantly overhaul the way that we managed memory and partition intermediate data adaptively. The resulting sampling and user-level memory management systems allow for fine-grained, policy-driven control of memory access in a way that allows jobs running in Themis to make progress in the face of significant amounts of skew without creating stragglers. Themis executes a wide range of MapReduce jobs with significantly higher per-node efficiency than existing systems.

The aggressive pipelining adopted by both TritonSort and Themis comes at a cost; the loss of any intermediate data requires that it be recomputed, since it was only materialized in one place. We have shown that, in many scenarios, the penalty imposed by complete re-computation on failure is significantly less than the performance penalty of intermediate materialization. Further, we have presented a modification to Themis that allows for proportional recovery from faults. The central principle of this recovery mechanism is that by taking advantage of the nature of multi-tenancy in modern MapReduce clusters and relaxing the assumption that each intermediate record is created exactly once, one can dramatically decrease the overhead of job re-execution.

We believe that this work holds a number of lessons for efficient data-intensive system design and scale-out architectures in general, and will help inform the construction of more efficient systems that will bridge the gap between scalability and per-node efficiency.

8.2 Limitations and Future Work

Themis’s high level of performance is predicated on its ability to tightly control access to its host machine’s I/O and memory. As a consequence, it is unclear how Themis would perform when sharing a cluster of machines with other applications. It is possible that some of Themis’s features (such as its unified control over disk I/O) might be incorporated into a lower-level service that all processes could share, but we have not explored this approach.

At present, phase one of Themis’s execution is limited by the speed of the slowest node, and is thus negatively affected by stragglers. Since Themis does not split its jobs into tasks, it is harder for it to support traditional methods of straggler mitigation such as speculative execution. Investigating alternate means of straggler mitigation is the subject of ongoing work.

A potential concern with the “scan-and-discard” method of fault tolerance that we have not addressed in this work is the CPU overhead involved in needlessly mapping input records whose intermediate data is not being recovered. Modifying our approach to account for this overhead is the subject of future work.

One clear avenue of future study is augmenting replicated storage systems like HDFS so that they achieve performance close to that of raw disk. Our primary whole-file replication approach, while fairly effective when the primary replica is available, is admittedly fragile, and more adaptive or workload-aware solutions could provide performance much closer to that of raw disks.

Currently, the number of workers in each stage is fixed. To make the system easier to configure, it would be valuable to dynamically determine the number of workers that a stage needs to not bottleneck previous stages. A stage's performance on synthetic data in isolation provides a reasonable upper-bound on its performance, but any synthetic analysis does not take runtime conditions such as CPU scheduling and cache contention into account. Therefore, some manner of online learning algorithm will be necessary to determine a good configuration at runtime.

Solid-state drives, or SSDs, are rapidly decreasing in cost per gigabyte but have not approached the low price provided by magnetic hard drives. Nevertheless, it is worth exploring the applicability of our design principles to solid-state storage like SSDs and PCI-attached flash.

It is also worth exploring the applicability of our user-level memory and disk management subsystems in a more general-purpose setting. For example, languages like Pig and Hive that currently compile to a sequence of MapReduce jobs could be compiled into a single distributed dataflow graph and thus forego a great deal of often unnecessary intermediate data materialization.

Bibliography

- [1] Alok Aggarwal and Jeffrey Vitter. The Input/Output Complexity of Sorting and Related Problems. *Communications of the ACM*, 31(9):1116–1127, September 1988.
- [2] Parag Agrawal, Daniel Kifer, and Christopher Olston. Scheduling Shared Scans of Large Data Files. *Proceedings of the VLDB Endowment*, 1(1):958–969, August 2008.
- [3] Mohammad Alizadeh, Albert Greenberg, David A. Maltz, Jitendra Padhye, Parveen Patel, Balaji Prabhakar, Sudipta Sengupta, and Murari Sridharan. Data Center TCP (DCTCP). In *ACM Special Interest Group on Data Communication (SIGCOMM)*, 2010.
- [4] Gene Amdahl. Validity of the Single Processor Approach to Achieving Large Scale Computational Capabilities. In *AFIPS Spring Joint Computer Conference*, 1967.
- [5] Gene Amdahl. Storage and I/O Parameters and System Potential. In *IEEE Computer Group Conference*, 1970.
- [6] Eric Anderson and Joseph Tucek. Efficiency Matters! In *USENIX Workshop on Hot Topics in Storage and File Systems (HotStorage)*, 2009.
- [7] Anon et al. A Measure of Transaction Processing Power. *Datamation*, 1985.
- [8] Apache Software Foundation. HDFS Architecture Guide. http://hadoop.apache.org/docs/hdfs/current/hdfs_design.html.
- [9] Andrea C. Arpaci-Dusseau, Remzi H. Arpaci-Dusseau, David E. Culler, Joseph M. Hellerstein, and David A. Patterson. High-Performance Sorting on Networks of Workstations. In *ACM Special Interest Group on the Management of Data (SIGMOD)*, 1997.
- [10] R.H. Arpaci-Dusseau, A.C. Arpaci-Dusseau, D.E. Culler, J.M. Hellerstein, and D.A. Patterson. The Architectural Costs of Streaming I/O: A Comparison of Workstations, Clusters, and SMPs. In *HPCA*, pages 90–101, 1998.

- [11] Magdalena Balazinska, Joeng-Hyon Hwang, and Mehul A. Shah. Fault Tolerance and High Availability in Data Stream Management Systems. <http://www.cs.washington.edu/homes/magda/encyclopedia-long.pdf>.
- [12] Eric Bauer, Xuemei Zhang, and Douglas Kimber. *Practical System Reliability* (pg. 226). Wiley-IEEE Press, 2009.
- [13] Rajendra Bose and James Frew. Lineage Retrieval for Scientific Data Processing: A Survey. *ACM Computing Surveys*, 37, 2005.
- [14] Yingyi Bu, Bill Howe, Magdalena Balazinska, and Michael D. Ernst. HaLoop: Efficient Iterative Data Processing on Large Clusters. In *Conference on Very Large Databases (VLDB)*, 2010.
- [15] George Candea, Shinichi Kawamoto, Yuichi Fujiki, Greg Friedman, and Armando Fox. Microreboot – A Technique for Cheap Recovery. In *USENIX Symposium on Operating Systems Design and Implementation (OSDI)*, 2004.
- [16] Biswapesh Chattopadhyay, Liang Lin, Weiran Liu, Sagar Mittal, Prathyusha Aragonda, Vera Lychagina, Younghee Kwon, and Michael Wong. Tenzing: A SQL Implementation On The MapReduce Framework. In *Proceedings of the VLDB Endowment*, 2011.
- [17] Yanpei Chen, Sara Alspaugh, and Randy Katz. Interactive Analytical Processing in Big Data Systems: A Cross-Industry Study of MapReduce Workloads. In *Conference on Very Large Databases (VLDB)*, 2012.
- [18] Dell and Cloudera Hadoop Platform. <http://www.cloudera.com/company/press-center/releases/dell-and-cloudera-collaborate-to-enable-large-scale-data-analysis-and-modeling-through-open-source/>.
- [19] Tyson Condie, Neil Conway, Peter Alvaro, Joseph M. Hellerstein, Khaled Elmelegy, and Russell Sears. MapReduce Online. In *USENIX Symposium on Networked Systems Design and Implementation (NSDI)*, 2010.
- [20] Yingwei Cui, Jennifer Widom, and Janet L. Wiener. Tracing the Lineage of View Data in a Warehousing Environment. *ACM Transactions on Database Systems (TODS)*, 25(2), June 2000.
- [21] Jeff Dean. Software Engineering Advice from Building Large-Scale Distributed Systems. <http://research.google.com/people/jeff/stanford-295-talk.pdf>.
- [22] Jeffrey Dean and Sanjay Ghemawat. MapReduce: Simplified Data Processing on Large Clusters. In *USENIX Symposium on Operating Systems Design and Implementation (OSDI)*, 2004.

- [23] Gary Demasi. More Renewable Energy for Our Data Centers. <http://googleblog.blogspot.com/2012/09/more-renewable-energy-for-our-data.html>, 2012.
- [24] David DeWitt and Jim Gray. Parallel Database Systems: The Future of High Performance Database Systems. *Communications of the ACM*, 35(6), June 1992.
- [25] D.J. DeWitt, S. Ghandeharizadeh, D.A. Schneider, A. Bricker, H.-I. Hsiao, and R. Rasmussen. The Gamma Database Machine Project. *IEEE Transactions on Knowledge and Data Engineering (TKDE)*, 1990.
- [26] D.J. DeWitt, J.F. Naughton, and D.a. Schneider. Parallel Sorting on a Shared-Nothing Architecture Using Probabilistic Splitting. In *International Conference on Parallel and Distributed Information Systems*, 1991.
- [27] Data, data everywhere. *The Economist*, February 2010.
- [28] E. N. (Mootaz) Elnozahy, Lorenzo Alvisi, Yi Wang, and David B. Johnson. A Survey of Rollback-Recovery Protocols in Message-Passing Systems. *ACM Computing Surveys*, 34(3), September 2002.
- [29] Robert Escriva, Bernard Wong, and Emin Gn Sirer. HyperDex: A Distributed, Searchable Key-Value Store. In *ACM Special Interest Group on Data Communication (SIGCOMM)*, 2012.
- [30] Daniel Ford, Francois Labelle, Florentina I. Popovici, Murray Stokely, Van-Anh Truong, Luiz Barroso, Carrie Grimes, and Sean Quinlan. Availability in Globally Distributed Storage Systems. In *USENIX Symposium on Operating Systems Design and Implementation (OSDI)*, 2010.
- [31] William Forrest, James Kaplan, and Noah Kindler. Data Centers: How to Cut Carbon Emissions and Costs. Technical report, McKinsey and Company, 2008.
- [32] G. Graefe. Volcano - An Extensible and Parallel Query Evaluation System. *IEEE Transactions on Knowledge and Data Engineering (TKDE)*, 1994.
- [33] Jim Gray and Gianfranco R. Putzolu. The 5 Minute Rule for Trading Memory for Disk Accesses and The 10 Byte Rule for Trading Memory for CPU Time. In *ACM Special Interest Group on the Management of Data (SIGMOD)*, 1987.
- [34] Jim Gray and Andreas Reuter. *Transaction Processing: Concepts and Techniques*. Morgan Kaufmann Publishers, 1993.
- [35] M. Hadjieleftheriou, J.W. Byers, and G. Kollios. Robust Sketching and Aggregation of Distributed Data Streams. Technical Report 2005-011, Boston University, 2005.
- [36] Hadoop PoweredBy Index. <http://wiki.apache.org/hadoop/PoweredBy>.

- [37] Bingsheng He, Mao Yang, Zhenyu Guo, Rishan Chen, Bing Su, Wei Lin, and Lidong Zhou. Comet: Batched Stream Processing for Data Intensive Distributed Computing. In *ACM Symposium on Cloud Computing (SoCC)*, 2010.
- [38] Tony Hey, Stewart Tansley, and Kristin Tolle. *The Fourth Paradigm: Data-Intensive Scientific Discovery*. Microsoft Corporation, 2009.
- [39] Bill Howe. lakewash_combined_v2.genes.nucleotide. https://dada.cs.washington.edu/research/projects/db-data-L1_bu/escience_datasets/seq_alignment/.
- [40] Michael Isard, Mihai Budiu, Yuan Yu, Andrew Birrell, and Dennis Fetterly. Dryad: Distributed Data-Parallel Programs From Sequential Building Blocks. In *European Conference on Computer Systems (EuroSys)*, 2007.
- [41] Jay Parikh. Big Data Whiteboard - 082212. <http://www.scribd.com/doc/103621762/Big-Data-Whiteboard-082212>.
- [42] Kestrel. <http://robey.github.com/kestrel/>.
- [43] Steven Y. Ko, Imranul Hoque, Brian Cho, and Indranil Gupta. Making Cloud Intermediate Data Fault-Tolerant. In *ACM Symposium on Cloud Computing (SoCC)*, 2010.
- [44] Jay Kreps, Neha Narkhede, and Jun Rao. Kafka: A Distributed Messaging System for Log Processing. In *International Workshop on Networking Meets Databases (NetDB)*, 2011.
- [45] Bradley C. Kuzmaul. TeraByte TokuSampleSort, 2007. <http://sortbenchmark.org/tokutera.pdf>.
- [46] YongChul Kwon, Magdalena Balazinska, Bill Howe, and Jerome Rolia. Skew-Resistant Parallel Processing of Feature-Extracting Scientific User-Defined Functions. In *ACM Symposium on Cloud Computing (SoCC)*, 2010.
- [47] YongChul Kwon, Magdalena Balazinska, Bill Howe, and Jerome Rolia. SkewTune: Mitigating Skew in MapReduce Applications. In *ACM Special Interest Group on the Management of Data (SIGMOD)*, 2012.
- [48] Avinash Lakshman and Prashant Malik. Cassandra: A Decentralized Structured Storage System. In *Large-Scale Distributed Systems and Middleware (LADIS)*, 2009.
- [49] Dionysios Logothetis, Christopher Olston, Benjamin Reed, Kevin C. Webb, and Ken Yocum. Stateful Bulk Processing for Incremental Analytics. In *ACM Symposium on Cloud Computing (SoCC)*, 2010.

- [50] Gurmeet Singh Manku, Sridhar Rajagopalan, and Bruce G. Lindsay. Random Sampling Techniques for Space Efficient Online Computation of Order Statistics of Large Datasets. In *ACM Special Interest Group on the Management of Data (SIGMOD)*, 1999.
- [51] Maurice de Kunder. WorldWideWebSize.com — The Daily Estimated Size of the World Wide Web. <http://www.worldwidewebsite.com/>.
- [52] James P. McDermott, G. Jogesh Babu, John C. Liechty, and Dennis K. Lin. Data Skeletons: Simultaneous Estimation of Multiple Quantiles for Massive Streaming Datasets with Applications to Density Estimation. *Statistics and Computing*, 17(4), December 2007.
- [53] Michael C Schatz. CloudBurst: Highly Sensitive Read Mapping with MapReduce. *Bioinformatics*, 25(11):1363–9, 2009.
- [54] Jeffrey C. Mogul and K. K. Ramakrishnan. Eliminating Receive Livelock in an Interrupt-Driven Kernel. *ACM Transactions on Computer Systems*, 15(3), August 1997.
- [55] Curt Monash. Petabyte-Scale Hadoop Clusters (Dozens of Them). <http://www.dbms2.com/2011/07/06/petabyte-hadoop-clusters/>.
- [56] Walid A Najjar, Edward A Lee, and Guang R Gao. Advances in the Dataflow Computational Model. *Parallel Computing*, 25(13):1907 – 1929, 1999.
- [57] Suman Nath, Haifeng Yu, Phillip B. Gibbons, and Srinivasan Seshan. Subtleties in Tolerating Correlated Failures in Wide-Area Storage Systems. In *USENIX Symposium on Networked Systems Design and Implementation (NSDI)*, 2006.
- [58] Chris Nyberg, Tom Barclay, Zarka Cvetanovic, Jim Gray, and Dave Lomet. Alphasort: A Cache-Sensitive Parallel External Sort. In *Conference on Very Large Databases (VLDB)*, 1995.
- [59] Chris Nyberg, Charles Koester, and Jim Gray. NSort: A Parallel Sorting Program for NUMA and SMP Machines, 1997.
- [60] Tomasz Nykiel, Michalis Potamias, Chaitanya Mishra, George Kollios, and Nick Koudas. MRShare: Sharing Across Multiple Queries in MapReduce. *Proceedings of the VLDB Endowment*, 3(1-2):494–505, September 2010.
- [61] Christopher Olston, Greg Chiou, Laukik Chitnis, Francis Liu, Yiping Han, Mattias Larsson, Andreas Neumann, Vellanki B.N. Rao, Vijayanand Sankarasubramanian, Siddharth Seth, Chao Tian, Topher ZiCornell, and Xiaodan Wang. Nova: Continuous Pig/Hadoop Workflows. In *ACM Special Interest Group on the Management of Data (SIGMOD)*, 2011.

- [62] Owen O'Malley and Arun C. Murthy. Winning a 60 Second Dash with a Yellow Elephant. <http://sortbenchmark.org/Yahoo2009.pdf>.
- [63] Diego Ongaro, Stephen M. Rumble, Ryan Stutsman, John Ousterhout, and Mendel Rosenblum. Fast Crash Recovery in RAMCloud. In *ACM Symposium on Operating Systems Principles (SOSP)*, 2011.
- [64] Lawrence Page, Sergey Brin, Rajeev Motwani, and Terry Winograd. The PageRank Citation Ranking: Bringing Order to the Web. Technical Report 1999-66, Stanford InfoLab, November 1999. Previous number = SIDL-WP-1999-0120.
- [65] Daniel Peng and Frank Dabek. Large-Scale Incremental Processing Using Distributed Transactions and Notifications. In *USENIX Symposium on Operating Systems Design and Implementation (OSDI)*, 2010.
- [66] Eduardo Pinheiro, Wolf Weber, and Luiz Andre Barroso. Failure Trends in a Large Disk Drive Population. In *USENIX Conference on File and Storage Technologies (FAST)*, 2007.
- [67] Mirko Rahn, Peter Sanders, Johannes Singler, and Tim Kieritz. DEMSort – Distributed External Memory Sort, 2009. <http://sortbenchmark.org/demsort.pdf>.
- [68] Sriram Rao, Raghu Ramakrishnan, Adam Silberstein, Mike Ovsiannikov, and Damian Reeves. Sailfish: A Framework for Large Scale Data Processing. In *ACM Symposium on Cloud Computing (SoCC)*, 2012.
- [69] Alexander Rasmussen, Michael Conley, Rishi Kapoor, Vinh The Lam, George Porter, and Amin Vahdat. Themis: An I/O-Efficient MapReduce. In *ACM Symposium on Cloud Computing (SoCC)*, 2012.
- [70] Alexander Rasmussen, George Porter, Michael Conley, Harsha V. Madhyastha, Radhika Niranjana Mysore, Alexander Pucher, and Amin Vahdat. TritonSort: A Balanced Large-Scale Sorting System. In *USENIX Symposium on Networked Systems Design and Implementation (NSDI)*, 2011.
- [71] Recovery-Oriented Computing. <http://roc.cs.berkeley.edu/>.
- [72] Redis. <http://www.redis.io/>.
- [73] Remzi H. Arpaci-Dusseau and Andrea C. Arpaci-Dusseau. Fail-Stutter Fault Tolerance. In *USENIX Workshop on Hot Topics in Operating Systems (HotOS)*, 2001.
- [74] J. H. Saltzer, D. P. Reed, and D. D. Clark. End-to-End Arguments in System Design. *ACM Transactions on Computer Systems*, 2(4), 1984.

- [75] Sunita Sarawagi. Query Processing in Tertiary Memory Databases. In *Conference on Very Large Databases (VLDB)*, 1995.
- [76] Bianca Schroeder and Garth Gibson. A Large-Scale Study of Failures in High-Performance Computing Systems. *IEEE Transactions on Dependable and Secure Computing*, 7(4), October 2010.
- [77] Bianca Schroeder and Garth A. Gibson. Understanding Disk Failure Rates: What Does an MTTF of 1,000,000 Hours Mean to You? *ACM Transactions on Storage (TOS)*, 3(3), October 2007.
- [78] Mehul A. Shah, Joseph M. Hellerstein, and Eric Brewer. Highly-Available, Fault-Tolerant, Parallel Dataflows. In *ACM Special Interest Group on the Management of Data (SIGMOD)*, 2004.
- [79] Andrew D Smith and Wen Chung. The RMAP Software for Short-Read Mapping. <http://rulai.cshl.edu/rmap/>.
- [80] Sort Benchmark Home Page. <http://sortbenchmark.org/>.
- [81] United States Securities and Exchange Commission. Facebook, Inc. Form S-1 Registration Statement, February 2012.
- [82] Jeffrey S. Vitter. Random Sampling with a Reservoir. *ACM Transactions on Mathematical Software (TOMS)*, 11(1), March 1985.
- [83] Xiaodan Wang, Christopher Olston, Anish Das Sarma, and Randal Burns. CoScan: Cooperative Scan Sharing in the Cloud. In *ACM Symposium on Cloud Computing (SoCC)*, 2011.
- [84] Matt Welsh, David Culler, and Eric Brewer. SEDA: An Architecture for Well-Conditioned, Scalable Internet Services. In *ACM Symposium on Operating Systems Principles (SOSP)*, 2001.
- [85] Freebase Wikipedia Extraction (WEX). <http://wiki.freebase.com/wiki/WEX>.
- [86] Joel Wolf, Andrey Balmin, Deepak Rajan, Kirsten Hildrum, Rohit Khandekar, Sujay Parekh, Kun-Lung Wu, and Rares Vernica. CIRCUMFLEX: A Scheduling Optimizer for MapReduce Workloads with Shared Scans. *SIGOPS Operating Systems Review*, 46(1), February 2012.
- [87] Sai Wu, Feng Li, Sharad Mehrotra, and Beng Chin Ooi. Query Optimization for Massively Parallel Data Processing. In *ACM Symposium on Cloud Computing (SoCC)*, 2011.
- [88] Jim Wyllie. Sorting on a Cluster Attached to a Storage-Area Network, 2005. http://sortbenchmark.org/2005_SCS_Wyllie.pdf.

- [89] Wei Xu, Eep Bhatkar, and R. Sekar. Taint-Enhanced Policy Enforcement: A Practical Approach to Defeat a Wide Range of Attacks. In *USENIX Security Symposium*, 2006.
- [90] Apache Hadoop. <http://hadoop.apache.org/>.
- [91] Matei Zaharia, Mosharaf Chowdhury, Tathagata Das, Ankur Dave, Justin Ma, Murphy McCauley, Michael J. Franklin, Scott Shenker, and Ion Stoica. Resilient Distributed Datasets: A Fault-Tolerant Abstraction for In-Memory Cluster Computing. In *USENIX Symposium on Networked Systems Design and Implementation (NSDI)*, 2012.
- [92] Matei Zaharia, Tathagata Das, Haoyuan Li, Scott Shenker, and Ion Stoica. Discretized Streams: An Efficient and Fault-Tolerant Model for Stream Processing on Large Clusters. In *USENIX Workshop on Hot Topics in Cloud Computing (HotCloud)*, 2012.
- [93] Matei Zaharia, Andy Konwinski, Anthony D Joseph, Randy Katz, and Ion Stoica. Improving MapReduce Performance in Heterogeneous Environments. In *USENIX Symposium on Operating Systems Design and Implementation (OSDI)*, 2008.
- [94] Zhuoyao Zhang. Processing Data-Intensive Workflows in the Cloud. Technical Report 2012-970, University of Pennsylvania, 2012.